2009

Mechanisms of iron reduction and phosphorus solubilization in an intermittently wet pasture soil

Jared L. Wilmoth
West Virginia University

Mechanisms of Iron Reduction and Phosphorus Solubilization in an Intermittently Wet Pasture Soil

Jared L. Wilmoth

Thesis submitted to the
Davis College of Agriculture, Forestry, and Consumer Sciences at
West Virginia University
in partial fulfillment of the requirements
for the degree of

Master of Science
in
Plant and Soil Science

Louis M. McDonald, Ph. D., Chair
William B. Bryan, Ph. D.
Alan J. Sexstone, Ph. D.

Division of Plant and Soil Sciences

Morgantown, WV
2009

Keywords: Anaerobic Incubation; AQDS; Humic Acid; Microbial Iron Reduction; Phosphorus Adsorption/Desorption; Platinum Electrode, Redox Potential

ABSTRACT

Mechanisms of Iron Reduction and Phosphorus Solubilization in an Intermittently Wet Pasture Soil

Jared L. Wilmoth

Microbial Fe-reduction in pasture soils may be of agronomic importance, because it has been shown to influence P cycling. The present study investigated the behavior of Fe and P in an intermittently wet, Appalachian pasture soil during a 42 day anaerobic incubation. Native humic acid (HA) extracted from the sampling location and anthraquinone-2,6-disulfonic acid (AQDS) were used in the experiment to determine their electron-mediating effects on Fe(III) reduction and P solubilization over time. Extracted HA and the International Humic Substance Society (IHSS) Elliott Soil HA standard were compared using ^{13}C-NMR, FT-IR, SEM, and CHNS analysis. Soil samples treated with 1.24 g native HA/kg dry soil and 0.2 g AQDS/kg dry soil displayed the highest, most similar, solubilized P rates during the anaerobic incubation. However, the soil alone, without an added electron mediator, was able to release biologically significant concentrations of P to solution at Eh values between 0 and -200 mV. Total soluble P increases were strongly related to soluble Fe(II) increases over time. Field Eh measurements, relative to naturally occurring seasonal changes, are also reported. The purpose of this research was to further define the mechanisms of Fe and P cycling in temperate, pasture soils.

TABLE OF CONTENTS

LIST OF FIGURES

LIST OF TABLES

ACKNOWLEDGEMENTS

This thesis is dedicated to Carly, Chloe, Emily, Gabrielle, Landon, and Olivia– all of my academic work and passion for knowledge have been meant for you.

I would like to give special thanks to the following individuals: Katy, for enduring all the sacrifices of young love, for listening, and for a mutual passion for knowledge; My family and friends, for their love, encouragement, support, and guidance; Mr. King, for being a real scientist and for emitting inspiration and imagination strong enough to propel me through my education; Mr. Hostuttler, for being a profound teacher, and for guiding and supporting my college education; My lab group, for their endless knowledge and friendship; Dr. Louis McDonald, for advice, intellect, and scientific imagination; Dr. Alan Sexstone, for teaching me microbiology and being enthusiastic about science; Dr. William Bryan, for introducing me to and guiding me through the field of plant and soil science; Dr. John Sencindiver, for being a true soil scientist and having faith in my academic ability; Dr. James Thompson, for support and for California; Dr. Novruz Akhmedov, for NMR training and for a mutual sense of humility and passion for science; and Bob at the WVU Agronomy Farm, for being a good man and a good mechanic.

CHAPTER 1: BIOGEOCHEMISTRY OF IRON AND PHOSPHORUS IN PASTURE SOILS

Overview

Iron and phosphorus are dynamic, critical elements in agricultural systems. Each contributes uniquely to the physiological development of plants and the biogeochemical evolution of soil. Biologically, iron is involved in multiple enzymatic pathways for electron transport. It is also a terminal electron acceptor for many soil bacteria in the absence of O_2. In circumneutral pasture soils, adsorption of phosphorus onto iron-oxides is of importance due to a generally low concentration of plant-available phosphorus in solution. Several natural systems (e.g. wetlands and lake sediments) exhibit microbial dissimilation of iron-oxides under reducing conditions, which can lead to an increase in available phosphorus. The chemistry of such mineral-microbe interactions is complex and inadequately defined. Historically, aquatic sediments and flooded agricultural lands have served as the primary models for reducing systems in the environment. This tradition has changed significantly in the last decade with new studies conducted on oxic tropical soils and on humic substances that can act as catalysts for microbial iron reduction. Studying temperate pasture soils with the same scrutiny is a natural and prospective extension of soil fertility and soil microbiology. Such research would broaden our understanding of iron/phosphorus interactions in pasture soils.

Literature Review

Pasture Soils

In 2002, livestock grazing was the major use of approximately 238 million hectares permanent (utilized five or more years) pasture lands in the United States. This accounted for 26 % of all land in the U.S. and about 50 % of all agricultural land in the U.S. (Lubowski et al., 2002). According to the 2000 U.S. Census Bureau, West Virginia contains 6,238,764 hectares of land. Approximately 0.71 million hectares of this land area is permanent pasture (Baker, 1996). Soils in WV pastures are often found on steep slopes, and are in general topographically variable (Baligar et al., 1985). They are typically acidic, shallow, low in native fertility, and often have physical and chemical limitations in the root zone. Phosphorus is a limiting nutrient in most of these pastures (Wright et al., 1984). Macronutrients, especially phosphorus (P), are essential for the growth and development of pasture grasses and legumes (Kleinman et al., 2003). These chemical, physical, and topographic factors limit the input and economic return of WV pastures.

A pasture may be thought of as a network, through which nutrients flow, are transformed, and exported (Pearson and Ison, 1997). Nutrients flow into the pasture system by soil weathering, atmospheric deposition, and fertilizer and soil amendments. Phosphorus in pasture soils is transformed through absorption by organic residues (Salas et al., 2003) and microorganisms (Turner and Haygarth, 2003), and adsorption to soil particles (Zhang et al., 2003). Most important is the transformation of phosphorus from biologically unavailable forms to biologically available forms (Pearson and Ison, 1997). Nutrients in pastures are exported by leaching, run-off and erosion, and by removal of animal products such as meat, milk, and wool (Pearson and Ison, 1997). Because P fertilizers are expensive, especially in the low input/low

return systems of WV, a better understanding of the internal soil-P cycle is needed to improve pasture productivity.

Phosphorus in Soils

Phosphorus is important for many biological and chemical processes (Schachtman et al., 1998). It exclusively fulfills many biochemical and physicochemical roles due to its ability to form more open and weaker bonds than elements in the Second Period, such as oxygen (O) and nitrogen (N); the possession of 3d orbitals, which allows valences beyond four; and the ability to form multiple bonds (Wald, 1962). Like nitrogen and sulfur, P forms complex anions with oxygen. Available soil P is the most critical element in the development of plants in the field, with the only likely exception being that of N. Even so, N uptake in soils is regulated by available P in some cases. A primary example of this is the high demand for P by legumes for growth and development, which then directly influences the amount of N that may be fixed (Brady, 1974). Phosphorus is required by living cells primarily for the synthesis of nucleic acids, phospholipids, and ATP (Westheimer, 1992; Madigan et al., 2003). Properties and functions of P in plants also include cell division, fat and albumin formation, flowering and fruiting, seed formation, crop maturation, root development, strength of straw in cereal crops, crop quality, and resistance to certain diseases (Brady, 1974). Excess soil phosphorus has been identified as an important source of surface water pollution, including eutrophication (Moore and Reddy, 1994; Kuo et al., 2008; Smith et al., 2007).

Total P in soil ranges from about 0 to 0.4%, with an average between 0.05 and 0.1% (1000-2000 kg/ha, in the furrow slice). Even among soils of the same order, P varies considerably in concentration (Troeh and Thompson, 2005). Total P in most agricultural systems is found in the inorganic form (50-70% total P), with much of the remaining P in organic

complexes. Only a small concentration of available P (<0.01 to 1 ppm) exists in the soil solution for biological uptake (Pierzynski et al., 2000).

Phosphates in the soil can be divided into three groups: (1) phosphates present in the soil solution; (2) phosphates present in soil organic matter; and (3) inorganic phosphates including both definite phosphate compounds and surface films of phosphate held on inorganic particles (Russell, 1973). In the soil solution, phosphorus occurs primarily as one of the ions of orthophosphoric acid (Hassett and Banwart, 1992). Plants preferentially take up phosphate ions in the form of $H_2PO_4^-$ and HPO_4^{2-}. However, plant uptake of HPO_4^{2-} is much slower (Tisdale et al., 1993).

Some low molecular weight, soluble organic P compounds exist in the soil solution and may be absorbed by plants, but are usually of minor importance (Tisdale et al., 1993). Soil organic P is derived from plant residues, and from soil flora and fauna tissues and residues, that can resist hydrolysis. Many organic P forms have not been adequately characterized (Kuo, 1996). The P in organic matter is held firmly in place and unavailable to plants until decomposition of the organic material takes place (Troeh and Thompson, 2005).

All soil inorganic P comes from the apatite minerals. Phosphorus can be exposed to the soil solution by mineral-weathering in place, and then dissolve if the surrounding solution has a lower P concentration and favorable pH for dissolution. Inorganic P is also produced in factories that process fertilizers, which can enter the soil through fertilizer amendments. In solution, inorganic P is formed by the mineralization of organic P (Troeh and Thompson, 2005).

Phosphorus may have relatively high, total concentrations in soils, but it is often immobilized and unavailable for plant uptake. It may become unavailable from the biological pool of nutrients through processes involving (1) conversion to organic substances; (2)

precipitation with Fe in acidic to circumneutral soils (or calcium (Ca) in alkaline soils); or (3) adsorption to soil minerals, especially Fe-oxides. Even if P is supplied to the soil in the form of fertilizer, due to these mechanisms, as much as 80% can be lost from the plant available pool (Holford, 1997; Schachtman et al., 1998).

Iron in Soils

Iron comprises approximately 5% of the earth's crust and is the fourth most abundant element in the lithosphere. Soil solution Fe exists as Fe^{2+} (ferrous) and Fe^{3+} (ferric), either free or as organic and inorganic complexes. Biologically, Fe is a critical component of cytochromes and iron-sulfur proteins involved in electron transport of soil organisms, which makes Fe important in cellular respiration (Madigan, et al., 2003).

Total iron in soils is highly variable because Fe can be concentrated or depleted during soil development. Estimates range from 0.7 to 55% (Tisdale et al., 1993). Fe exists in soils primarily as Fe oxides such as hematite, goethite, lepidocrocite, magnetite, maghemite, and ferrihydrite (Loeppert and Inskeep, 1996; Schwertmann, 1988; Schwertmann and Taylor, 1989). Each of these Fe oxides is an Fe(III)-mineral existing predominantly in the clay-size fraction of soils. The exception is magnetite, which contains both Fe^{2+} and Fe^{3+}, and can occur in the silt- and sand-size fraction (Loeppert and Inskeep, 1996). The octahedron is the basic structural unit for all Fe oxides. Each Fe atom is surrounded by six oxygens or both O^{2-} and hydroxide (OH^-) ions (Sparks, 2003).

The solubility of Fe oxide minerals increases in the following order (Schwertmann, 1991; Loeppert and Inskeep, 1996):

$$\text{hematite} = \text{goethite} << \text{lepidocrocite} = \text{magnetite} < \text{ferrihydrite}.$$

Reactivity of Fe oxide in the soil is a consequence of its mineral phase solubility, which is in part determined by particle size and surface reactivity (Loeppert and Inskeep, 1996; Glasauer et al., 2001; Sparks, 2003). Ferrihydrite is the least stable of these minerals. Ferrihydrite is an amorphous mineral (Reyes and Torrent, 1997), being more hydrated with short range crystalline order and typical particle sizes of 10 nm or less (Loeppert and Inskeep, 1996). It is likely to exist in most soils, usually in small quantities, but is a frequent component of soils that exhibit fluctuating redox potentials (Loeppert and Inskeep, 1996). Ferrihydrite and related amorphous Fe minerals are important in rendering Fe more bioavailable in soils, which impacts plants (Loeppert and Inskeep, 1996; Schmidt, 1999), microorganisms (Lovley and Phillips, 1987; Zachara et al., 1998; Lovley and Blunt-Harris 1999), and soil chemical properties (Willett and Higgins, 1978; Golterman, 1995; Finneran et al., 2001; Sparks, 2003).

Phosphorus Adsorption in Soils

In addition to forming precipitates with Fe^{3+} and Al^{3+} in acid soils, and with Ca^{2+} in alkaline soils, P is strongly adsorbed by Fe^{3+}, Al^{3+}, and Ca^{2+} minerals (Figure 1. 1). It has been experimentally determined that there is an active hydroxyl site every 22 to 24 $Å^2$ of an iron oxide-hydroxide mineral's surface (Hassett and Banwart, 1992). The PO_4^{3-} tetrahedron has a base of approximately 21.6 $Å^2$, leading to the notion that every hydroxyl site is able to absorb PO_4^{3-} without steric hindrance (Hassett and Banwart, 1992).

Redox Chemistry of Soils

Chemical species in a given soil vary in their tendency to become oxidized or reduced. This is measured as a reduction potential (Eh), expressed in millivolts by the Nernst equation:

$$Eh(mV) = E^0 - \frac{59.1}{n} log \frac{(Red)}{(Ox)} + 59.1 \frac{m}{n} pH \qquad \text{[eq. 1]}$$

where *Eh* is the electrode potential; E^o is the standard half cell potential; *59* is equal to the gas constant (*R*) multiplied by standard temperature (298 K) devided by the Faraday constant (*F*); (*n*)

is the number of electrons exchanged in the half-cell reaction; (m) is the number of protons exchanged; and the activities of the reduced and oxidized species are shown in parentheses (Patrick et al., 1996).

Given thermodynamic constants for solubility and reduction potential, an Eh-pH diagram of the Fe redox system can be constructed to indicate the most stable oxidation state and mineral form (Figure 1. 2). Although not a thermodynamic property, the negative log of electron activity (pe), analogous to the negative log of proton activity (pH), can be calculated as,

$$pe = \frac{Eh(mV)}{59.1} \qquad \text{[eq. 2]}$$

Soils have the ability to buffer against changes in pH. Likewise, they also have the ability to buffer changes in Eh. This buffering capacity of soils for changes in Eh is called poising. The poising of a substance is the ability of that substance to retard the change in Eh when small amounts of oxidants or reductants are added to the system (Liu, 1997). All soils differ in their degree of poising (Patrick et al., 1996). An example of this would be the continuous donation of electrons from organic residues (buffering against oxidation) and the continuous acceptance of electrons from oxygen (buffering against reduction). Such a process becomes complicated since there are often many redox couples participating in the poise of a given soil. Although measuring Eh is complex, it provides an excellent tool for detecting relative redox changes in the environment as a function of varying conditions (Evangelou, 1998).

Conditions that induce and influence redox fluctuation are always present and always changing in the soil environment. Temperature effects redox reactions by hastening the degradation of organic residues that release electrons to the soil solution (Evangelou, 1998). Biological processes double in reaction rate with every 10°C increase (Madigan et al., 2003).

Thus, temperature may affect the rate at which redox reactions occur in the soil (Yao and Conrad, 2000). Soil microorganisms such as fungi and bacteria effect redox reactions, indirectly and directly, through electron transport, localized changes in pH, and assimilation and liberation of redox sensitive species (Zachara et al., 1998; Essington et al., 2005; Deacon, 2006).

Many studies have dealt with the effects of water, either in submerged terrestrial soil systems (e.g., rice paddies and wetlands) (Ponnamperuma, 1972; Patrick and Khalid, 1974; Zhang et al., 2003) or lake sediments (Moore and Reddy, 1994). In all cases, one of the most obvious and influential consequences of water saturation in soils is the disappearance of oxygen (Ponnamperuma, 1972). When a soil becomes saturated, pores that were once occupied by oxygen become filled with water (Ponnamperuma, 1972). In many soils, this process can occur in cycles, manifesting itself in redoximorphic features such as red and bluish-green-grey colors from Fe, and dark or black concretions of Mn (Buol et al., 2002). When oxygen has been sufficiently depleted from a soil, bacteria must use the next most efficient chemical species to complete a circuit of electrical energy between electron donor, bacterial membrane, and electron acceptor to maintain their life cycle (Zachara et al., 1998; Lovley and Blunt-Harris, 1999; Finneran et al., 2001).

Microbial Reduction of Iron and Its Effects on P Solubility

Bacteria play an important role in the redox chemistry of Fe and P in soils (Lovley and Phillips, 1986; Zachara et al., 1998; Roh et al., 2003; Essington et al., 2005; Peretyazhko and Sposito, 2005; Chacon et al., 2006a and b). Indeed, much research and development in soil science has either been the direct or indirect result of studying the processes of microbial metabolism, which influence many chemical and biological transformations in the environment (Lovley and Phillips, 1987). Two mechanisms for the conservation of energy in microbial

metabolism are known – fermentation and respiration (Madigan et al., 2003). Simply stated, the oxidation in fermentation is coupled to the reduction of a compound generated from the initial substrate (Madigan et al., 2003). In respiration, redox reactions proceed in the presence of a terminal electron acceptor (e.g., Fe^{3+}), after electrons have been transferred from a donor (e.g., organic matter or H_2) (Zachara et al., 1998). There is now evidence that many bacteria can channel electrons toward the reduction of Fe^{3+} under sufficient anaerobic conditions (e.g., *Shewanella putrefaciens*, and members of *Geobacter*, *Geospirillum*, and *Geovibrio*) (Madigan et al., 2003), including some fermenting bacteria (Benz et al., 1998).

Oxygen is not the only electron acceptor and a preferential series of electron acceptors follow when O_2 becomes deficient (Finneran et al., 2001). This includes, but is not limited to, NO_3^-, Mn^{4+}, Fe^{3+}, SO_4^{2-}, and CO_2 (Madigan et al., 2003). Ferric iron (especially in amorphous minerals, but also in crystalline minerals) is extremely important in anaerobic respiration due to its abundance in the environment (Zachara et al., 1998) and the slightly electropositive reduction potential of the Fe^{3+}/Fe^{2+} redox couple (Madigan et al., 2003). This allows the reduction of Fe^{3+} to be coupled to the oxidation of many organic and inorganic electron donors (Madigan et al., 2003).

Energy from the transfer of electrons (e.g., from organic substance to ferric oxyhydroxide) is conserved in the bacterial cell via the proton motive force. The cell membranes of iron reducing bacteria (and many other microorganisms) contain membrane-bound proteins and chemical complexes (electron carriers) that have access to both the outside environment and the inside of the cell. Each carrier follows in a series within the membrane to form a transport system for electrons (Madigan et al., 2003). In order for a flow of electrons to proceed through the membrane, each electron carrier must be slightly more electropositive than the former carrier

in the direction of transport. While electrons are flowing through the membrane, electron carriers are positioned in such a way that they release protons to the outside of the cell. Reactions with water inside the cell produce protons which are used in further reactions and hydroxides that remain inside the cell. The charge of hydroxide ions and protons impedes their migration across the membrane. Electron transport through the cell membrane results in a slightly acidic, slightly positive environment outside the cell and a slightly alkaline, slightly negative environment inside the cell (Madigan et al., 2003).

The establishment of a pH gradient and electrical potential across the membrane of a bacterium energizes the cell analogous to an energized battery. This energy can be used directly for maintenance of cellular components or indirectly for the production of ATP. At a critical point in the transport, protons flow into the cell through a wall-bound enzyme (ATPase). As the protons move into the cell through ATPase, they cause part of the membrane-bound portion of the enzyme to rotate. The second main portion of ATPase, located inside the cell and attached to the membrane-bound portion, undergoes conformational changes because it is fixed in position relative to the turning motion. Ultimately, the flow of protons into the cell due to the pH gradient and electrical potential across the membrane create torque in ATPase, which is conserved as chemical energy in the enzyme and can be used to couple ADP and inorganic P to establish a high-energy phosphate bond in ATP (Madigan et al., 2003).

Iron-reducing bacteria gain energy to live by generating electrical energy from the transfer of electrons from a sufficient electron donor to Fe^{3+}, or Fe^{3+} containing minerals such as ferric oxyhydroxides (Lovley and Phillips, 1987; Zachara et al., 1998; Finneran et al., 2001). Amorphous ferric oxyhydroxides, such as ferrihydrite, are more favorable to iron-reducing

bacteria as terminal electron acceptors since the surface of poorly-crystalline minerals are more reactive and unstable, compared to highly-crystalline ferric minerals (Lovley and Phillips, 1987).

Until recently (within the last few decades), it had been generally thought that iron-reducing bacteria must physically come into contact with Fe minerals for reduction to occur (Finneran et al., 2001). However, research now shows that bacteria can use organic mediators in electron transfer between the microbial cell and the ferric mineral. These organic electron mediators (e.g. humic acid) are known as electron shuttles. It has also been shown that quinone moieties are largely responsible for the electron carrying capacity of humic substances (Lovley et al., 1996; Lovley and Blunt-Harris, 1999; Finneran et al., 2001). Following this research, investigations into electron shuttling processes involved in Fe^{3+} reduction have included the use of synthetic humic substances, such as anthraquinone-2,6-disulfonic acid (AQDS) (Figure 1.3) (Pereyazhko and Sposito, 2005; Chacon et al., 2006a).

Experiments using humic-like substances to probe the mechanisms of electron shuttling in soils and sediments have shown that the addition of AQDS (and related compounds) stimulates the reduction of Fe^{3+}, dissolution of ferric minerals, and solubilization of P sorbed to those ferric minerals (Pereyazhko and Sposito, 2005; Chacon et al., 2006a). The importance of electron shuttling compounds is that they can catalyze dissolution of otherwise inaccessible ferric minerals, making microbial iron reduction more efficient (Finneran et al., 2001). However, there seem to be few examples of research that have investigated iron reduction in soils with native microbial populations coupled to local electron shuttling substances, such as native humic acids (Pereyazhko and Sposito, 2005).

Numerous studies have shown that P is released under anaerobic conditions into the soil solution (Mortimer, 1941; Ponnamperuma, 1972; Patrick and Khalid, 1974; Gale et al., 1992;

Moore and Reddy, 1994; Sigua et al., 2006). It can be deduced from these studies that many soils and sediments exhibit a buffering capacity which controls fluxes of P and Fe (Burkitt et al., 2006), largely due to formation of secondary complexes and the redox potential of the system (Ponnamperuma, 1972). The reductive transformation of Fe oxides can lead to an increase in available P (Mortimer, 1941; Ponnamperuma, 1972; Patrick and Khalid, 1974; Gale et al., 1992; Moore and Reddy, 1994; Sigua et al., 2006), or lead to a decline in available P through complexation with reduced amorphous Fe during dissolution. (Patrick and Khalid, 1974; Moore and Reddy, 1994).

Recent studies have looked at the relationship between Fe reduction and subsequent P mobilization in tropical forest soils that undergo periods of high rainfall and cycles of flooding (de Mello et al., 1998; Peretyazhko and Sposito, 2005; Chacon et al., 2006a and b). The novelty of these studies was that they examined the effects of anoxic soil conditions on Fe and P cycling in highly weathered tropical systems that have traditionally been assumed to be oxic (Peretyazhko and Sposito, 2005). Results from these recent experiments indicate that the reduction of Fe oxides can solubilize P in tropical soils that undergo periods of high rainfall. The prospect of finding similar results for other assumed oxic systems that contain reducible Fe and accompanying sorption phenomena of P seems plausible.

Hypothesis

Microbial reduction of Fe oxides and the presence of natural electron mediating compounds will increase the availability of P in a temperate, seasonally wet pasture soil.

Conditions Set by Hypothesis

The following conditions were established to support the stated hypothesis: (1) Phosphorus is bound to Fe oxides in the soil and can be solubilized by microbial reduction of the associated oxide. (2) Iron oxide-bound P that can be solubilized through non-reductive and/or abiotic-reductive dissolution yields significantly lower solution concentrations over time than P solubilized through microbial reduction. (3) Natural humic substances of the soil can catalyze microbial reduction of Fe oxides by acting as electron mediators. (4) The soil demonstrates sufficiently low redox conditions to reduce Fe oxides.

References

Albers, C.N., Banta, G.T., Jacobsen, O.S., Hansen, P.E., 2008. Characterization and structural modeling of humic substances in field soil displaying significant differences from previously proposed structures. European Journal of Soil Science 59, 693-705.

Baker, B. 1996. Permanent Pasture Management. West Virginia University Extension Service; http://www.caf.wvu.edu/~forage/5728.htm

Baligar, V.C., R.J. Wright, O.L. Bennett, J.L. Hern, H.D. Perry, and M.D. Smedley. 1985. Lime effect on forage legume growth and mineral composition in an acid subsoil. Communications in Plant Science and Soil Analysis 16:1079-1093.

Benz, M., B. Schink, and A. Brune. 1998. Humic acid reduction by *Propionibacterium freudenreichii* and other fermenting bacteria. Applied and Environmental Microbiology 64:4507-4512.

Brady, N.C. 1974. The Nature and Properties of Soils 8th. MacMillan Publishing Co., NY.

Buol, S.W., R.J. Southard, R.C. Graham, and P.A. McDaniel. 2002. Soil Genesis and Classification. Iowa State Press.

Burkitt, L.L., C.J.P. Gourley, M.C. Hannah, and P.W.G. Sale. 2006. Assessing alternative approaches to predicting soil phosphorus sorption. Soil Use and Management, 22:325-333.

Chacon, N., S. Flores, and A. Gonzalez. 2006a. Implications of iron solubilization on soil phosphorus release in seasonally flooded forests of the lower Orinoco River, Venezuela. Soil Biology and Biochemistry. 38:1494-1499.

Chacon, N., W. L. Silver, E. A. Dubinsky, and D. F. Cusack. 2006b. Iron reduction and soil phosphorus solubilization in humid tropical forests soils: The roles of labile carbon pools and an electron shuttle compound. Biogeochemistry. 78:67-84.

Deacon, J. 2006. Fungal Biology 4th. Blackwell Publishing.

de Mello, J.W.V., V. Barron, and J. Torrent. 1998. Phosphorus and iron mobilization in flooded soils from Brazil. Soil Science 163:122-132.

Essington, M.E., J.B. Nelson, and W.L. Holden. 2005. Gibbsite and goethite solubility: The influence of 2-ketogluconate and citrate. Soil Science Society of America Journal 69:996-1008.

Evangelou, V.P. 1998. Environmental Soil and Water Chemistry: Principles and Applications. John Wiley & Sons.

Finneran, K., D. Lovley, and E. Moyer. 2001. Anaerobic strategies for enhanced MTBE and TBA bioremediation. AEHS Magazine: Soil, Sediment, & Water Spring 2001 Special Oxygenated Fuels Issue.

Gale, P.M., K.R. Reddy,and D.A. Graetz. 1992. Mineralization of sediment organic matter under anoxic conditions. Journal of Environmental Quality 77:789-792.

Glasauer, S., S. Langley, and T.J. Beveridge. 2001. Sorption of Fe (hydr)oxides to the surface of *Shewanella putrefaciens*: Cell-bound fine-grained minerals are not always formed *de novo*. Applied and Environmental Microbiology 67:5544-5550.

Golterman, H.L. 1995. Theoretical aspects of the adsorption of ortho-phosphate onto iron-hydroxide. Hydrobiologia 315:59-68.

Hassett, J.J., and W.L. Banwart. 1992. Soils & Their Environments. Prentice Hall NJ.

Holford I.C.R. 1997. Soil phosphorus: Its measurement, and its uptake by plants. Australian Journal of Soil Research 35:227-239.

Kleinman, P.J.A., B.A. Needelman, A.N. Sharpley, and R.W. McDowell. 2003. Using soil phosphrous profile data to assess phosphorus leaching potential in manured soils. Soil Science Society of America Journal 67:215-224.

Kuo, S. 1996. Phosphorus. p. 869-919. *In* D.L. Sparks et al. (*ed*.) Methods of Soil Analysis. Part 3. Chemical Methods. SSSA, Madison, WI.

Kuo, J.-T., P.-H. Hsieh, and W.-S. Jou. 2008. Lake eutrophication management modeling using dynamic programming. Journal of Environmental Management 88:677-687.

Liu, Z.G., C.P. Ding, Y.X. Wu, S.Z. Pan, and R.K. Xu. 1997. Oxidation-Reduction Reactions. p. 442-472. *In* T.R. Yu (*ed*.) Chemistry of Variable Charge Soils. Oxford University Press, NY.

Loeppert, R.L., and W.P. Inskeep. 1996. Iron. p. 639-664. *In* D.L. Sparks et al. (*ed*.) Methods of Soil Analysis. Part 3. Chemical Methods. SSSA, Madison, WI.

Lovley, D.R., and E.L. Blunt-Harris. 1999. Role of humic-bound iron as an electron transfer agent in dissimilatory Fe(III) reduction. Applied and Environmental Microbiology 65:4252-4254.

Lovley, D.R., and E.J.P. Phillips. 1986. Organic matter mineralization with reduction of ferric iron in anaerobic sediments. Applied and Environmental Microbiology 51:683-689.

Lovley, D.R., and E.J.P. Phillips. 1987. Rapid assay for microbially reducible ferric iron in aquatic sediments. Applied and Environmental Microbiology 53:1536-1540.

Lovley, D.R., J.D. Coates, E.L. Blunt-Harris, E.J.P. Phillips, and J.C. Woodward. 1996. Humic substances as electron acceptors for microbial respiration. Nature 382:445-448.

Lubowski, R.N., M. Vesterby, S. Bucholtz, A. Baez, and M.J. Roberts. 2002. Major Uses of Land in the United States. EIB-14. Economic Research Service/USDA.

Madigan, M.T., J.M. Martinko, and J. Parker. 2003. Brock Biology of Microorganisms 10th. Prentice Hall NJ.

Moore, P.A., and K.R. Reddy. 1994. Role of Eh and pH on phosphorus geochemistry in sediments of Lake Okeechobee, Florida. Journal of Environmental Quality 23:955-964.

Mortimer, C.H. 1941. The exchange of dissolved substances between mud and water in lakes. Journal of Ecology. 29:280-329.

Patrick, W.H., R.P. Gambrell, and S.P. Faulkner. 1996. p. 1255-1273. *In* D.L. Sparks et al. (*ed.*) Methods of Soil Analysis. Part 3. Chemical Methods. SSSA, Madison, WI.

Patrick, W.H., and R.A. Khalid. 1974. Phosphate release and sorption by soils and sediments: Effect of aerobic and anaerobic conditions. Science 186:53-55.

Pearson, C.J., and R.L. Ison. 1997. Agronomy of Grassland Systems 2nd. Cambridge University Press NY.

Peretyazhko, T. and G. Sposito. 2005. Iron(III) reduction and phosphorous solubilization in humid tropical forest soils. Geochimica et Cosmochimica Acta 69:3643-3652.

Pierzynski, G.M., J.T. Sims, and G.F. Vance. 2000. Soils and Environmental Quality 2nd. CRC Press LLC Florida.

Ponnamperuma, F.N. 1972. The chemistry of submerged soils. Advances in Agronomy 24:29-96.

Reyes, I., and J. Torrent. 1997. Citrate-ascorbate as a highly selective extractant for poorly crystalline iron oxides. Soil Science Society of America Journal 61:1647-1654.

Roh, Y., C.-L. Zhang, H. Vali, R.J. Lauf, J. Zhou, and T.J. Phelps. 2003. Biogeochemical and environmental factors in Fe biomineralization: Magnetite and siderite formation. Clays Clay Minerals 51:83-95.

Russell, E.W. 1973. Soil Conditions and Plant Growth 10th. Longman, London.

Salas, A.M., E.T. Elliott, D.G. Westfall, C.V. Cole, and J. Six. 2003. The role of particulate organic matter in phosphorus cycling. Soil Science Society of America Journal 67:181-189.

Sigua, G.C., W.J. Kang, and S.W. Coleman. 2006. Soil profile distribution of phosphorus and other nutrients following wetland conversion to beef cattle pasture. Journal of Environmental Quality. 35:2374-2382.

Sparks, D.L. 2003. Environmental Soil Chemistry 2nd. Academic Press.

Schachtman, D.P., R.J. Reid, and S.M. Ayling. 1998. Phosphorus uptake by plants: From soil to cell. Plant Physiology 116:447-453.

Schmidt, W. 1999. Mechanisms and regulation of reduction-based iron uptake in plants. New Phytologist 141:1-26.

Schwertmann, U. 1988. Some properties of soil and synthetic iron oxides. p. 203-251. *In* J.W. Stucki et al. (*ed*.) Iron in Soils and Clay minerals. Reidel, Dordrecht, the Netherlands.

Schwertmann, U. 1991. Solubility and dissolution of iron oxides. p. 3-27. *In* Y. Chen and Y. Hadar (*eds*.) Iron Nutrition and Interactions in Plants. Kluwer, Dordrecht, the Netherlands.

Schwertmann, U., and R.M. Taylor. 1989. Iron oxides. P. 379-438. *In* J.B. Dixon and S.B Weed (*ed*.) Minerals in Soil Environments. SSSA, Madison, WI.

Smith, D.R., P.R. Owens, A.B. Leytem, E.A. Warnemuende. 2007. Nutrient losses from manure and fertilizer applications as impacted by time to first runoff event. Environmental Pollution 147:131-137.

Tisdale, S. L., W.L. Nelson, J.D. Beaton, and J.L. Havlin. 1993. Soil Fertility and Fertilizers 5th. Macmillan Publishing Co.

Troeh, F.R., and L.M. Thompson. 2005. Soils and Soil Fertility 6th. Blackwell Publishing.

Turner, B.L., and P.M. Haygarth. 2003. Changes in bicarbonate-extractable inorganic and organic phosphorus by drying pasture soils. Soil Science Society of America Journal 67:344-350.

U.S. Census Bureau. 2000. <http://www.census.gov/>

Wald, G. 1962. Life in the second and third periods; or why phosphorus and sulfur for high-energy bonds? *In* Kasha, M. and Pullman, B. (*eds*.) Horizons In Biochemistry. Academic Press, NY, 127-141.

Westheimer, F.H. 1992. The role of phosphorus in chemistry and biochemistry. p. 1-17. *In* Walsh et al. (*ed*.) Phosphorus chemistry. Developments in American Science. American Chemical Society, 202nd meeting, NY.

Willett, I.R., and M.L. Higgins. 1978. Phosphate sorption by reduced and reoxidized rice soils. Australian Journal of Soil Research 16:319-326.

Wright, R.J., M.C. Carter, T.B. Kinraide, and O.L. Bennett. 1984. Phosphorus requirements for the early growth of red clover, trefoil, and flatpea. Communications in Soil Science and Plant Analysis 15:49-63.

Yao, H., and R. Conrad. 2000. Effect of temperature on reduction of iron and production of carbon dioxide and methane in anoxic wetland rice soils. Biology and Fertility of Soils, 32:135-141.

Zachara, J.M., J.K. Fredrickson, S.M. Li, D.W. Kennedy, S.C. Smith, and P.L. Gassman. 1998. Bacterial reduction of crystalline Fe^{3+} oxides in single suspensions and subsurface materials. American Mineralogist 83:1426-1443.

Zhang, Y., X. Lin, and W. Werner. 2003. The effect of soil flooding on the transformation of Fe oxides and the adsorption/desorption behavior of phosphate. Journal of Plant Nutrition and Soil Science 166:68-75.

Figures

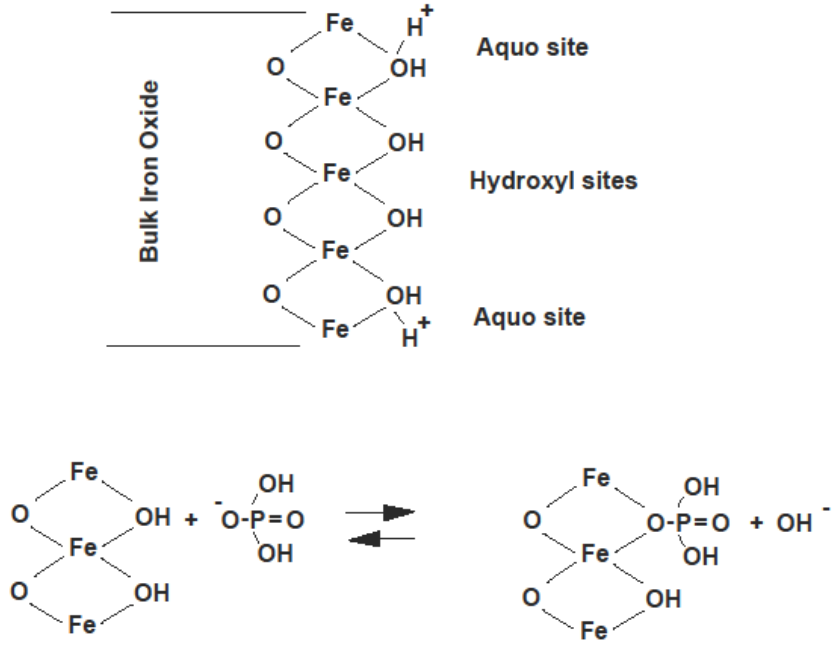

Figure 1. 1 Schematic representation of a monodentate phosphate surface complex on an iron oxyhydroxide (Hassett and Banwart, 1992).

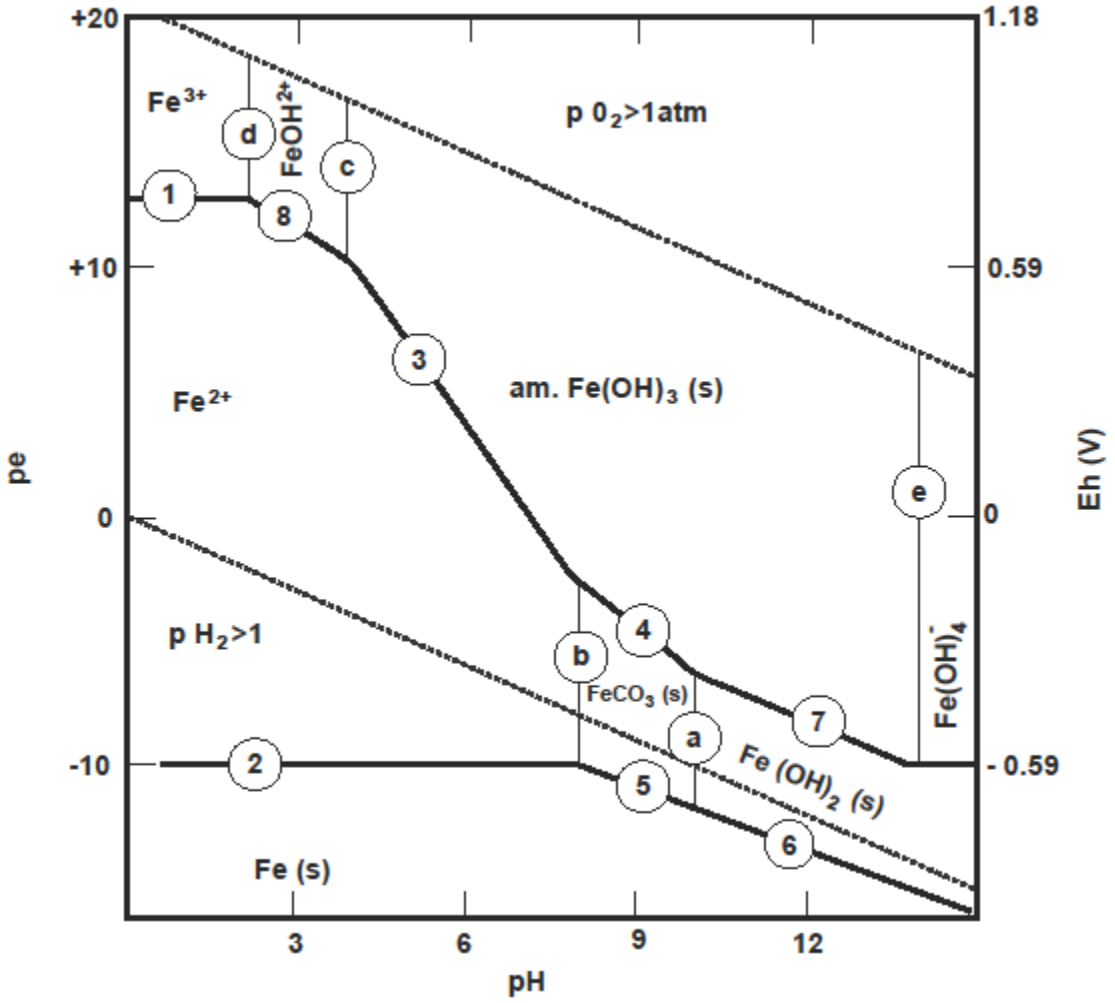

Figure 1. 2 Eh-pH diagram for the iron redox system (Evangelou, 1998).

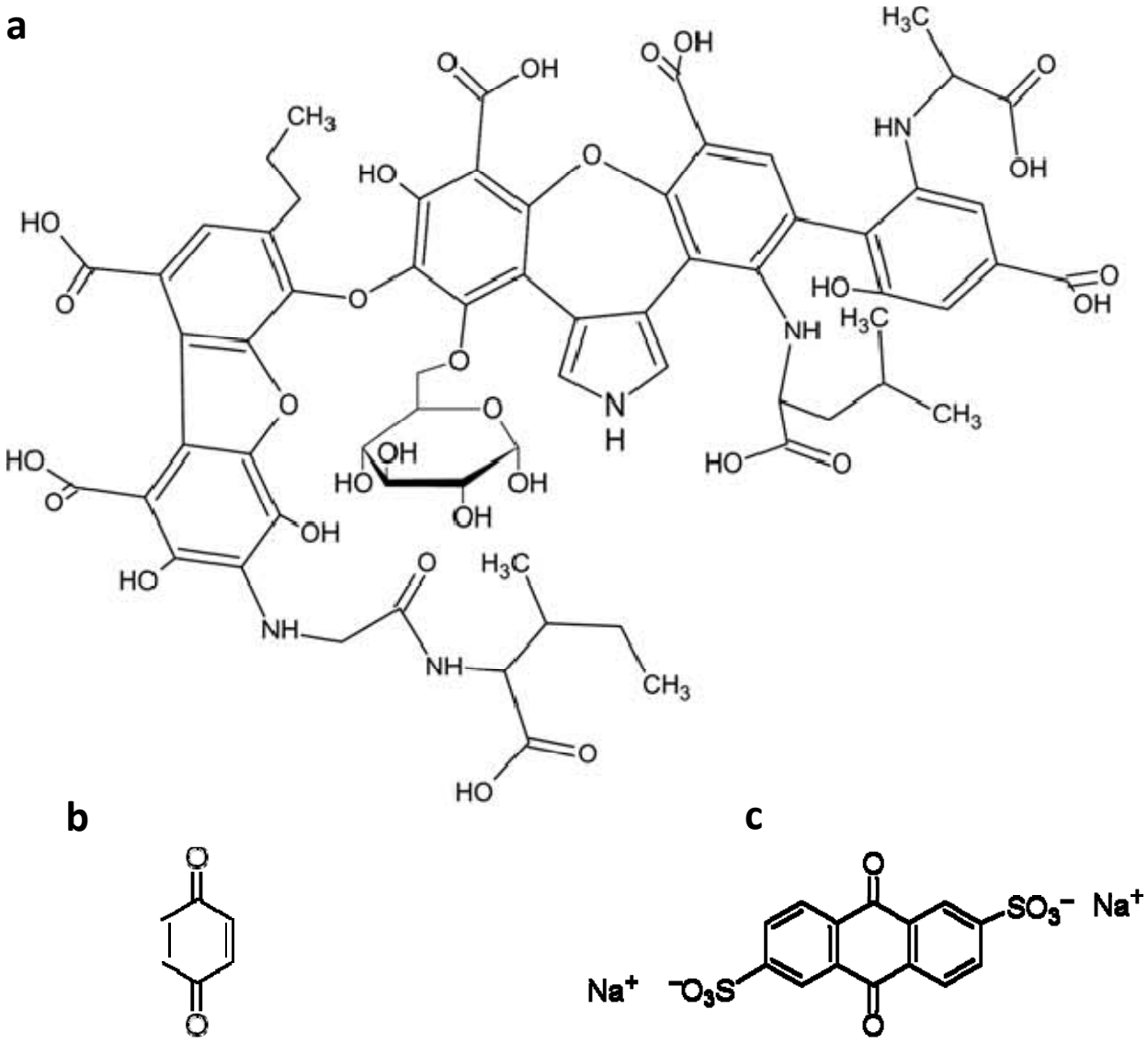

Figure 1. 3 (a) A proposed structure of humic acid extracted from soil (quinone moieties are not shown) (Albers et al., 2008). (b) Molecular structure of benzoquinone. (c) Molecular structure of anthraquinone-2,6-disulfonic acid.

CHAPTER 2: MECHANISMS OF IRON REDUCTION AND PHOSPHORUS SOLUBILIZATION IN AN INTERMITTENTLY WET PASTURE SOIL

Abstract

There is no general agreement in the literature on the biogeochemical processes that exist between Fe(III)-reducing bacteria and Fe-mineral surfaces in solution. Microbial Fe-reduction in pasture soils may be of agronomic importance, because it has been shown to influence P cycling. The present study investigated the behavior of Fe and P in an intermittently wet, Appalachian pasture soil during a 42 day anaerobic incubation. Native humic acid (HA) extracted from the sampling location and anthraquinone-2,6-disulfonic acid (AQDS) were used in the experiment to determine their electron-mediating effects on Fe(III) reduction and P solubilization over time. Extracted HA and the International Humic Substance Society (IHSS) Elliott Soil HA standard were compared using ^{13}C-NMR, FT-IR, SEM, and CHNS analysis. Soil samples treated with 1.24 g native HA/kg dry soil and 0.2 g AQDS/kg dry soil displayed the highest, most similar, solubilized P rates during the anaerobic incubation. However, the soil alone, without an added electron mediator, was able to release biologically significant concentrations of P to solution at Eh values between 0 and -200 mV. Total soluble P increases were strongly related to soluble Fe(II) increases over time. Field Eh measurements, relative to naturally occurring seasonal changes, are also reported. The purpose of this research was to further define the mechanisms of Fe and P cycling in temperate, pasture soils.

Introduction

Soils of Appalachian pastures generally lack adequate concentrations of phosphorus to sustain crops and grazing livestock in agricultural systems (Elrashidi et al., 2008). Economically viable organic and inorganic P fertilizers are applied to pastures of low fertility in order to elevate yield and forage quality (Alloush et al., 2003). These methods are usually sufficient to meet nutritional demands, and often exceed plant requirements (Green et al., 2007). Environmental hazards are inherent in such practices (Smith et al., 2007). Consequently, research in Appalachian pastures frequently addresses P availability and P transformation in the context of leaching and runoff (Alloush et al., 2003; Brauer et al., 2007; Elrashidi et al., 2008). Data from these reports may give insight into processes leading to loss of native and applied P, but presents limited quantitative information to explain fundamental, mechanistic relationships that influence P biogeochemistry at the mineral/solution interface in pasture soils.

Kinetic studies have been used to examine P interactions between mineral surfaces and plants in the soil solution (Sharpley et al., 1981; Raven and Hossner, 1994). These interactions are important, primarily because native P and P added to soils as fertilizer becomes adsorbed to minerals like iron (Fe) oxides (Hassett and Banwart, 1992). Plant growth and development have been related to the rate of P sorption and desorption from mineral surfaces (Raven and Hossner, 1994). Interactions between soil and water (e.g. precipitation) have been shown to initiate significant P desorption depending on the intensity, duration, soil type, and initial concentration of available and sorbed P (Sharpley et al, 1981).

Plant nutritional studies have traditionally focused on available P, rather than the process of P release from mineral surfaces (Raven and Hossner, 1994). More recently, P desorption has become important in evaluating nutrient translocation and loading of aquatic systems from

common agricultural landscapes (Zhang et al., 2005). Yet, the majority of information and theory derived from relevant soil-P studies has been framed within the context of oxic soil conditions (Shober and Sims, 2009). Much less research has examined the effects of redox fluctuation on P desorption in natural, non-flooded soil systems, such as temperate pastures.

Iron minerals largely control the soil solution P composition in neutral to acidic soils (Essington et al., 2005). Reductive dissolution of Fe(III) oxyhydroxides can release P adsorbed to the surface of Fe minerals in the soil (Ponnamperuma, 1972; Patrick and Khalid, 1974; de Mello et al., 1998; Peretyazhko and Sposito, 2005; Chacon et al., 2006a). In the past, this chemical relationship between Fe and P has been evaluated using wetlands (Ponnamperuma, 1972), lake sediments (Moore and Reddy, 1994), and flooded agricultural lands (Patrick and Khalid, 1974; Zhang et al., 2003) as model reducing environments. Consequently, Fe/P redox-relationships reflect the conditions of these unique systems, but prevent their complete application to more common landscapes of agronomic importance.

Peretyazhko and Sposito (2005) examined the relationship between Fe(III) mineral reduction, organic matter accumulation, and P desorption in an Ultisol of a humid tropical forest in Puerto Rico. The results showed that soil from a toposequence displayed significant Fe reduction and P desorption when incubated in the laboratory under anaerobic conditions. Phosphorus released during the incubation accumulated primarily in organic form. Chacon et al. (2006a) studied the role of labile carbon (C) sources in Fe reduction and P desorption in the same type of soil. These results showed that pulsed additions of glucose and acetate, used to mimic naturally pulsed C inputs in the environment, significantly increased Fe(III) mineral reduction and P solubilization.

Lovley and Phillips (1988) showed that organic substances, when oxidized to carbon dioxide by a consortium of Fe(III)-reducing bacteria, can serve as primary electron donors to Fe(III) under anaerobic conditions. They described a model whereby complex OM is metabolized to fermentation products, which then serve as organic electron donors for the reduction of Fe(III). Subsequent research by Lovley et al. (1996) showed that humic acid (HA), and the synthetic HA analog anthraquinone-2,6-disulfonic acid (AQDS), could both mediate the transfer of electrons from organic substrates to Fe(III). They proposed that HA can act as a catalyst for Fe(III) reduction via a two-step mechanism. In the first step, Fe(III) reducers transfer electrons to HA, with quinone moieties possibly serving as the main electron-carrying functional groups. In the second step, HA abioticaly reduces Fe(III), thus becoming oxidized for further cycles of electron acceptance and donation.

Peretyazhko and Sposito (2005) and Chacon et al. (2006a) used AQDS in laboratory incubations of oxic tropical soils to determine its effect on Fe(III) reduction and P solubilization. The results showed that low concentrations of AQDS where able to catalyze Fe(III) reduction, releasing significant amounts of P in solution. Peretyazhko and Sposito (2005) pointed out, however, that a similar role for HA in soil is unclear and deserves further study. Additionally, it must be noted that AQDS, with its lower molecular weight and smaller diversity of electron carrying moieties, is not necessarily a good model for high-molecular-weight, highly substituted HA associated with the mineral fraction of soil (Benz et al., 1998).

Although the results of Alloush et al. (2003) and Elrashidi et al. (2008) showed significant correlations between organic and inorganic fertilizer input, OM, P concentration, topography, and precipitation in Appalachian pasture soils; no redox mechanisms corresponding to these factors were examined. Theoretically, wetting from precipitation and/or groundwater

could stimulate reducing conditions at various points on a rugged Appalachian toposequence, due to decreased flow rate and increased infiltration of water. Phosphorus desorption from minerals such as Fe(III) oxyhydroxides could occur as the redox potential falls, continuing efficiently if labile C sources for electron donation are present (Chacon et al., 2006a). This P could then be taken up by plants (Schachtman et al., 1998) and microorganisms (Whitton et al., 1991), lost from the system through leaching and runoff (Kleinman et al., 2003), re-adsorbed to mineral surfaces (Willett and Higgins, 1978; Chacon et al., 2006b), or become incorporated into accumulating OM as particle translocation progresses downslope (Peretyazhko and Sposito, 2005).

The hypothesis of the present research was that microbial reduction of Fe oxides and the presence of natural electron mediating compounds would increase the availability of P in a temperate, seasonally wet pasture soil. The following conditions were established to test this hypothesis: (1) Phosphorus must be adsorbed to Fe oxides in the soil and can be solubilized by microbial reduction of the associated oxide. (2) Iron oxide-bound P that can be solubilized through non-reductive and/or abiotic-reductive dissolution yields significantly lower solution concentrations over time than P solubilized through microbial reduction. (3) Natural humic substances of the soil can catalyze microbial reduction of Fe oxides by acting as electron mediators. (4) The soil can demonstrate sufficiently low redox conditions to reduce Fe oxides.

Materials and Methods

Field Site and Sampling Location

Soil samples were collected from a slightly concave position on a NW-facing sideslope (12-15% slope) located at the West Virginia University Agronomy Farm in Morgantown, WV

(39°39'16.70"N, 79°54'7.16"W). The site does not receive frequent (i.e. annual) applications of lime or fertilizer, and does not presently contain grazing livestock. It is topographically variable, including steep slopes and natural drainages, with grass (harvested for livestock forage) serving as the main source of productivity. The vegetation was examined in the field to identify potential indicator species for wet and/or poorly drained soil. A species of the *Cyperaceae* family was observed (similar to field sedges), but exact identification was not possible due to lack of maturity.

Soils formed primarily from parent material of the Allegheny Formation and Pottsville Group, mainly from interbedded shale, siltstone, sandstone, and some limestone. Dekalb (loamy-skeletal, mixed, mesic Typic Dystrochrepts) and Gilpin (Fine-loamy, mixed, mesic Typic Hapludults) are the dominant residual soils in the area and are generally more acid than the surrounding soils. Some of the local soils have a seasonal high water table (Wright et al., 1982).

A 46 m (down slope) x 23 m (across slope) plot was identified, from which 30 soil samples were collected from an average depth of 20 cm, and then composited. After roots had been separated, the sample was air-dried, then ground and passed through a 2 mm sieve. It was stored at 23-25°C under standard laboratory conditions, and subsequently used to determine soil chemical and physical characteristics relevant to this study.

A duplicate composite of 30 soil samples from the same area and soil depth was also collected. After roots were separated, the field-moist soil (approximately 30% moisture by weight) was carefully mixed and used directly in a 42 day anaerobic incubation. In order to prevent microbial cell lysis, as well as other chemical changes in the soil, such as the oxidation of ferrous Fe (Fe(II)) to Fe(III), the soil was not air-dried prior to the incubation experiment.

Soil Chemical and Physical Characterizations

pH, Particle Size, Bulk Density, and Porosity

The following soil chemical and physical characterizations were conducted on the air-dried composite sample (unless noted otherwise) prior to the anaerobic incubation. Soil pH was measured in a 1:1 soil to water ratio (Chacon et al., 2006a) using a combination pH electrode (Mettler-Toledo, Inc., Columbus, OH, USA). Soil particle-size distribution was determined by pipette analysis after dispersion with sodium hexametaphosphate (Tan, 1996). Bulk density and porosity at the field site were determined based upon six core samples taken to a depth of 20 cm after the sod had been removed (Hassett and Banwart, 1992).

Organic Matter and Organic Carbon

Total OM% (TOM) was determined by loss on ignition (Nelson and Sommers, 1996). Soil samples (1.25 g) were placed in ceramic crucibles and dried at 105°C for 24 hours. The samples were then ignited at 400°C for 16 hours. The mass lost during ignition was used to calculate TOM. Total residual OM% (TROM) was determined by recording the dry mass (105°C for 24 hours) of separate 1.25 g soil samples, then treating them with a minimum amount of 35% H_2O_2 until gas evolution ceased. The dry mass of the H_2O_2 treated soil was then recorded. Finally, the samples were ignited at 400°C for 16 hours. The mass lost during ignition (non-H_2O_2 reactive OM) was used to calculate TROM (Peretyazhko and Sposito, 2005). Total labile OM% (TLOM (H_2O_2 reactive OM)) was calculated as the difference between TOM and TROM. Total organic C% (TOC) was determined by dry combustion using a TruSpec CHN analyzer (Leco, Corp., St. Joseph, Michigan, USA). Total residual OC% (TROC) was determined by using H_2O_2 treated soil samples in the same analysis as TOC. Total labile organic C% (TLOC) was calculated as the difference between TOC and TROC.

Fe and P Characterizations

Soil Fe and P forms were characterized following the methods of Peretyazhko and Sposito (2005). Citrate-bicarbonate-dithionite (CBD) extraction (Loeppert and Inskeep, 1996) was used to operationally measure total free Fe oxides. For this method, sodium dithionite ($Na_2S_2O_4$) was used to reduce Fe(III) in crystalline oxides. The solubilized Fe(II) was determined by a colorimetric reaction with 1,10-phenanthroline (Loeppert and Inskeep, 1996) at 510 nm using a Cary 50 UV Spectrophotometer (Varian, Inc., Palo Alto, CA, USA). Total P in $Na_2S_2O_4$ extracts was determined using an Optima 2100 DV Inductively Coupled Plasma-Atomic Emission Spectrophotometer (ICP-AES) (PerkinElmer, Waltham, Massachusetts, USA). The extracted P is reported here as an estimate of P chemically associated with $Na_2S_2O_4$-reducible Fe(III) oxides in the soil (Peretyazhko and Sposito, 2005).

Amorphous Fe oxide concentration was operationally determined using a citrate-ascorbate (CA) extraction developed by Reyes and Torrent (1997). Soils were shaken (3 cycles/s) in 50 ml of a 0.2 M sodium citrate-0.05 M sodium ascorbate solution at pH 6 for 16 hours. Addition of ascorbic acid results in the reductive dissolution of poorly crystalline Fe(III) oxides. Citrate serves as a chelator, forming aqueous complexes with Fe(II), which maintains Fe(II) solubility and stimulates the solubilization of Fe(III). However, citrate can also extract Fe(III) from organic complexes (Reyes and Torrent, 1997). Following the recommendation of Reyes and Torrent (1997), amorphous Fe oxide concentration is reported here as the difference between citrate-ascorbate extracted Fe and citrate extracted Fe. Reduced Fe and total P in solution were determined as described above.

Total Fe and P in the soil were determined by a microwave digest with concentrated HNO_3. Approximately 0.5 g of soil was placed in Teflon microwave vessels with 10 mL of trace

metal grade HNO_3. The reaction was carried out in a Mars 5 microwave (CEM, Corp., Matthews, NC, USA). Fe and P from digested filtrates were determined by ICP.

Microbially reducible Fe(III) in field moist soil was estimated according to the procedure set forth by Lovley and Phillips (1987). Approximately 0.2 g-samples of moist soil were extracted for 1 hour, under standard conditions, in 5 ml of one of two solution treatments: The first treatment was a solution of 0.5 M HCl; and the second treatment was a solution of 0.25 M hydroxylamine hydrochloride in 0.25 M HCl. After 1 hour, the solutions were passed through a 25 mm 0.2 μm filter (Millipore Corp., Billerica, MA, USA), and 0.1 ml of each filtrate was added to 5 ml of 1 g/L ferrozine (3-(2-pyridyl)-5,6-diphenyl-1,2,4-triazine-p,p'-disulfonic acid, disodium salt hydrate) in 50 mM HEPES (*N*-2-hydroxyethylpiperazine-N'-2-ethanesulfonic acid) buffer adjusted to pH 7 with 1 M NaOH. Standards were made using ferrous ethylenediammonium sulfate tetrahydrate (Lovley and Phillips, 1986). Absorbance at 562 nm of the resulting solutions was determined as described above. Detection limits for the ferrozine analysis were established according to Eaton et al. (1995) (Appendix 1).

Lovley and Phillips (1987) stated that Fe reduction, estimated by hydroxylamine hydrochloride dissolution, might be preferred over long term anaerobic incubations for an initial screening of Fe reduction in natural environments. Furthermore, the 0.5 M HCl extraction allows inherent Fe(II) in samples to be distinguished from chemically reduced Fe(III) (Lovely and Phillips, 1987). Hydroxylamine hydrochloride reducible Fe in the moist soil samples used for the present study was detected in the laboratory. No Fe(II) was detected in 0.5 M HCl extracts. If 0.5 M HCl-extractable Fe(II) was present in the moist samples, it existed in a concentration too low to be quantified with ferrozine. Table 2. 1 summarizes the results of the soil chemical and physical characterizations.

Humic Acid Extraction

Humic acid (HA) was extracted from the soil according to the procedures of Swift (1996). The method used was one set forth by the International Humic Substance Society (IHSS). IHSS is a supplier of highly purified HA suitable for anaerobic experiments with Fe(III) reducing bacteria (Lovley and Blunt-Harris, 1999). The soil sample was first acidified with 1 and 0.1 M HCl, followed by extraction with 1 and 0.1 M NaOH under an atmosphere of N_2 gas, precipitation of HA with 6 M HCl, re-dissolution with a minimum amount of 0.1 M KOH with the addition of solid KCl (0.3 M K^+ final concentration) under N_2, precipitation of HA with 6 M HCl, and removal of inorganic materials by 0.1 M HCl/0.3 M HF treatment followed by dialysis against DDI water. The HA slurry from the dialysis tubing was freeze dried and kept in a sealed, dark glass vial under laboratory conditions. The yield was 7.37 g HA/kg dry soil; 0.74% of the dry soil was operationally defined as HA (Table 2. 1).

Humic Acid Characterization

Although Benz et al. (1998) treated in-lab extracted HA (fractionated from sediments of Lake Constance in Germany) and commercial HA (Aldrich) with 1 M HCl, they were unable to completely remove residual Fe. Consequently, the HA extracted for the present study was analyzed for total Fe and P (ICP), as well as hydroxylamine/HCl-reducible Fe(III) and acid-extractable Fe(II) (following the procedure of Lovley and Phillips, 1987). FT-IR, ^{13}C-NMR, SEM, and CHNS analyses were used to compare other important chemical and physical properties between the extracted HA (HA Ex) and the IHSS Elliott Soil HA standard (HA St) (University of MN, St. Paul, MN, USA).

FT-IR: Fourier transformed infrared spectra were recorded in absorbance mode with a Spectrum One spectrophotometer (PerkinElmer, Waltham, Massachusetts, USA). Samples were

prepared as pellets containing 0.5 mg freeze-dried HA and 300 mg potassium bromide (Drosos et al., 2009).

^{13}C-NMR: Liquid state normal broadband ^{13}C-NMR analysis of HA samples was performed on a 600 Inova spectrometer (Varian, Inc., Palo Alto, CA, USA) at 150 MHz (Albers et al., 2008). Samples were prepared by dissolving 150 mg of freeze-dried HA in 1.5 ml of 3 M sodium deuteroxide in deuterium oxide (3 M NaOD in D_2O), shaken for 24 hours and then centrifuged at 11 000 g for 15 minutes (Dou et al., 2008). The supernatant (700 µl) was transferred to 5 mm, high precision (900 MHz) NMR tubes (Wilmad-LabGlass, Buena, NJ, USA). Chemical shifts of the spectra were referred to D_2O, and the deuterium signal of the solvent was used as an internal lock. Acquisition of spectra was stopped at 90 000 transients and a line broadening function (LB = 50 Hz) was applied before Fourier transformations.

SEM: SEM images of gold-coated, freeze-dried HA samples were recorded on an S-4700 field emission scanning electron microscope (Hitachi, HTA Inc., Pleasanton, CA, USA) using an accelerating voltage of 5.0 kV.

Elemental Analysis: Percentages of carbon (C %), hydrogen (H %), nitrogen (N %), and sulfur (S %) were determined using a Flash 1112 series elemental analyzer (CE Instruments, Hindley Green, UK). Oxygen content (O %) was estimated by mass difference (Drosos et al., 2009).

Anaerobic Incubation of Soil

Approximately 30 g of moist soil was added to autoclaved 125 ml clear glass serum bottles (Wheaton, Inc., Millville, NJ, USA). The inside opening of each bottle was 13 mm in diameter (outer diameter was 20 mm). Soil aggregates equal to or larger than 13 mm in diameter

were not forced through bottle openings, and were omitted from the incubation. The exact amount of soil (by mass) in each bottle was recorded after each addition.

The experimental design of the incubation was arranged such that seven treatments could be sampled 12 times at three replicates over a 42 day period (total number of individual samples = 252). Peretyazhko and Sposito (2005) and Chacon et al. (2006a) conducted similar experiments in tropical soils over a much shorter duration (14 and 13 days respectively). The 42 day incubation reported in the present study was chosen because little information exists on the rate and biogeochemical processes that govern Fe reduction in the natural pasture soil selected for analysis. It was hypothesized that a longer incubation time would more accurately demonstrate redox fluctuation in the environment, which would allow biological and chemical parameters to approach values representative of anaerobic cycles in the field.

Sodium Azide Treatment

Soil treated with sodium azide (NaN_3) was used as a microbe-inhibiting control throughout the incubation. Sodium azide inhibits cytochrome c oxidase, which is the last electron transport-enzyme in the respiratory electron transport chain of bacteria and mitochondria. Among species of bacteria, NaN_3 most effectively inhibits gram-negative bacteria (i.e. Fe-reducing bacteria) (Cunningham and Williams, 1995). The treatment was applied to soils according to Wolf et al. (1989). Samples were treated with NaN_3 (36 serum bottles) at a rate of 0.28 g/kg dry soil (3.08 mmol/kg moist soil). Samples containing NaN_3 and soil were partially sealed by blocking the opening of each glass bottle with approximately 3 sheets of twisted laboratory paper (Kimwipe). The treated samples were allowed to vent under a fume hood for 72 hours at standard laboratory conditions. The treatment was finally prepared by adding 50 ml of boiled, highly purified 18 $M\Omega\ cm^{-1}$ water (Milli-Q Synthesis A10, Millipore

Corp., Billerica, MA, USA) to each of the 36 serum bottles (1 trt x 3 reps x 12 sampling periods = 36 bottles).

Propylene Oxide Treatment

Serum bottles (n = 36) with added soil were treated with propylene oxide according to Wolf et al. (1989). Propylene oxide toxicity is related to esterification of carboxyl groups in protein (Wolf et al., 1989; Fraenkel-Conrat, 1944). Thus, the treatment served here as a microbe-inhibiting control during the incubation. Propylene oxide was added to the soil at a rate of 593.04 g/kg dry soil (7.15 mol/kg moist soil). After the addition of propylene oxide, serum bottles were sealed with autoclaved 13 mm I.D. x 20 mm O.D. butyl rubber stoppers (Wheaton). The sealed serum bottles were left under a fume hood for 48 hours. After 48 hours, the stoppers were removed, and the open serum bottles were allowed to vent for 48 hours under the hood. After this venting period, no observable propylene oxide liquid remained. The treatment was finally prepared as above by adding 50 ml of boiled, highly purified water to each of the 36 serum bottles.

Soil and Water Treatment

Water treated soil samples were prepared by adding 50 ml of boiled, highly purified water to 36 serum bottles containing soil.

AQDS Treatment

As little as 100 μM (Lovley et al., 1996) and 150 μM (Peretyazhko and Sposito, 2005) of AQDS have been shown to catalyze the reduction of Fe in anaerobic incubations. For the AQDS treatment in the present study, AQDS was added at a rate of 0.2 g/kg dry soil (200 μM) as a solution made with boiled, highly purified water. This solution (50 ml) was added to 36 serum

bottles containing soil samples. The ultimate purpose for using AQDS treated soil was to test the implications of the AQDS-related studies previously mentioned, and to have a comparative model for evaluating the effect(s) of HA in separate treatments.

HA Treatments

Lovley et al. (1996) reported that 100 μM AQDS and HA (2 g/L) displayed similar catalytic Fe reducing activity under anaerobic conditions. Iron reduction linked to the presence of HA has also been shown to be important for many species of bacteria in the environment (Benz et al., 1998). In the present study, three levels of HA (extracted from the field site soil) were used in three additional soil treatments during the laboratory incubation. Each of three treatment groups, comprised of 36 serum bottles filled with soil, either received 50 ml of solution with added HA at a rate of 1.24 g/kg dry soil (0.5 g/L), 4.96 g/kg dry soil (2 g/L), or 9.92 g/kg dry soil (4 g/L). HA solutions were prepared as above with boiled, highly purified water.

Gas Evacuation With Argon

After all the soil treatments had been prepared, each serum bottle was sealed with an autoclaved butyl rubber stopper (Geo-Microbial Technologies, Inc., Ochelata, OK, USA) and a 20 mm crimped aluminum cap (Wheaton, Inc., Millville, NJ, USA). In order to initiate anaerobic conditions, each sample was then gas evacuated under vacuum and filled with argon (Ar) (Peretyazhko and Sposito, 2005). The apparatus used to evacuate and fill was built and maintained in the WVU Biology Department, located in the WVU Life Sciences building. It was composed of three essential components: a vacuum pump, an Ar gas tank, and a manifold of copper tubing mounted with a pressure gage.

For each of three rounds of gas evacuation and filling, 9 serum bottles containing treated soil samples were gently swirled and the septums pierced with a 3.8 cm 18 gauge needle attached to a one-way stopcock (Baxter Healthcare Corp., Deerfield, IL, USA). The bottles with needle-stopcock assemblies were then attached to the copper manifold via copper lines each fitted with a two-way stopcock. Atmospheric gas was then pumped out of the bottles until bubbles stopped forming in solution, after which Ar was injected.

Measurement of Biogeochemical Parameters During Incubation

Three replicates from each of the seven treatments were analyzed for various biogeochemical parameters on days 0, 2, 5, 7, 12, 16, 19, 23, 30, 35, 40, and 42 (12 sampling-day groups, each comprised of 21 (3 reps x 7 treatments) individual sample bottles). Day 0 measurements of biogeochemical parameters are defined here as the measurements performed after all of the incubation bottles had been evacuated and filled with Ar, but before the first 24 hours of the incubation had passed (i.e. day 0 is the original day of the experiment). Ultimately, data corresponding to a given sampling day represents data collected at the end, or very near the end, of that sampling day. Before analysis, the samples were stored in the dark with intermittent, gentle shaking during the incubation. Laboratory temperature fluctuated between 22 and 24°C, but on average was 23°C.

Incubation CO_2

The first analytical procedure to take place on each sampling date was gas collection from the incubated serum bottles. A 20 ml syringe fitted with a one-way stopcock was filled with 10 ml Ar, which was then injected into the headspace of a soil-incubation bottle so that a vacuum would not be formed during gas withdraw. During the addition of 10 ml Ar, the syringe was pumped several times to mix the headspace gas. After the gas had been thoroughly mixed,

10 ml of headspace gas was drawn into the syringe, the stopcock was closed, and the sample was then injected into another autoclaved 125 ml serum bottle (at atmospheric conditions) fitted with an autoclaved stopper and crimped aluminum cap. An additional 20 ml of Ar was then injected into each soil sample bottle so that an equal volume (approximately 20 ml) of solution could be withdrawn for Fe and P analysis without creating a vacuum. The gas sample bottles were stored in the dark at 23°C for later analysis by gas chromatography.

Carbon dioxide in gas sample bottles was analyzed with a Carle AGC Series 100 gas chromatograph (Hach Co., Loveland, CO, USA) connected to a BD40 chart recorder (Kipp & Zonen, inc., Bohemia, NY, USA). Standards were made by diluting appropriate volumes of CO_2 with Ar in a 60 ml syringe. A standard was measured every 21 samples to monitor instrument drift over time. Carbon dioxide concentrations were calculated based upon peak height measurements taken from the chart recorder graphs. Evolution of CO_2 was used as an indicator of microbial metabolism.

Incubation Fe and P Measurements

For measurement of Fe and P in solution, serum bottles containing incubated soil were centrifuged at 680 g for 15 to 20 min. A centrifuge carriage capable of holding 250 ml centrifuge bottles was modified to accommodate the Wheaton 125 ml serum bottles used for the incubation. Centrifugation was used primarily to avoid subsequent filter clogging problems (Peretyazhko and Sposito, 2005).

A syringe was used to withdraw approximately 20 ml of solution from the centrifuged serum bottles, which was then passed through a 0.2 μm filter. For Fe(II) quantification, 0.1 to 4 ml of sample was added to 5 ml of ferrozine, and the absorbance at 562 nm was determined as described above. New standards were prepared before each Fe(II)-ferrozine analysis. A separate

5 ml sample was added to a 15 ml polystyrene conical centrifuge tube (Fisher Scientific, Pittsburgh, PA, USA), diluted to 7 ml with DDI water, and then acidified with 1 M HCl to achieve a 0.5 M HCl solution. Total Fe and P in this acidified sample were determined by ICP.

Inorganic P was determined by the ammonium molybdate method (Murphy and Riley, 1962; Kuo, 1996). Filtered solution (5 ml) was added to a 50 ml polypropylene centrifuge tube (Fisher Scientific), then diluted to 20 ml with DDI water. Ammonium molybdate reagent (8 ml) was added to the diluted sample. After reagent addition and mixing, the solution was diluted to 50 ml with DDI water. The solution was allowed to stand for at least 15 min, or longer, for full color development. Absorbance at 880 nm was determined as described above.

Colorimetric solutions for Fe(II) (ferrozine) and inorganic P (ammonium molybdate) were allowed to develop according to preliminary experiments that monitored for potential absorbance changes of ferrozine and ammonium molybdate standards over a 24 hour period. The results of the experiments showed that negligible absorbance fluctuation, relative to the methods outlined in this study, occurred within 24 hours after colorimetric solutions were thoroughly mixed. In accordance with these results, samples and standards were analyzed within 24 hours after being reacted with colorimetric reagents (Appendix 1).

Incubation Eh and pH Measurements

Eh measurements were collected with a platinum electrode and AgCl reference electrode, which had both been built in the lab specifically for the incubation. The platinum electrode design was fundamentally similar to that used by Wafer et al. (2004). The electrode was assembled by first drilling a 1.6 mm diameter, 3 mm deep hole into the end of a 3.18 mm diameter low-fume-bare bronze brazing rod (LFBB) (Radnor Welding Products, Radnor, PA, USA) cut to a length of 23 cm. A propane torch and 1.5 mm electrical rosin core solder (Lenox,

East Longmeadow, MA, USA) were used to attach a 10 mm length x 0.5 mm diameter solid platinum wire (Sigma-Aldrich, St Louis, MO, USA) to the drilled opening. The bronze rod and platinum/rod junction were covered with a thin layer of Loctite Marine epoxy (Henkel, Hagen, Germany), except for a few cm of the unsoldered end, which was left bare for electrical contact. Approximately 7 mm of the platinum wire was left exposed.

The Ag/AgCl reference electrode was assembled using a method similar to that of Sawyer et al. (1995). A 4 mm diameter Vycor porous-glass frit (#G0100) (Princeton Applied Research, Oak Ridge, TN, USA) was attached to the end of a 15 cm length x 4 mm diameter Pyrex glass tube (Fisher Scientific) by heat-shrink Teflon tubing (Princeton Applied Research, # G0100). The glass tube was then filled with a saturated KCl solution and an 11 cm length of 0.5 mm silver wire (Aldrich). Teflon tubing was used as a cap, with 4 mm of silver wire left exposed for electrical contact. The silver wire was electroplated with AgCl by using a counter platinum electrode in circuit with a 9V battery and a 1MΩ resistor (RadioShack, Fort Worth, TX, USA).

After incubated serum bottles had been analyzed for Fe and P, Eh (mV) was determined by using an auto-range digital multimeter (RadioShack, Fort Worth, TX, USA) connected to a platinum electrode and a AgCl reference electrode. This was accomplished by removing the aluminum seal and stopper from each serum bottle, and then quickly immersing both electrodes into the incubated solution to measure the reduction potential. Probe function was checked with two standard solutions made up of a small fraction of quinhydrone mixed in either a pH 4 or pH 7 buffer (Fisher Scientific) (Patrick et al., 1996). The pH of incubated samples was measured as described previously in an aliquot of solution that had been poured into a plastic container.

Qualitative Eh Validation With Tetramethylthionine Chloride (Methylene Blue)

On day 23 of the incubation, two randomly selected replicates were removed from the soil and water treatment group after Fe and P analysis. Three drops of methylene blue (tetramethylthionine chloride, 0.23% w/v) alkaline dye was dispensed from an 18 gauge needle into a sealed serum bottle (Eh and pH not measured). The remaining serum bottle was opened, and treated with 3 drops of methylene blue dye after Eh and pH values had been recorded. Both of the serum bottles, one sealed and one open, were allowed to sit overnight. Methylene blue dye is dark blue under oxic conditions. But under anaerobic conditions, it converts to colorless leuco methylene blue and HCl, resulting from the addition of 2 electrons and 2 protons (Galagan and Su, 2008). This procedure was carried out to qualitatively verify that reducing conditions were present in the serum bottles. The soil and water replicates were selected because they only contained soil, and no additional electron mediating or microbe-inhibiting compound.

Statistical Analysis

Statistical analysis of Fe(II), Fe-ICP, P-ICP, and CO_2 versus time graphs was performed using SAS ver 9.1 (SAS Institute, Inc., Cary, NC, USA). In all other graphs with trend lines, parameter relationships are shown using lines that best fit the data. When present, error bars represent an average plus or minus the standard deviation of 3 sample replicates.

Results and Discussion

HA Chemical and Physical Properties

Fe and P in HA: The total residual Fe concentration, 0.181 μmol/mg (in units reported by Benz et al. (1998)), was extremely close to the total Fe concentrations reported by Benz et al. (1998) (0.187 μmol/mg Aldrich HA and 0.210 μmol/mg lake sediment HA). In the present

study, HCl extractable Fe(II) was determined to be 8.79 times lower than total Fe. Hydroxylamine hydrochloride reducible Fe(III) and extracted inherent Fe(II) produced a similar value, indicating that nearly all of the acid soluble Fe was in the reduced state. Ultimately, total Fe made up approximately 1% of the HA by mass, of which 12% was acid soluble and mainly in the ferrous form. Phosphorus was also detected in the HA, making up approximately 0.6% of HA by mass (Table 2. 2).

FT-IR: FT-IR spectra of the extracted HA and the IHSS standard HA were very similar (Figure 2. 1). All spectral bands characteristic of humic substances were present for both samples: in the regions of 3410 cm^{-1} (H-bonded OH groups); 2920 cm^{-1} (aliphatic C-H stretching); 1720 cm^{-1} (C=O stretching of COOH and ketones); 1620 cm^{-1} (aromatic C=C, H-bonded C=O, and/or dissociated COOH groups); 1530 cm^{-1} (aromatic ring vibrations characteristic for lignins); 1400 cm^{-1} (O-H deformation, CH_3 bending, C-O stretching of phenolic OH, and COO^- antisymmetric stretching of aryl esters); 1250 cm^{-1} (C-O stretching and OH deformation of COOH, C-O stretching of aryl esters); and 1034 cm^{-1} (possibly due to C-O stretching of polysaccharide-like substances or other C-O-H containing groups like alcohols or lignin; or mineral stretching of silicon-type (Si) impurities) (Drosos et al., 2009). The most apparent differences between the two spectra occur between the regions of 1226 cm^{-1} and 1712 cm^{-1}, with slight differences occurring around 2917 cm^{-1} and 2846 cm^{-1}.

^{13}C-NMR: Solution state ^{13}C-NMR spectra of the extracted HA and the IHSS standard HA were very similar, and displayed unique spectral characteristics of humic substances: 0-48 ppm (aliphatic-C); 48-90 ppm (C-O and carbohydrate-C); 90-108 ppm (acetal-C atoms connected with one bond or with two O atoms, carbohydrate-C (e.g. cyclic poly-sugars)); 108-145 ppm (C or H substituted aromatic-C); 145-167 ppm (aromatic-C bonded to O and/or OH

groups (phenolic-C)); 167-185 ppm (carboxylic-C esters, amide-C, and possibly phenolic-C close to quinonoid groups); and 185-220 ppm (C=O) (Schnitzer and Preston, 1986; Albers et al., 2008) (Figure 2. 2).

SEM: SEM images of both HA samples revealed some unique topographic features. At a relative scale of 200 μm, the extracted HA (on average) was found to be composed of slightly larger, more topographically variable plate-like and blocky structures when compared to the IHSS standard HA. In general, the IHSS standard HA displayed smaller, angular, plate-like aggregates with smoother surfaces. At scales of 10 and 5 μm, irregular fissures were clearly observed in the surfaces of extracted HA aggregates. These surface features were not observed in the IHSS standard HA (Figure 2. 3).

Elemental Analysis: Elemental analysis showed very similar values for both HA samples (Table 2. 3). Ultimately, and most importantly, chemical characterization of the HA samples showed that the extracted HA used in the incubation was indeed HA (relative to a universal HA standard, the IHSS Elliott Soil HA standard). In the following discussion of incubation chemical parameters, the results of the propylene oxide (PO) treatment have been omitted because of the large amount of variability in chemical parameters measured during the incubation, which could not be adequately explained. The removed data for the PO treatment is in Appendix 2.

Incubation Chemical Parameters

Eh and pH

The redox potential (approximately +300 mV) of the incubation samples decreased slowly from day 0 to day 16 of the experiment (Figure 2. 4). Beginning at day 16, the redox potential for all treatments, except the sodium azide (NaN_3) treatment, dropped steeply from

+150 mV to below -100 mV by day 23, after which it decreased slowly to -200 mV by day 42. The redox potential of the NaN_3 treatment continued to decrease, approaching just below +100 mV by day 42.

Soil and water (SW) treatment bottles that had been mixed with methylene blue on day 23 were evaluated after setting overnight. The sample bottle that had been left open had a purple-blue tinted solution, while the sealed bottle displayed a slightly hazy, yet relatively clear solution– indicative of reduced methylene blue. On day 16, it was observed that one of the AQDS treatment (AQDS 0.2) replicates displayed a yellow-green colored solution. By day 23, all AQDS treated samples displayed an orange-gold colored solution. Reduced AQDS (anthrahydroquinone-2,6-disulfonic acid (AHDS)) absorbs light at 450 nm (Lovley et al., 1996), which explains the color change in solution as the redox potential fell during the incubation.

The pH of all incubation treatments fluctuated between pH 6.4 and 7.4 (Figure 2. 4). Peretyazhko and Sposito (2005) observed a similar pH fluctuation of 1 unit during their anaerobic incubation of tropical forest soil. In this study, three of the seven treatments were recognized as being distinct from the others. The 9.92 g HA/kg dry soil treatment (HA 9.92) started with the lowest pH (pH of 6.4); and the 4.96 g HA/kg dry soil treatment (HA 4.96) started with the second lowest pH (pH of 6.6). The low pH values for the two highest HA concentrations might be explained by the dissociable protons left over from the extraction of HA. Both HA treatments stabilized around pH 7 by day 16 of the incubation. Finally, the AQDS 0.2 treatment reached the highest pH value by the end of the incubation (pH of 7.2). This could be explained by the conversion of AQDS to AHDS, which would account for the decreased proton activity in solution over time, and reflects the observed color change in solution.

Soluble Fe(II)

The rate of Fe(II) release remained unchanged for the NaN_3 treatment during the incubation. Overall, the NaN_3 treatment displayed the lowest adj r^2 and slope values for all chemical parameters (Table 2. 4). Table 2. 4 shows the SAS regression output for the Fe(II), Fe-ICP, P-ICP, and CO_2 parameters over time. The slope for SW treatment Fe(II) was 0.70 mg kg^{-1} day, which exceeded the rate of Fe(II) release for the NaN_3 treatment. Soluble Fe(II) for the AQDS 0.2 treatment displayed a rate similar to that of the SW treatment (slope = 0.57 mg kg^{-1} day). Although the AQDS 0.2 and SW treatments shared the same general linear trend during the incubation, between day 0 and 19, and between day 30 and 42, the rate of Fe(II) release displayed a slightly higher value for the AQDS 0.2 treatment (slope = 0.49 mg kg^{-1} day (day 0-19) and 1.26 mg kg^{-1} day (day 30-42) for AQDS 0.2 treatment; 0.35 mg kg^{-1} day (day 0-19) and 0.86 mg kg^{-1} day (day 30-42) for SW treatment). The reason that the AQDS 0.2 treatment displayed higher rates of Fe(II) release than the SW treatment at the beginning and end of the incubation, but not in the middle, seems to be attributed to the lag phase observed for the AQDS 0.2 treatment between day 19 and 30. The Fe(II) slopes for HA 1.24 g/kg dry soil (HA 1.24), HA 4.96, and HA 9.92 treatments were 0.89, 1.36, and 1.80 mg kg^{-1} day respectively, together displaying the highest rates of Fe(II) release during the experiment (Figure 2. 5).

Total Fe

The rate of Fe-ICP release did not change for the NaN_3 treatment during the incubation, although concentrations were slightly elevated above soluble Fe(II) concentrations. The SW treatment slope for Fe-ICP was 0.65 mg kg^{-1} day, and 0.79 mg kg^{-1} day for the AQDS 0.2 treatment. The difference between the rates of Fe-ICP and Fe(II) for the AQDS 0.2 treatment is interesting when compared to all other treatments. These results suggest that AQDS solubilized

Fe(III) over the entire course of the incubation, beyond the first 12 to 16 days. A similar relationship between AQDS and solution Fe(III) was also reported by Peretyazhco and Sposito (2005). However, a key study published by Lovley et al. (1996), linking HA to AQDS as a model compound for natural humic substances, reported that no Fe(III) was observed to have been solubilized by AQDS during anaerobic incubations. Ultimately, the Fe(III)-solubilizing potential of AQDS is not clearly defined in the literature. The Fe-ICP slopes for HA 1.24, 4.96, and 9.92 treatments were 0.84, 1.23, and 1.61 mg kg^{-1} day respectively (Figure 2. 6).

Based upon HCl and hydroxylamine hydrochloride extractions performed on the bulk HA sample (extractions also performed by Benz et al. (1998) for their anaerobic incubation of HA), only a small amount of Fe (mostly in the reduced state) would have been added to solution by HA treatments. According to the results of HCl and hydroxylamine extractions, Fe(II) and Fe-ICP measured during the incubation could have included the following values of extractable Fe added from HA treatments: HA 1.24 = 1.54 mg Fe/kg dry soil, HA 4.96 = 6.15 mg Fe/kg dry soil, and HA 9.92 = 12.29 mg Fe/kg dry soil. However, since 93% of extractable Fe in the HA was Fe(II), and HA soluble Fe(II) graphs did not show concentrations above 4.0 mg/kg dry soil until day 5, the potential Fe additions from HA treatments were not significantly present at the beginning of the incubation. Alternatively, the elevated concentrations of Fe-ICP for HA 2 and 4, between day 0 and day 16, were possibly the result of Fe(III) solubilization due to interactions between the soil and HA (Xie and Shang, 2005). However, it is also possible that Fe(II) could have been oxidized once released from HA, thereby adding to total Fe. In either case, the inherent Fe concentrations in HA did not contribute significantly to Fe(II) or Fe-ICP after day 5.

Total P

The concentrations of inorganic P throughout the incubation were too low to determine using ammonium molybdate. This is most likely because the soil used in this study was (1) not highly weathered and (2) had not received regular fertilizer amendments in the past. The P-ICP slope for the NaN_3 treatment was 2.39 μg kg^{-1} day. As mentioned previously, NaN_3 does not function as a complete sterilization treatment of soil. Rather it acts as a microbial inhibitor, including both gram-negative bacteria and fungi (Wolf et al., 1989). It is important to note that the P solubilized over time in the NaN_3 treatment is most likely indicative of P released non-reductively or abiotically from the soil and/or P solubilized via microorganisms other than Fe-reducing bacteria, such as fungi and other bacterial species. The P-ICP slope for the SW treatment was 7.71 μg kg^{-1} day. If the assumption is that NaN_3 P-ICP represents P released by non-biological or non-Fe-reducing-bacterial processes, then NaN_3 P-ICP can be subtracted from SW P-ICP to equal SW P-ICP values most likely due to microbial Fe-reduction. For example, when the P-ICP concentrations on day 42 for both treatments is considered, and the difference between them calculated in terms of μg/L P (solution P), 27 μg/L P was released by microbial reduction of Fe by the end of the experiment for the SW treatment.

Pierzynski et al. (2000) mentioned that most agricultural soils have solution concentrations of P between <0.01 and 1 mg P/L. At the beginning of the incubation, virtually no P-ICP was detected in solution. The data show that as much as 0.027 mg/L P was added to solution over time, due to microbial reduction primarily of Fe(III) oxyhydroxides. It should also be noted that as little as 20 μg/L P can negatively impact natural water bodies (Pierzynski et al., 2000; Elrashidi et al., 2008). Even if such a concentration of P (0.027 mg/L) were only

periodically released into solution from redox-fluctuating pasture soils, it could significantly add to biologically available P, and possibly to runoff.

The P-ICP slope for the AQDS 0.2 treatment was 8.71 μg kg^{-1} day, which was greater than the SW treatment slope. The higher rate of P-ICP release for the AQDS 0.2 treatment might be partially explained by Fe(III) solubilization, in addition to soluble Fe(II) release over time. However, the decrease in Eh coupled with the increase in both Fe(II) and P-ICP by day 30, supports a strong relationship between Fe(III) reduction and P solubilization for the AQDS 0.2 treatment.

The P-ICP slopes for HA 1.24, 4.96, and 9.92 treatments were 8.65, 7.18, and 0.46 μg kg^{-1} day respectively. The HA 1.24 P-ICP slope was essentially equal to that of AQDS 0.2. It is also important to note that the Fe(II) slope for the HA 1.24 treatment (0.89 mg kg^{-1} day) was larger than the Fe(II) slope for the SW treatment (0.70 mg kg^{-1} day). Even though both P-ICP slopes for the HA 1.24 and SW treatments show overlapping standard deviations between day 19 and day 40, they are separated between day 5 and day 19, as well as at day 42. This is important because day 5 marked the beginning of Fe(II) increase in solution, and also the separation of HA 1.24 P-ICP from NaN_3 P-ICP, approximately 10 days earlier than SW P-ICP separation from NaN_3 P-ICP (Figure 2. 7).

The HA 4.96 and 9.92 treatments were elevated in day 0 P-ICP concentration relative to the other treatments. When day 0 P-ICP for all three HA treatments is plotted as a function of HA concentration, a positive linear trend is obtained (data not shown). This relationship indicates that HA 4.96 and 9.92 treatments were elevated in P-ICP at day 0 because of P addition from HA. However, this does not completely rule out interactions between HA and the soil. Since day 0 measurements were finished 12-16 hours after serum bottles were flushed with Ar,

there may have been time for reactions between soil-P and HA to have occurred by day 0 measurements.

The fact that the HA 9.92 P-ICP slope did not change over time relative to the HA 4 Fe(II) slope needs to be addressed. Even if elevated HA P-ICP at day 0 could be completely explained by added P from HA treatments, HA 9.92 P-ICP should still have increased over time similar to HA 4.96, because of continued Fe reduction and P solubilization in the soil. Alternatively, the elevated level of HA 9.92 P-ICP may have remained static over time due to a P-equilibrium of the system. Another possible explanation for elevated initial P concentrations is direct interactions between HA and the soil.

HA has been shown to compete with adsorbed P at the Fe-mineral surface (Sibanda and Young, 1986). Xie and Shang (2005) also noted the dominance of natural organic matter (i.e. HA) adsorption onto Fe-mineral surfaces over other chemical species in solution. In the present study, HA could have exchanged with adsorbed P at Fe-mineral surfaces in the soil, thereby elevating P-ICP by day 0 measurements. If this reaction between HA 9.92 and the soil was sufficient enough, it would explain why P-ICP remained unchanged during the incubation, but why Fe(II) increased over time. In other words, the limited concentration of P initially adsorbed to Fe(III) oxyhydroxides in the soil may have been largely solubilized early in the incubation via an exchange mechanism with HA, while HA-complexed-Fe(III) and/or free Fe(III) oxyhydroxides were reduced over time.

The HA/soil-P exchange model would also help explain why the rate of P-ICP release for the HA 1.24 treatment was greater than that of the SW treatment, but why the rate of P-ICP release for the HA 4.96 treatment was less than that of the SW treatment. Such a result would be expected if the HA 4.96 treatment had significantly stimulated the release of exchangeable P

adsorbed to Fe(III) at the beginning of the incubation. HA 1.24 did not show an elevated day 0 P-ICP concentration. Consequently for HA 1.24, more adsorbed P would have been available for solubilization as the redox potential decreased during the incubation. Although evidence for such HA-soil interactions can be speculated based upon the data, no single mechanism was directly investigated during the experiment, and therefore deserves future study.

Relationship Between Soluble Fe(II) and Total P

By plotting P-ICP as a function of F(II) released during the incubation, the positive effect of Fe reduction on P solubilization can be observed (Figure 2. 8). The data shows for the NaN_3 treatment, in which Fe-reducing bacteria were theoretically inhibited, that P-ICP did not follow an ordered trend. The reason for this decoupling of Fe reduction and P release is most likely due to inhibition of Fe-reducing bacteria. The SW, AQDS 0.2, HA 1.24, and HA 4.96 treatments each displayed a very strong, positive relationship between Fe(II) and P-ICP during the incubation. Such a relationship was not observed for the HA 9.92 treatment because of an unchanged P-ICP concentration over time, which is further complicated by the elevated levels of initial P-ICP (P vs Fe(II) graph for HA 9.92 is not shown). Overall, these data give evidence that P was adsorbed to Fe(III) oxides in the soil, and that this P could be released through microbial-reduction of the associated oxide.

CO_2 Evolution

The CO_2 slope for the NaN_3 treatment was 0.55 $\mu g\ g^{-1}$ day. When compared with Fe(II), Fe-ICP, and P-ICP, it seems that the NaN_3 treatment was in fact an effective microbial inhibitor during the incubation. The CO_2 slopes for the SW, AQDS 0.2, HA 1.24, HA 4.96, and HA 9.92 treatments were 1.29, 1.23, 1.47, 1.85, and 2.28 $\mu g\ g^{-1}$ day respectively (Figure 2. 9). Concentrations of CO_2 increased over time as P-ICP and Fe increased in solution. A high degree

of similarity between CO_2 evolution, soluble Fe(II), and total P in solution over time suggests that bacteria able to oxidize OM and donate electrons to Fe(III) oxides functioned as the primary Fe-reducing agents during the incubation; and that microbial-dissociation of Fe(III) minerals led to an increase in soluble P. This point is further strengthened by comparing the chemical parameters of the NaN_3 treatment with the chemical parameters of all other treatments, in which the NaN_3 treatment always displayed the lowest rates.

1st Derivative Analysis of the AQDS Treatment

Between day 19 and day 30, a distinguished lag in the rate of Fe(II) occurred for the AQDS 0.2 treatment. This lag phase was also observed for Fe-ICP and P-ICP, and to a less obvious extent for CO_2, until it appeared to terminate near day 30. The increase in concentration for all AQDS 0.2 chemical parameters seemed to be related to the steep drop in Eh around day 19, which began to level around day 30 at almost -200 mV. The lag phase shared by these chemical parameters, and its effects on their rates, can be more clearly demonstrated by first fitting each parameter's data set with a best fit polynomial function, obtaining the first derivative of that function, then solving the derivative using incubation time as the variable. When the solutions are plotted against time, the curvature between day 19 and 30 is accentuated, and the simultaneous shift toward a more positive slope around day 20 for all chemical parameters is revealed (Figure 2. 10).

The AQDS 0.2 lag phase was important because it reinforced a direct link between Eh, Fe(II), Fe-ICP, P-ICP, CO_2 and the metabolic activity of Fe-reducing bacteria. In other words, the AQDS 0.2 lag phase made it possible to link Eh, Fe(II), Fe-ICP, P-ICP, and CO_2 (microbial respiration) together, because all of these AQDS 0.2 parameters shared the same deviation in chemical rate at approximately the same time. Relative to AQDS 0.2, all other treatments were

either too linear or too variable to represent such a comparison between treatment-specific chemical parameters (i.e. 1st derivative analysis of other treatments did not show simultaneous inflection similar to the AQDS 0.2 treatment).

It should be noted that around day 19 the AQDS in solution had began to be converted to AHDS. The lag phase might possibly be explained by loading of electrons on AQDS. By day 19, respiring bacteria under anaerobic conditions (solution Eh approaching -100 mV from +150 mV) may have preferentially reduced AQDS since it was available and abundant in solution. A lag in Fe reduction could have been due to a slower abiotic-Fe-reduction rate (dependent on day 30 Eh, -200 mV) of AHDS compared to the initial reduction of AQDS by Fe-reducing bacteria. This slow second step involving abiotic Fe-reduction by AHDS could likely be explained by a relatively low concentration of Fe(III) oxyhydroxides versus the concentration of AHDS in solution, and/or the Eh dependency of AHDS to reduce Fe(III) oxyhydroxides.

Possible Role of Redox-Active Species other than Fe

In general, the primary terminal electron acceptors for organic matter decomposition in anaerobic sediments are nitrate (NO_3^-), manganese (Mn(IV)), Fe(III), sulfate (SO_4^{2-}), and CO_2 (Lovley and Phillips, 1988). At pH 7, SO_4^{2-} and CO_2 have very electronegative reduction potentials (equal to -200 mV and below) in the environment compared to the other chemical species (Masscheleyn et al., 1990). Such reduction potentials theoretically would not be favorable to facultative metal-reducing bacteria in pasture soils where values reach a lower limit of -200 mV, as observed in this study. Manganese and NO_3^- have greater electropositive reduction potentials compared to the other chemical species (between +200 and +300 mV). In the context of P availability under anaerobic conditions, NO_3^- reduction would not influence

available P through adsorption/desorption, which leaves Mn(IV) reduction as a possible mechanism for P solubilization observed during the incubation.

The reduction potential for the Fe(III)/Fe(II) redox couple is approximately +50 mV at pH 7 (Masscheleyn et al., 1990) and Fe(III) is generally much more abundant in soils than Mn(IV), especially if a given soil has not been regularly fertilized with compounds containing Mn (i.e. the pasture soil used in this study). For the SW treatment, P-ICP did not completely diverge from NaN_3 P-ICP until day 19, when the Eh was 0 mV. It could be hypothesized that if P solubilization was primarily controlled by Mn(IV), SW P-ICP should have been higher than NaN_3 P-ICP before day 19, due to a more electropositive potential of the system during that time. However, biologically significant SW P-ICP concentrations were not observed until around day 19, when Fe(III) would have been more favorable as a terminal electron acceptor for Fe-reducing bacteria (Eh = 0 mV). When taking into account that Fe(II) and P-ICP were shown to be strongly related, and that first derivative analysis of AQDS 0.2 chemical parameters showed a simultaneous increase near day 19 (relative to an Eh of 0 mV), it is most likely that P solubilization was primarily the result of Fe(III) reduction during the incubation.

Conclusion

Recent discoveries of novel metal-reducing-bacteria have allowed traditional ideas concerning anaerobic metabolism to be reevaluated. A species of bacteria that can directly couple organic C oxidation to Fe(III)-reduction, with Fe(III) as the sole terminal electron accepter, was not isolated until the late 1980's (Lovley and Phillips, 1988). Since then, related organisms have been shown to assemble highly organized biofilms that regulate electrical current at electrode surfaces (e.g. microbial fuel cells) (Marsili et al., 2008), develop electrically conductive pili (Gorby et al., 2006), degrade organic contaminants (Finneran et al., 2001),

remove radioactive metals such as uranium (U) (Lovley and Phillips, 1991), and reduce soluble electron shuttles that can abiotically reduce Fe(III) (Lovley et al., 1996).

Current data from Eh fluctuating tropical soils, thought to be predominantly oxidized, has shown that significant concentrations of P are released to solution during microbial reduction of Fe(III) oxyhydroxides (Peretyazhco and Sposito, 2005). This data has also shown that soluble electron mediators, such as the HA-model-compound AQDS, catalyze Fe(III) reduction and P solubilization. However, such research has not fully examined the effects of soil-specific HA during laboratory incubations, leaving the role of native HA in soils unknown and deserving future study.

There is no general agreement in the literature on the mechanistic relationships that exist between Fe-reducing bacteria, HA, AQDS, and Fe-mineral surfaces in solution. The results of this study show that 0.2 g AQDS/kg dry pasture soil and 1.24 g native HA/kg dry pasture soil treatments displayed more similar and higher solubilized P rates when compared with untreated pasture soil during a laboratory anaerobic incubation. However, the soil alone, without an added electron mediator, was able to release biologically significant concentrations of P to solution at Eh values between 0 and -200 mV. Increases in available P were shown to be strongly related to soluble Fe(II) increases over time.

The experiments described here extended modern microbial-Fe-reduction research to a temperate pasture soil. Fe(III) reduction in pastures may be of agronomic importance because it influences P cycling. In general, the data show a strong relationship between Eh, Fe(II), solubilized P, and CO_2 evolution for the selected pasture soil under anaerobic conditions (Eh = 0 to -200 mV during the incubation). To complement the incubation, field Eh, soil moisture, and precipitation at the sample location were measured in the summer and autumn of 2007 and 2008.

The field data demonstrated a stabilized Eh of approximately -200 mV for a 60 day interval during the summer of 2008. Field Eh was dependent upon soil moisture and frequency of precipitation (Ch. 3).

The observed relationship between Eh, Fe(II), and solubilized P during the incubation, combined with field Eh data, presents evidence that P solubilization from microbial reduction of Fe(III) oxyhydroxides, coupled to HA electron mediation, occurs in intermittently wet pasture soils. Accordingly, these processes would exist even if the natural system was dominated by oxidizing conditions, so long as seasonal Eh fluctuations (approximating -200 mV for a sufficient duration) occur. The results of this study warrant future research that could further elucidate the mechanistic relationships between microbial-Fe-reduction and P solubilization in temperate, agricultural systems.

References

Albers, C.N., Banta, G.T., Jacobsen, O.S., Hansen, P.E., 2008. Characterization and structural modeling of humic substances in field soil displaying significant differences from previously proposed structures. European Journal of Soil Science 59, 693-705.

Alloush, G.A., Boyer, D.G., Belesky, D.P., Halvorson, J.J., 2003. Phosphorus mobility in a karst landscape under pasture grazing system. Agronomie 23, 593-600.

Benz, M., Schink, B., Brune, A., 1998. Humic acid reduction by *Propionibacterium freudenreichii* and other fermenting bacteria. Applied and Environmental Microbiology 64, 4507-4512.

Brauer, D., Turner, K., Belesky, D., 2007. Effects of source and amount of phosphorus on sorption kinetics in the topsoil of a highly weathered soil. Communications in Soil Science and Plant Analysis 38, 885-893.

Chacon, N., Silver, W.L., Dubinsky, E.A., Cusack, D.f., 2006a. Iron reduction and soil phosphorus solubilization in humid tropical forests soils: the roles of labile carbon pools and an electron shuttle compound. Biogeochemistry 78, 67-84.

Chacon, N., Flores, S., Gonzalez, A., 2006b. Implications of iron solubilization on soil phosphorus release in seasonally flooded forests of the lower Orinoco River, Venezuela. Soil Biology & Biochemistry 38, 1494-1499.

Cunningham, L., Williams, H.D., 1995. Isolation and characterization of mutants defective in the cyanide-insensitive respiratory pathway of *Pseudomonas aeruginosa*. Journal of Bacteriology 177, 432-438.

De Mello, J.W.V., Barron, V., Torrent, J., 1998. Phosphorus and iron mobilization in flooded soils from Brazil. Soil Science 163, 122-132.

Dou, S., Zhang, J.J., Li, K., 2008. Effect of organic matter applications on ^{13}C-NMR spectra of humic acids of soil. European Journal of Soil Science 59, 532-539.

Drosos, M., Jerzykiewicz, M., Deligiannakis, Y., 2009. H-binding groups in lignite *vs*. soil humic acids: NICA-Donnan and spectroscopic parameters. Journal of Colloid and Interface Science 332, 78–84.

Eaton, A.D., Clesceri, L.S., Greenberg, A.E., Franson, M.A.H., 1995. Standard Methods for the Examination of Water and Wastewater. APHA, Washington, USA.

Elrashidi, M.A., Seybold, C.A., Wysocki, D.A., Peaslee, S.D., Ferguson R., West, L.T., 2008. Phosphorus in runoff from two watersheds in Lost River Basin, West Virginia. Soil Science 173, 792-806.

Essington, M.E., Nelson, J.B., Holden, W.L., 2005. Gibbsite and goethite solubility: the influence of 2-ketogluconate and citrate. Soil Science of America Journal 69, 996-1008.

Finneran, K., Lovley, D., Moyer, E., 2001. Anaerobic strategies for enhanced MTBE and TBA bioremediation. AEHS: Contaminated Soil Sediment and Water, Special Issue Spring 2001, 91-94.

Fraenkel-Conrat, H., 1944. The action of 1,2-epoxides on proteins. Journal of Biological Chemistry 154, 227-238.

Galagan, Y., Su, W.F., 2008. Reversible photoreduction of methylene blue in acrylate media containing benzyl dimethyl ketal. Jounal of Photochemistry and Photobiology A: Chemistry 195, 378-383.

Gorby, Y., Yanina, S., McLean, J.S., 2006. Electrically conductive bacterial nanowires produced by *Shewanella oneidensis* strain MR-1 and other microorganisms. PNAS 103, 11358-11363.

Green, V.S., Dao, T.H., Stone, G., Cavigelli, M.A., Baumhardt, R.L., Devine, T.E., 2007. Biotactive phosphorus in simulated runoff from a phosphorus-enriched soil under two forage management systems. Soil Science 172, 721-732.

Hassett, J.J., Banwart, W.L., 1992. Soils & Their Environment. Prentice-Hall, Inc., Englewood Cliffs, NJ, pp. 16-19, 276-282.

Kleinman, P.J.A., Needelman, B.A., Sharpley, A.N., McDowell, R.W., 2003. Using soil phosphorus profile data to assess phosphorus leaching potentialin manured soils. Soil Science Society of America Journal 67, 215-224.

Kuo, S., 1996. Phosphorus. In: Sparks, D.L. (Ed.), Methods of Soil Analysis: Part 3, Chemical Methods. Soil Science Society of America, Madison, WI, pp. 908-909.

Loeppert, R.L., Inskeep, W.P., 1996. Iron. In: Sparks, D.L. (Ed.), Methods of Soil Analysis: Part 3, Chemical Methods. Soil Science Society of America, Madison, WI, pp. 639-661.

Lovley, D.R., Phillips, E.J.P., 1986. Organic matter mineralization with reduction of ferric ironin anaerobic sediments. Applied and Environmental Microbiology 51, 683-689.

Lovley, D.R., Phillips, E.J.P., 1987. Rapid assay for microbially reducible ferric iron in aquatic sediments. Applied and Environmental Microbiology 53, 1536-1540.

Lovley, D.R., Phillips, E.J.P., 1988. Novel mode of microbial energy metabolism: organic carbon oxidation coupled to dissimilatory reduction of iron or manganese. Applied and Environmental Microbiology 54, 1472-1480.

Lovley, D.R., Phillips, E.J.P., 1991. Reduction of uranium by *Desulfovibrio desulfuricans*. Applied and Environmental Microbiology 58, 850-856.

Lovley, D.R., Coatest, J.D., Blunt-Harris, E.L., Philipps, E.J.P., Woodward, J.C., 1996. Humic substances as electron acceptors for microbial respiration. Nature 382, 445-448.

Lovley, D.R., Blunt-Harris, E.L., 1999. Role of humic-bound iron as an electron transfer agent in dissimilatory fe(III) reduction. Applied and Environmental Microbiology 65, 4252-4254.

Marsili, E., Rollefson, J.B., Baron, D.B., Hozalski, R.M., Bond, D.R., 2008. Microbial biofilmvoltammetry: direct electrochemical characterization of catalytic electrode-attached biofilms. Applied and Environmental Microbiology 74, 7329-7337.

Masscheleyn, P.H., DeLaune, R.K., and Patrick, Jr., W.H., 1990. Transformations of selenium as affected by sediment oxidation-reduction potential and pH. Journal of Environmental Science and Technology 24, 91-97.

Moore, P.A., Reddy, K.R., 1994. Role of Eh and pH on phosphorus geochemistry in sediments of Lake Okeechobee, Florida. Journal of Environmental Quality 23, 955-964.

Murphy, J., Riley, J.P., 1962. A modified single solution method for the determination of phosphate in natural waters. Analitica Chimica Acta 27, 31-36.

Nelson, D.W., Sommers, L.E., 1996. Total Carbon, Organic Carbon, and Organic Matter. In: Sparks, D.L. (Ed.), Methods of Soil Analysis: Part 3, Chemical Methods. Soil Science Society of America, Madison, WI, pp. 1004-1005.

Patrick, W.K., Khalid, R.A., 1974. Phosphate release and sorption by soils and sediments: effect of aerobic and anaerobic conditions. Science 186, 53-55.

Patrick, W.H., Gambrell, R.P., Faulkner, S.P., 1996. Redox Measurements of Soils. In: Sparks, D.L. (Ed.), Methods of Soil Analysis: Part 3, Chemical Methods. Soil Science Society of America, Madison, WI, pp. 1255-1271.

Peretyazhko, T., Sposito, G., 2005. Iron(III) reduction and phosphorous solubilization in humid tropical forest soils. Geochimica et Cosmochimica Acta 69, 3643-3652.

Pierzynski, G.M., Sims, J.T., Vance, G.F., 2000. Soils and Environmental Quality. CRC Press, Boca Raton, FL, pp. 155-205.

Ponnamperuma, F.N., 1972. The chemistry of submerged soils. Advances in Agronomy 26, 29-96.

Raven, K.P., Hossner, L.R., 1994. Soil phosphorus desorption kinetics and its relationship with plant growth. Soil Science Society of America Journal 58, 416-423.

Reyes, I., Torrent, J., 1997. Citrate-ascorbate as a highly selective extractant for poorly crystalline iron oxides. Soil Science Society of America Journal 61, 1647-1654.

Sawyer, D.T., Sobkowiak, A., Roberts, J.L., 1995. Electrochemistry for Chemists. John Wiley & Sons, Inc., New York, NY.

Schachtman, D.P., Reid, R.J., Ayling, S.M., 1998. Phosphorus uptake by plants: from soil to cell. Plant Physiology 116, 447-453.

Schnitzer, M., Preston, C.M., 1986. Analysis of humic acids by solution and solid-state carbon-13 Nuclear Magnetic Resonance. Soil Science Society of America Journal 50, 326-331.

Sharpley, A.N., Ahuja, L.R., Yamamoto, M., Menzel, R.G., 1981. The kinetics of phosphorus desorption from soil. Soil Science Society of America Journal 45, 493-496.

Shober, A.L., Sims, J.T., 2009**.** Evaluating phosphorus release from biosolids and manure amended soils under anoxic conditions. Journal of Environmental Quality 38, 309-318.

Sibanda, H.M., Young, S.D., 1986. Competitive adsorption of humus acids and phosphate on goethite, gibbsite, and two tropical soils. Journal of Soil Science 37, 197–204.

Smith, D.R., Owens, P.R., Leytem, A.B., Warnemuende, E.A., 2007. Nutrient losses from manure and fertilizer applications as impacted by time to first runoff event. Environmental Pollution 147, 131-137.

Swift, R.S., 1996. Organic matter characterization. In: Sparks, D.L. (Ed.), Methods of Soil Analysis: Part 3, Chemical Methods. Soil Science Society of America, Madison, WI, pp. 1011-1069.

Tan, K.H., 1996. Soil Sampling, Preparation and Analysis. Marcel Dekker, Inc., New York, NY, pp. 169-170.

Wafer, C.C., Richards, J.B., Osmond, D.L., 2004. Construction of platinum-tipped redox probes for determining soil redox potential. Journal of Environmental Quality 33, 2375-2379.

Whitton, B.A., Grainger, S.L.J., Hawley, G.R.W., Simon, J.W., 1991. Cell-bound and extracellular phosphatase activities of cyanobacterial isolates. Microbial Ecology 21, 85-98.

Willet, I.R., Higgins, M.L., 1978. Phosphate sorption by reduced and reoxidized rice soils. Australian Journal of Soil Research 16, 319-326.

Wolf, D.C., Dao, T.H., Scott, H.D., Lavy, T.L., 1989. Influence of sterilization methods on selected soil microbiological, physical, and chemical properties. Journal of Environmental Quality 18, 39-44.

Wright, E.L., Delp,C.H., Sponaugle, K., Cole, C., Ammons, J.T., Gorman, J., Childs, F.D., 1982. Soil Survey of Marion and Monongalia Counties, West Virginia. USDA, Soil Conservation Service.

Xie, L., Shang, C., 2005. Role of humic acid and quinone model compounds in bromated reduction by zerovalent iron. Environmental Science and Technology 39, 1092-1100.

Zhang, Y., Lin, X., Werner, W., 2003. The effect of soil flooding on the transformation of Fe oxides and the adsorption/desorption behavior of phosphate. Journal of Plant Nutrition and Soil Science 166, 68-75.

Zhang, H., Schroder, J.L., Fuhrman, J.K., Basta, N.T., Storm, D.E., Payton, M.E., 2005. Path and multiple regression analyses of phosphorus sorption capacity. Soil Science Society of America Journal 69, 96-106.

Figures and Tables

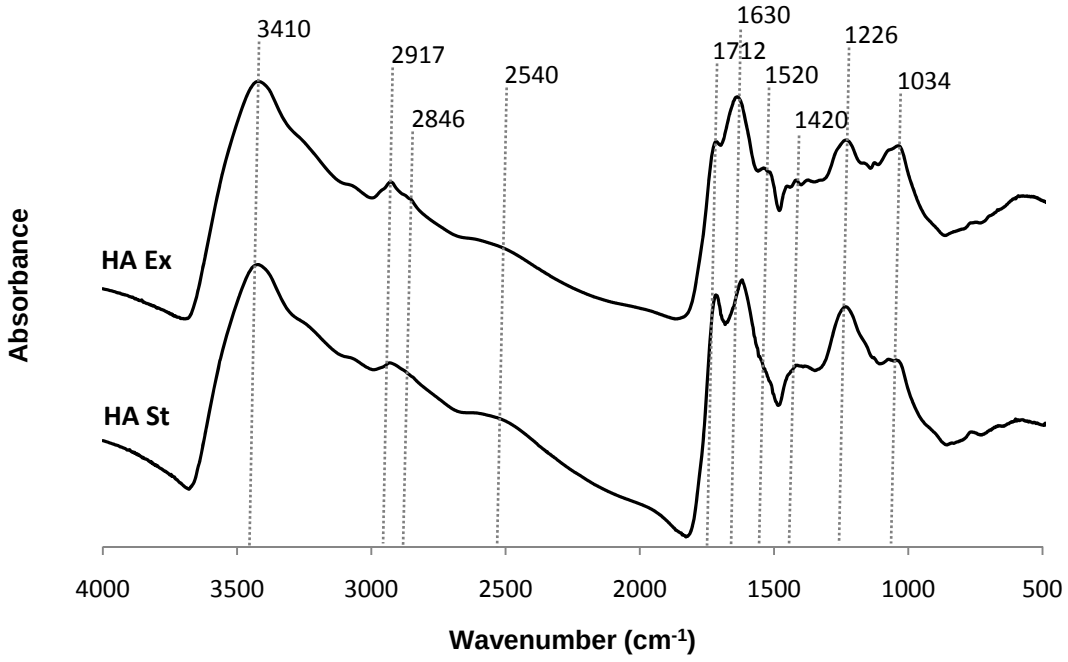

Figure 2. 1 FT-IR spectra of HA samples. (HA Ex) humic acid extracted from soil. (HA St) IHSS Elliott Soil humic acid standard.

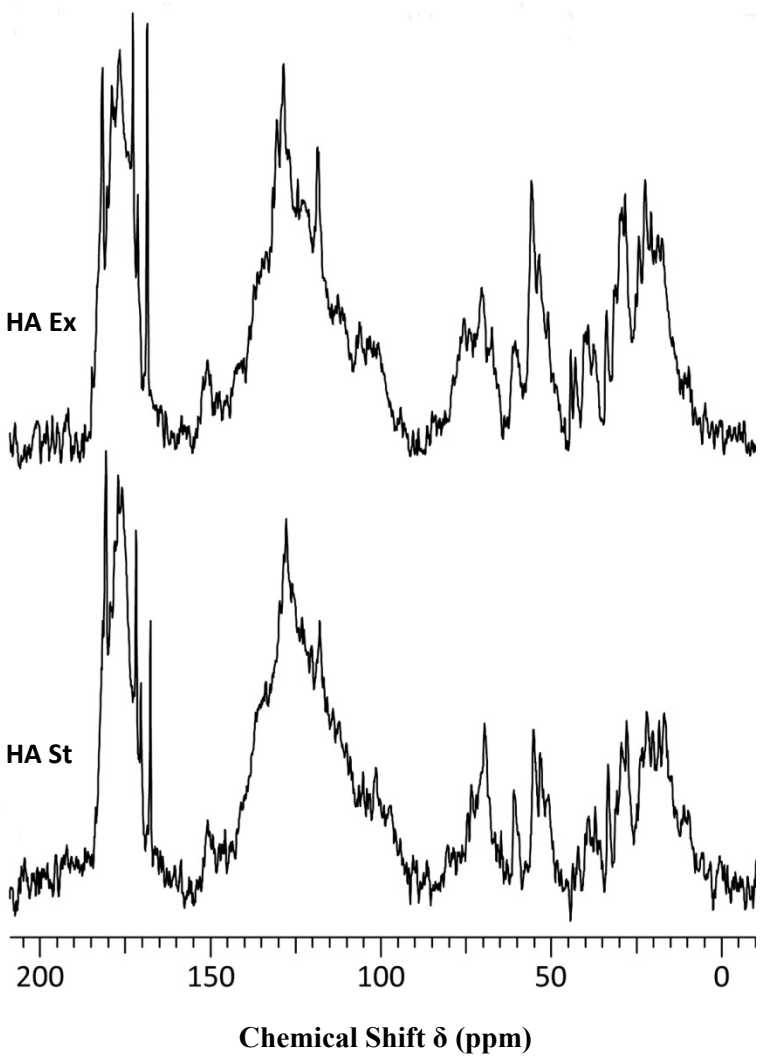

Figure 2. 2 ^{13}C-NMR spectra of HA samples. (HA Ex) humic acid extracted from soil. (HA St) IHSS Elliott Soil humic acid standard.

a

HA Ex

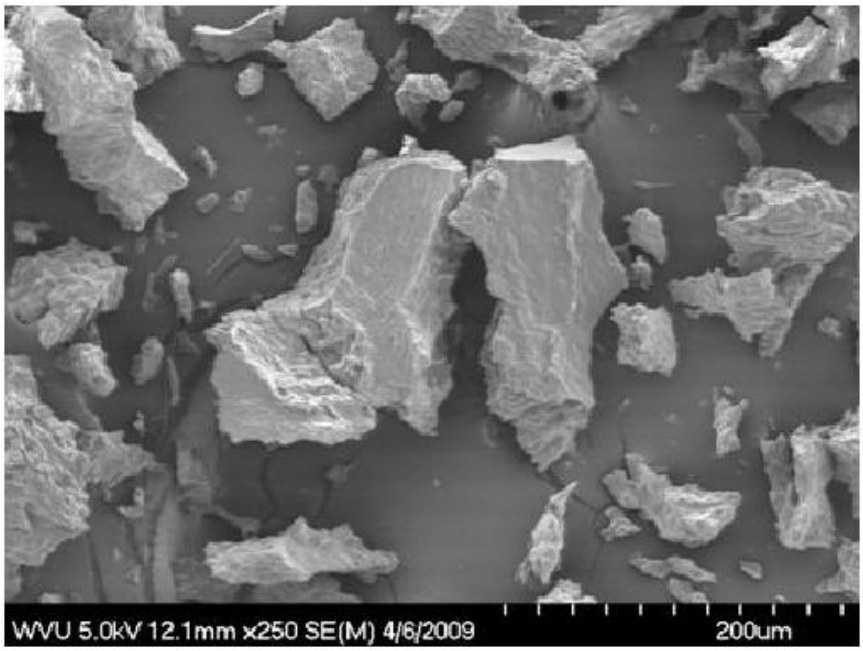
WVU 5.0kV 12.1mm x250 SE(M) 4/6/2009
200um

b

HA St

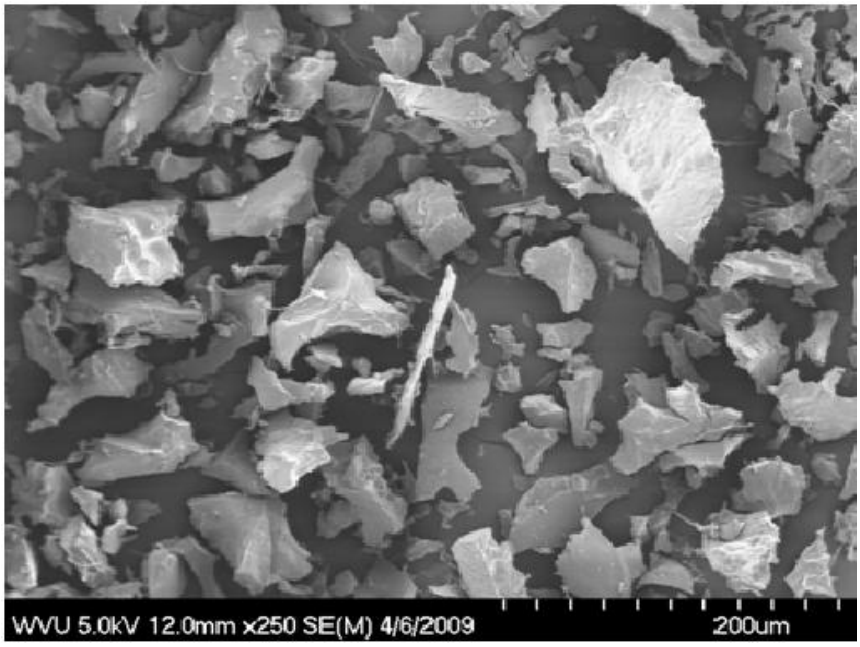
WVU 5.0kV 12.0mm x250 SE(M) 4/6/2009
200um

c

HA Ex

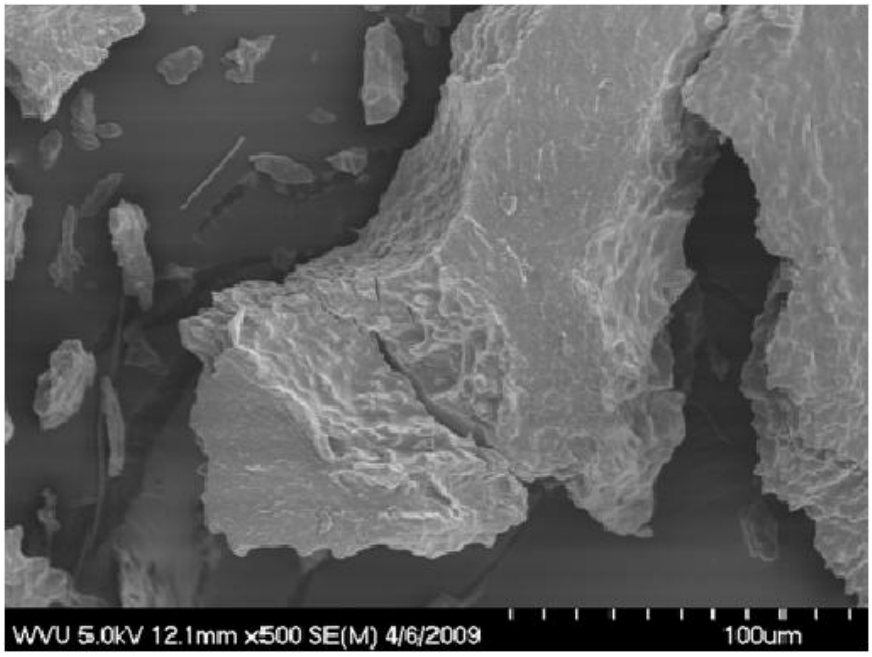
WVU 5.0kV 12.1mm x500 SE(M) 4/6/2009
100um

d

HA St

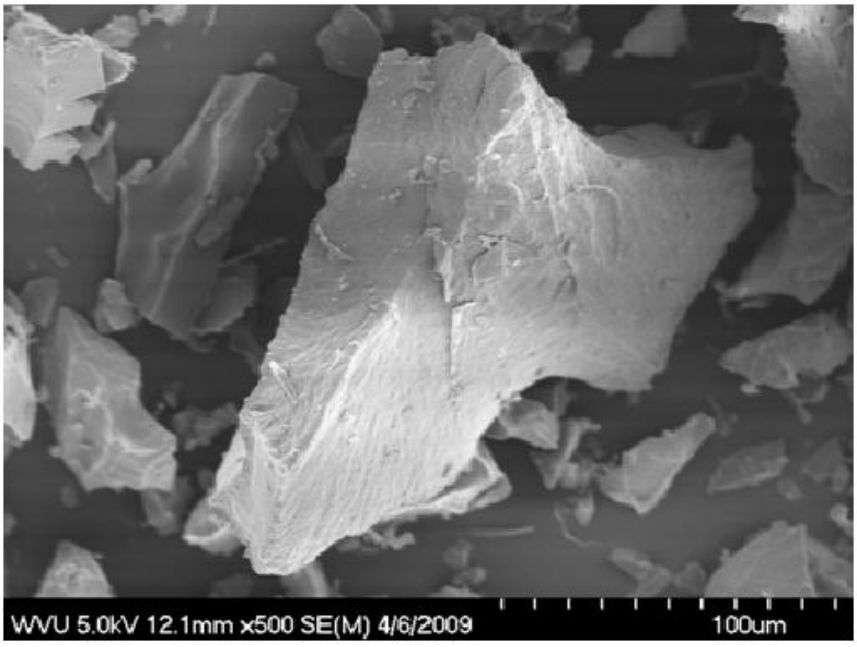
WVU 5.0kV 12.1mm x500 SE(M) 4/6/2009
100um

e

HA Ex

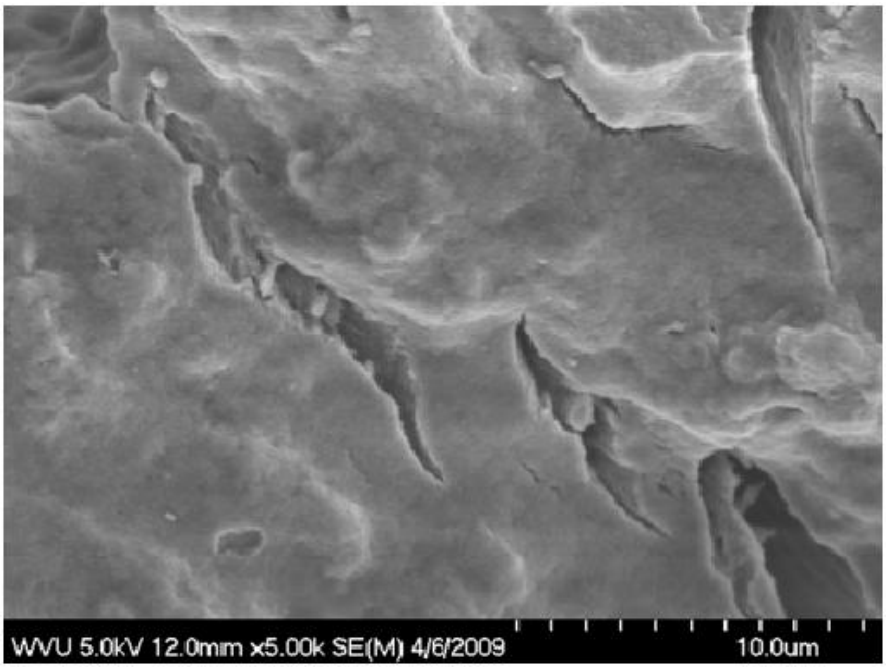
WVU 5.0kV 12.0mm x5.00k SE(M) 4/6/2009
10.0um

f

HA St

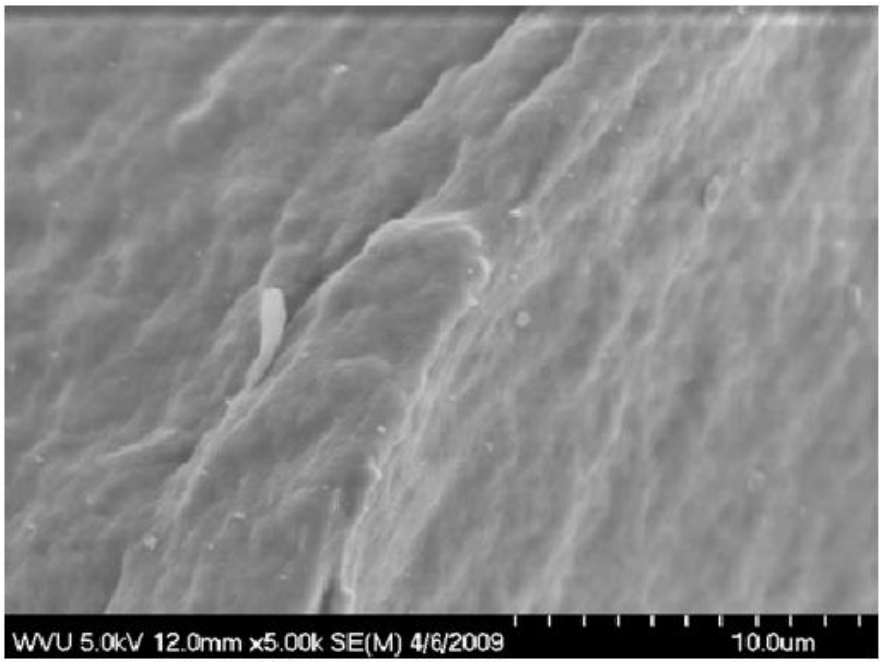
WVU 5.0kV 12.0mm x5.00k SE(M) 4/6/2009
10.0um

g

HA Ex

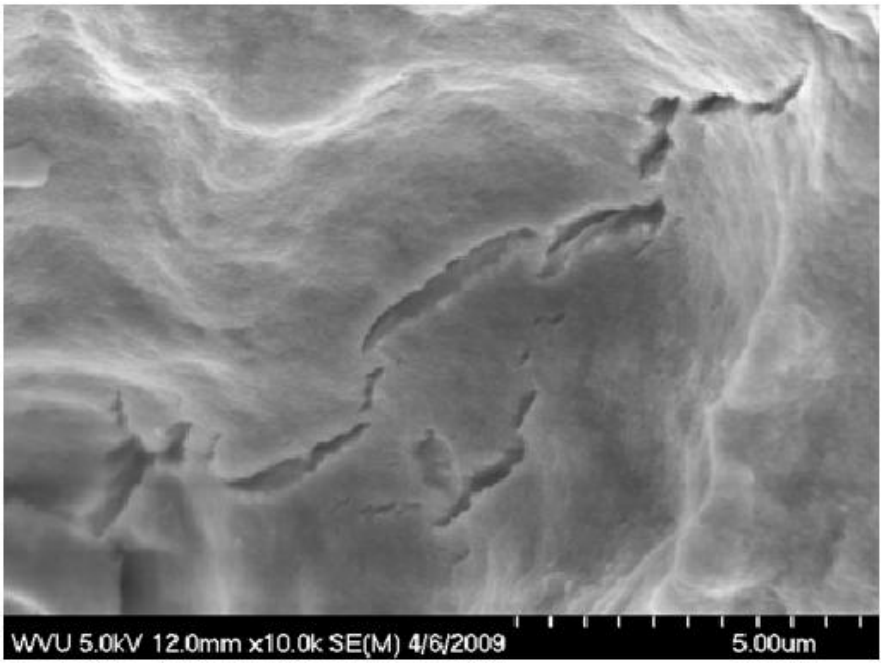

h

HA St

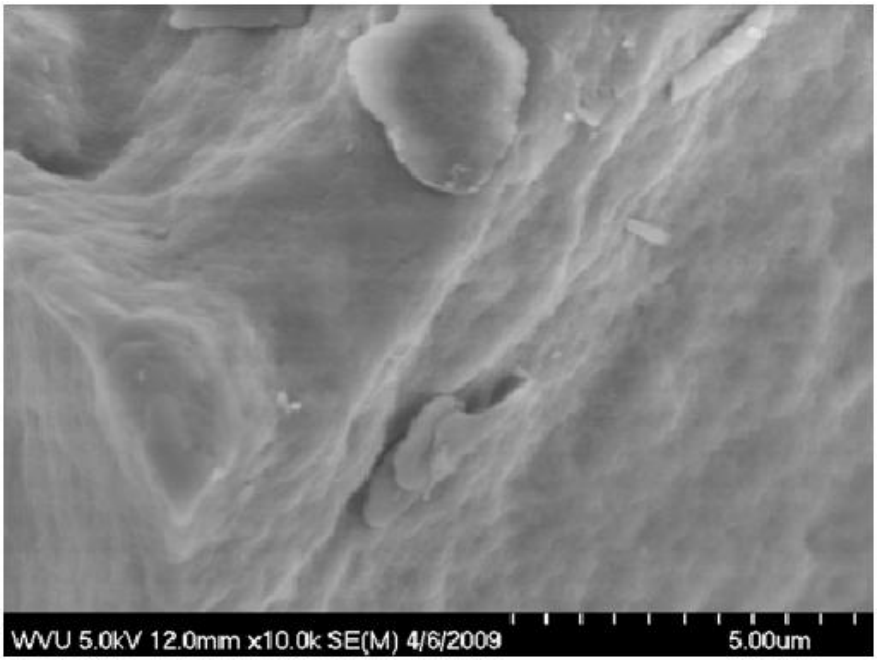

Figure 2. 3 SEM images of HA samples. (a),(c),(e),(g) Extracted humic acid (HA Ex) and (b),(d),(f),(h) IHSS standard humic acid (HA St) at different levels of magnification. White, dashed scale bars at the bottom of images indicate relative length (μm).

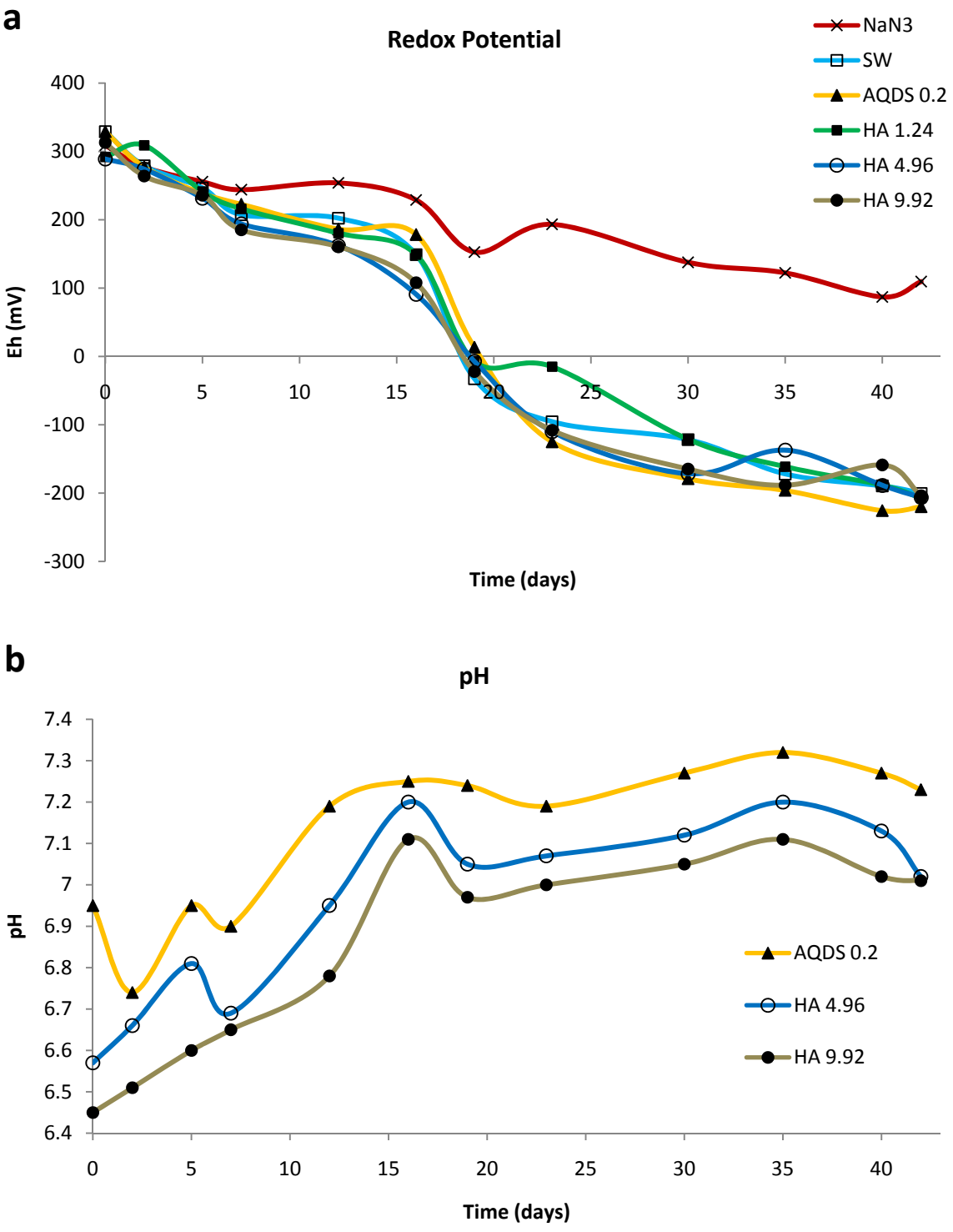

Figure 2. 4 Incubation Eh and pH. (a) Eh fluctuation during the incubation. (b) pH fluctuation of selected treatments during the incuabation.

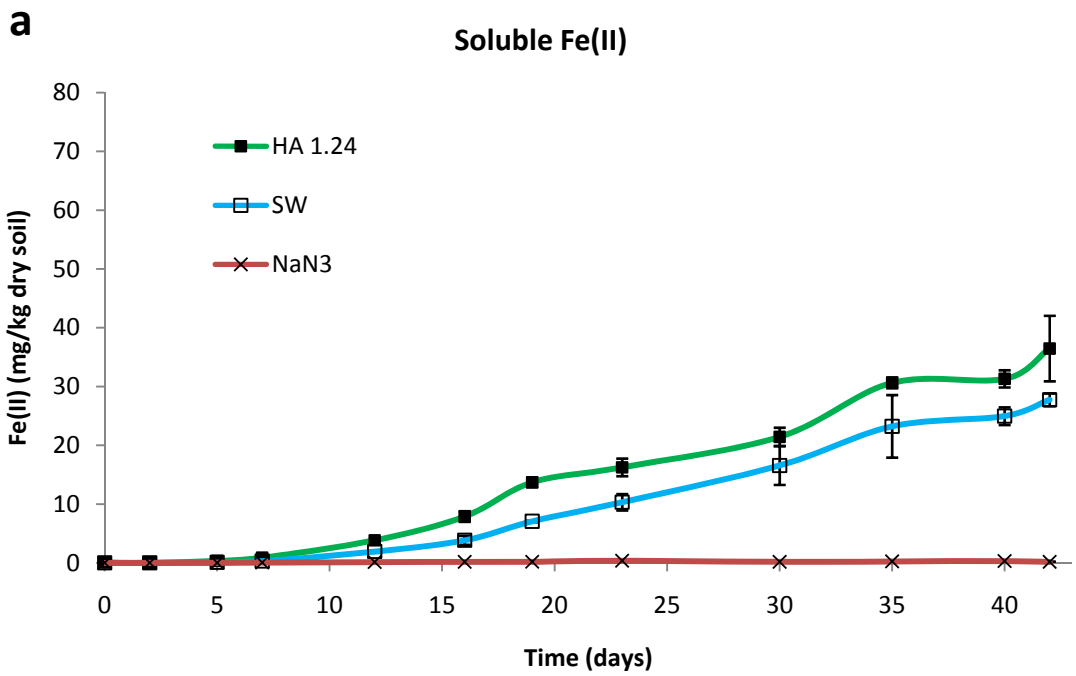

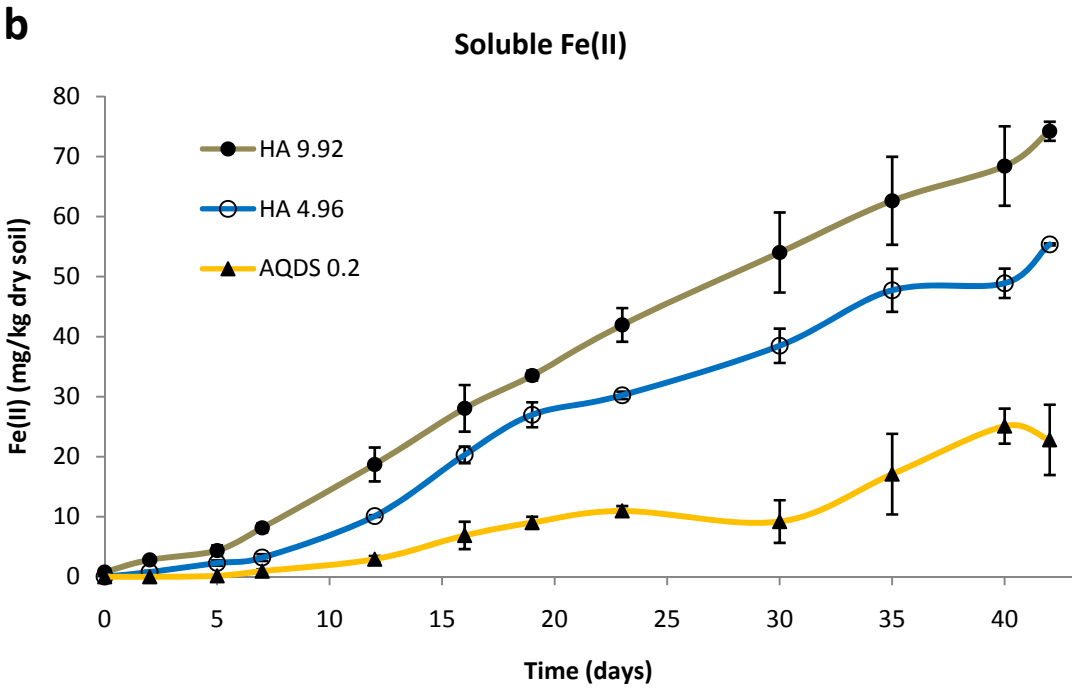

Figure 2. 5 Incubation soluble Fe(II). (a) Soluble Fe(II) during the incubation for NaN_3, SW, and HA 1.24 treatments. (b) Soluble Fe(II) during the incubation for AQDS 0.2, HA 4.96, and HA 9.92 treatments. Data are means ± one standard deviation.

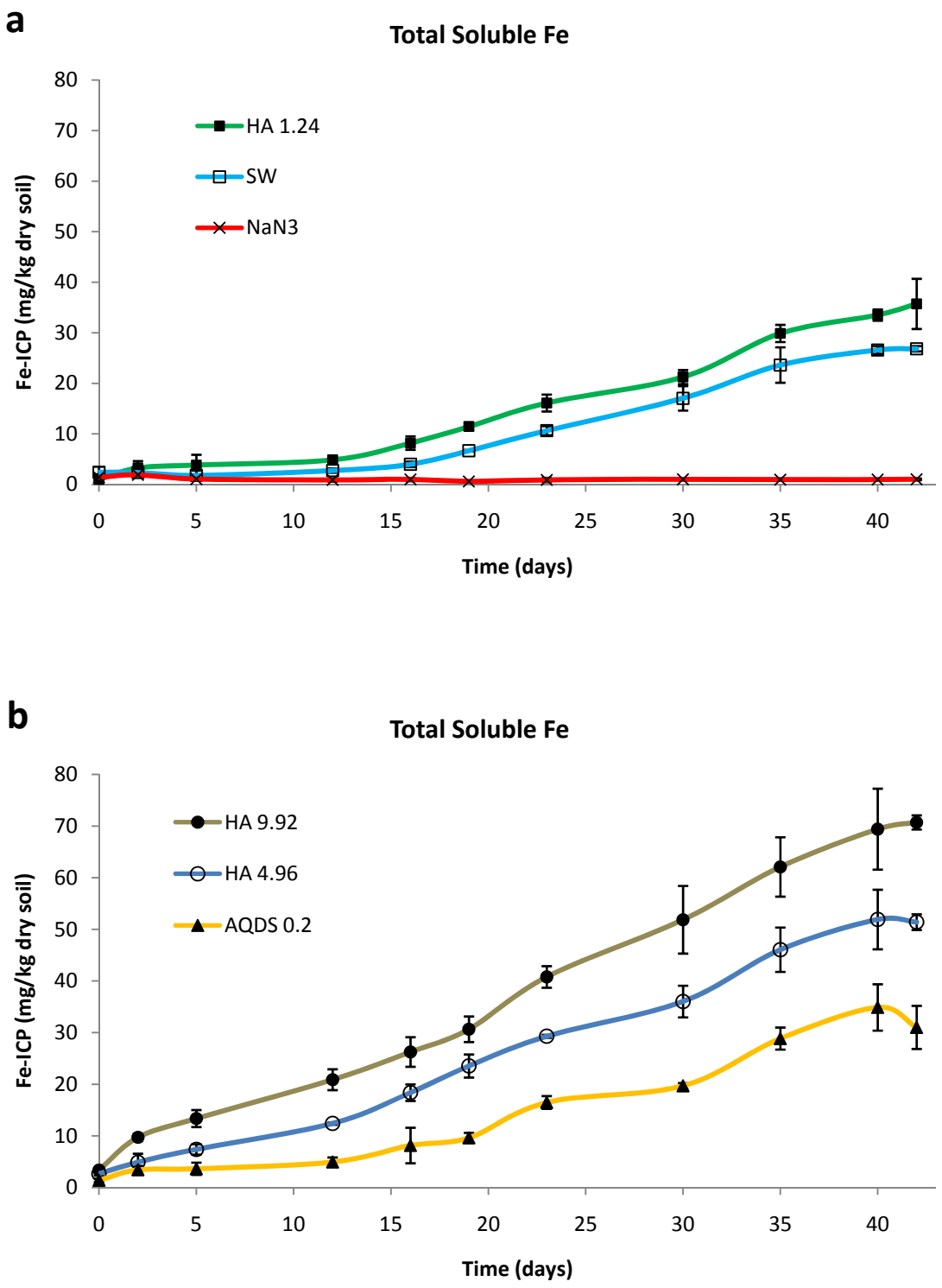

Figure 2. 6 Incubation total Fe. (a) Total soluble Fe during the incubation for NaN_3, SW, and HA 1.24 treatments. (b) Total soluble Fe during the incubation for AQDS 0.2, HA 4.96, and HA 9.92 treatments. Data are means ± one standard deviation. Day 7 Fe-ICP concentrations were not determined.

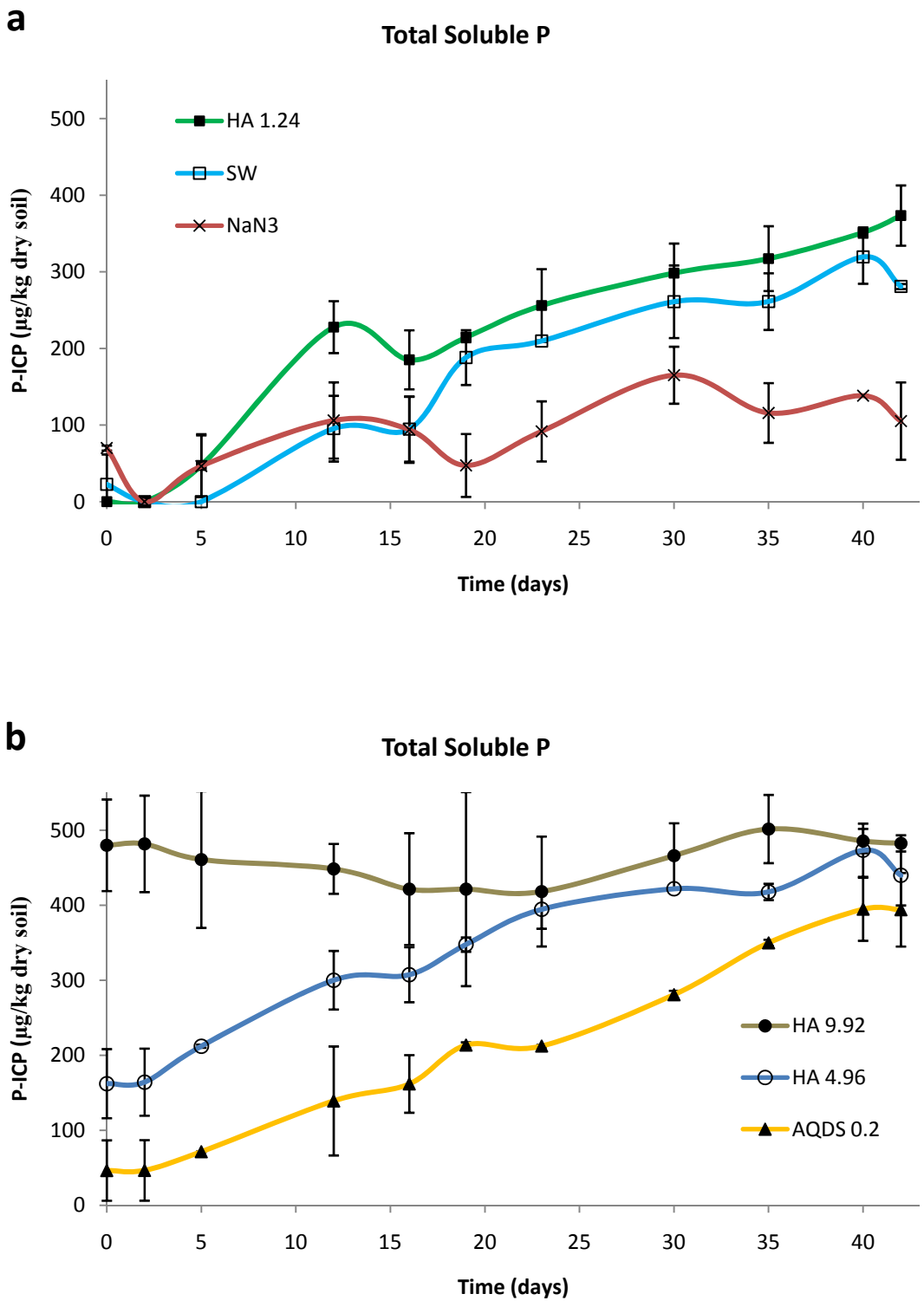

Figure 2. 7 Incubation total P. (a) Total soluble P during the incubation for NaN_3, SW, and HA 1.24 treatments. (b) Total soluble P during the incubation for AQDS 0.2, HA 4.96, and HA 9.92 treatments. Data are means ± one standard deviation. Day 7 P-ICP concentrations were not determined.

a

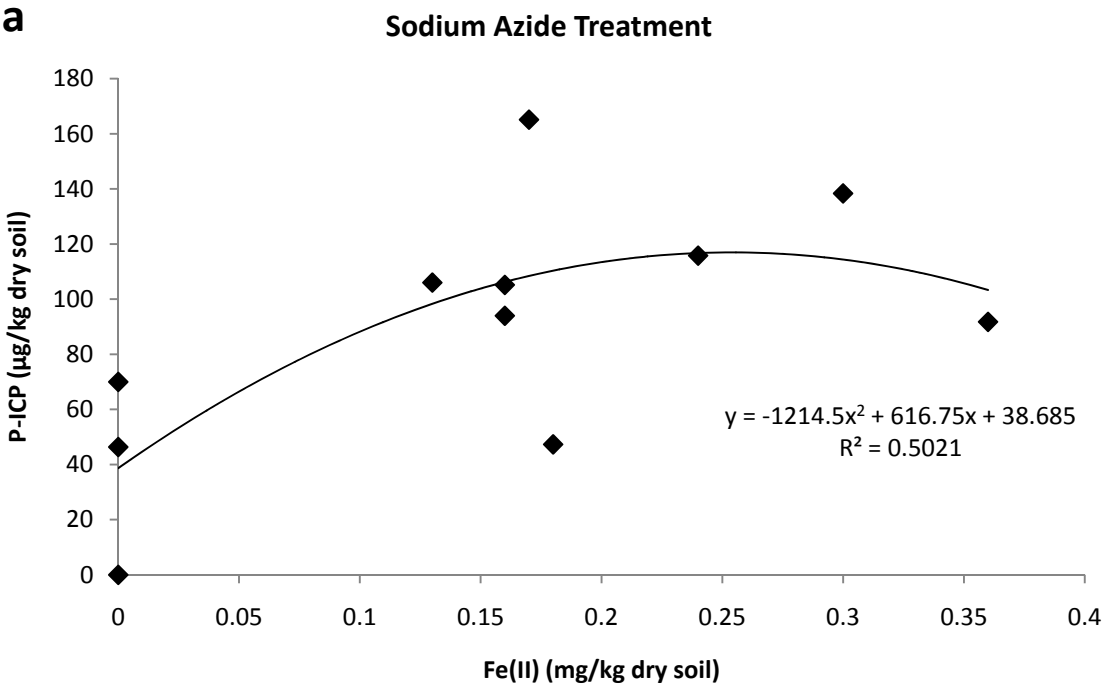
Sodium Azide Treatment
P-ICP (µg/kg dry soil)
180
160
140
120
100
80
60
40
20
0
0
0.05
0.1
0.15
0.2
0.25
0.3
0.35
0.4
Fe(II) (mg/kg dry soil)
y = -1214.5x² + 616.75x + 38.685
R² = 0.5021

b

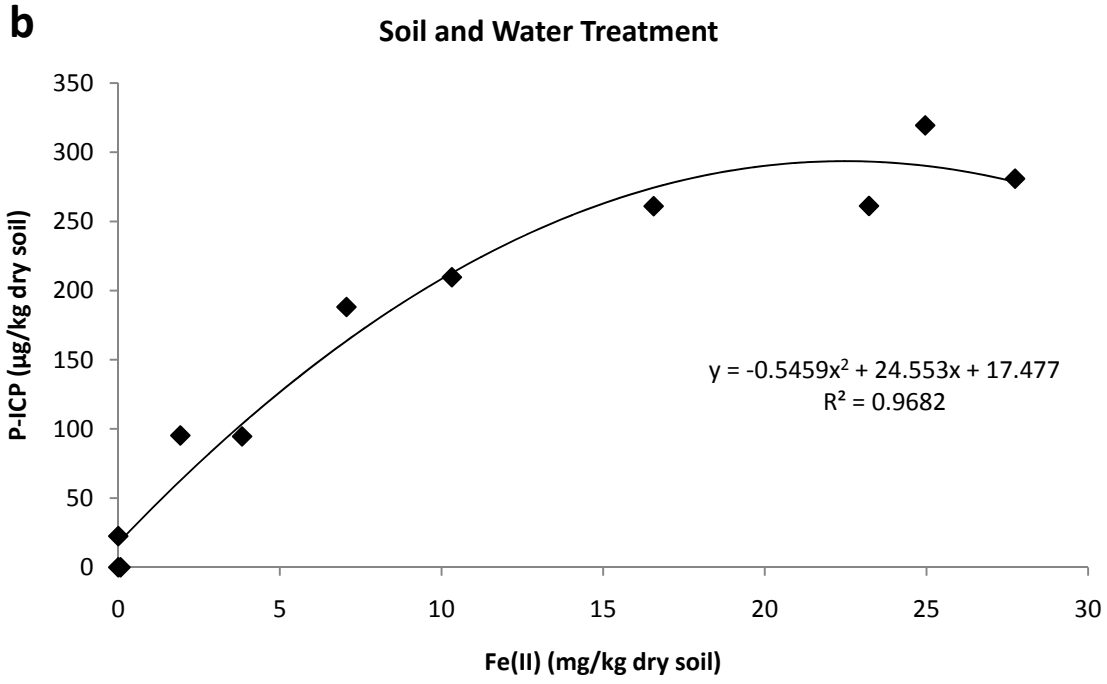
Soil and Water Treatment
P-ICP (µg/kg dry soil)
350
300
250
200
150
100
50
0
0
5
10
15
20
25
30
Fe(II) (mg/kg dry soil)
y = -0.5459x² + 24.553x + 17.477
R² = 0.9682

c

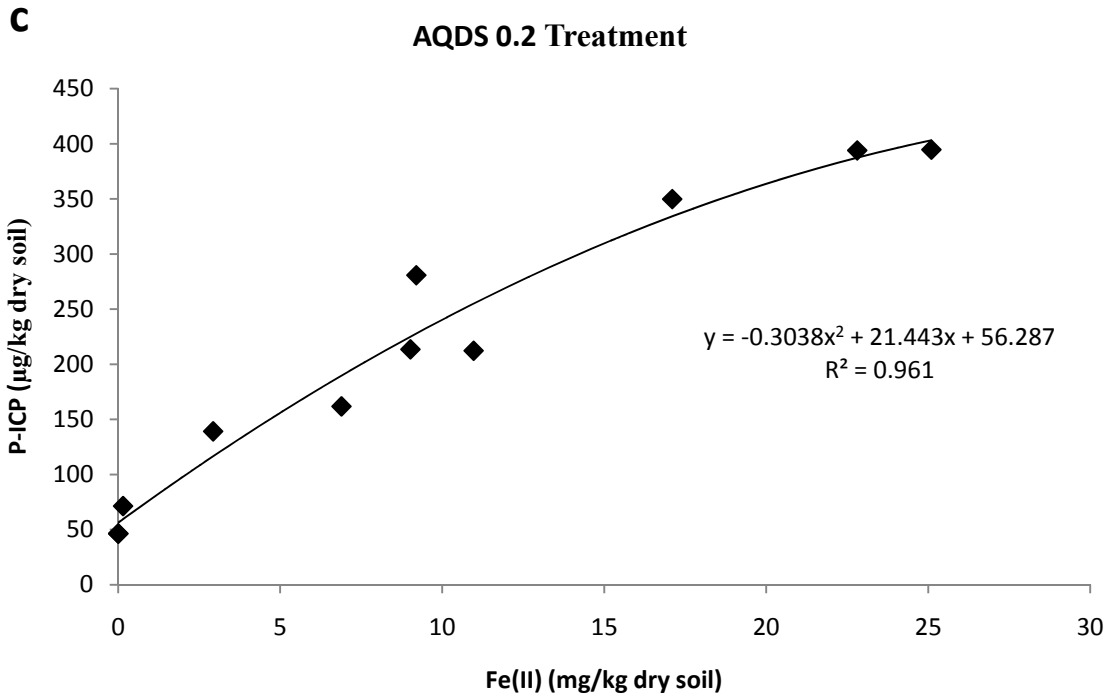
AQDS 0.2 Treatment
P-ICP (µg/kg dry soil)
Fe(II) (mg/kg dry soil)
y = -0.3038x² + 21.443x + 56.287
R² = 0.961
0
50
100
150
200
250
300
350
400
450
0
5
10
15
20
25
30

d

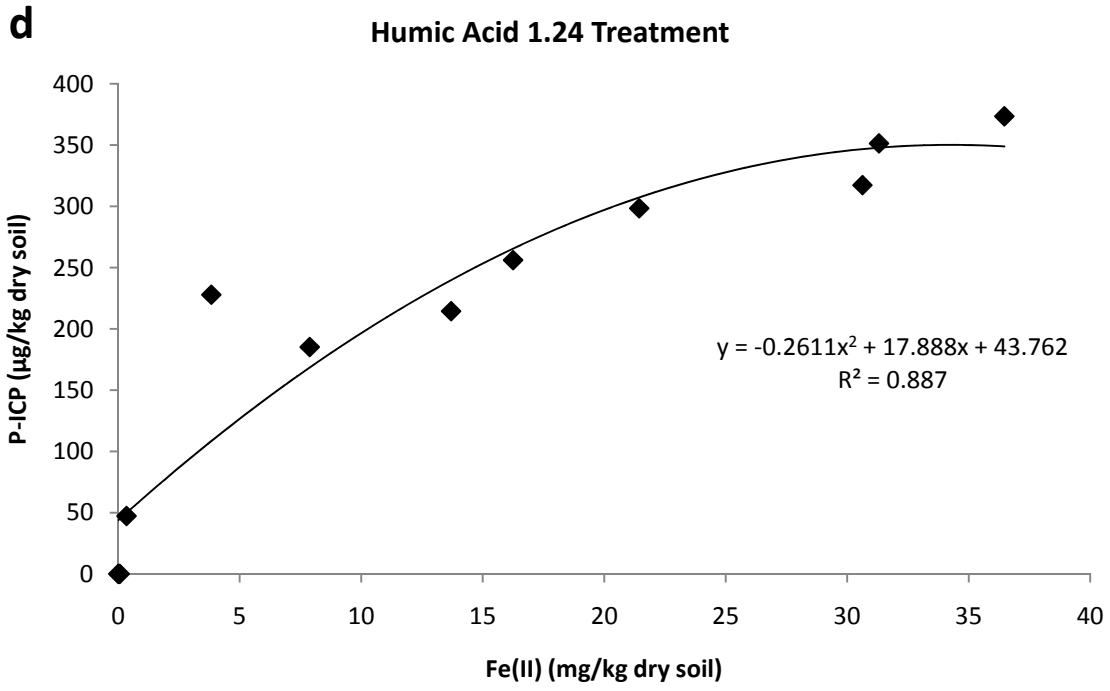
Humic Acid 1.24 Treatment
P-ICP (µg/kg dry soil)
Fe(II) (mg/kg dry soil)
y = -0.2611x² + 17.888x + 43.762
R² = 0.887
0
50
100
150
200
250
300
350
400
0
5
10
15
20
25
30
35
40

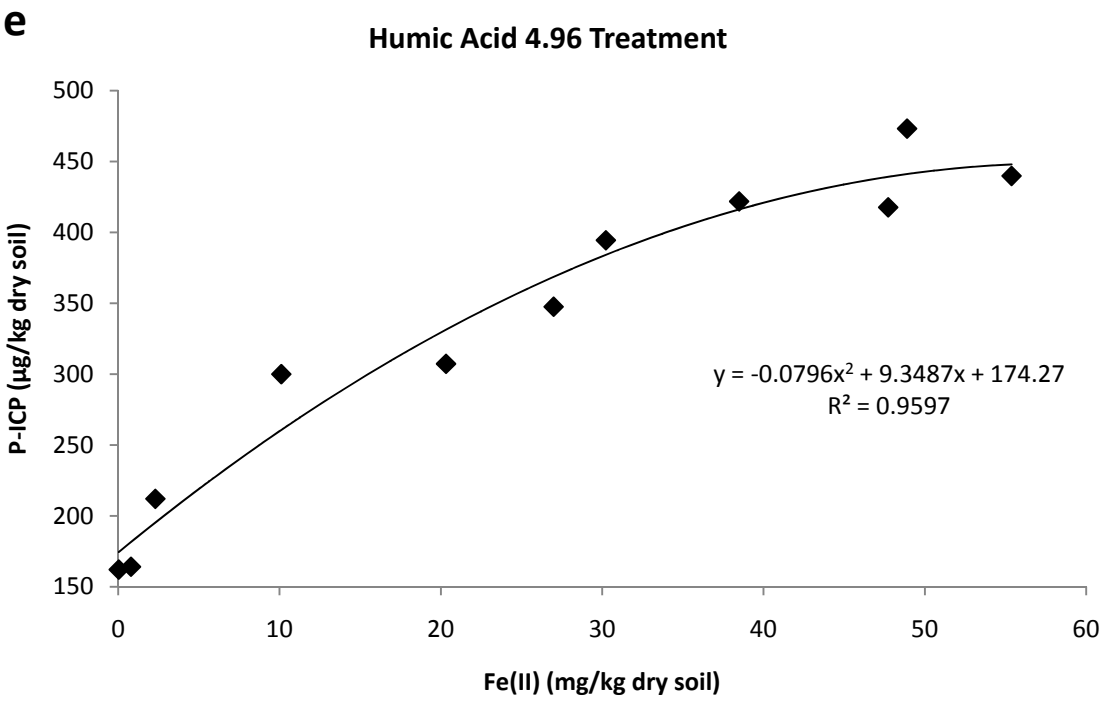

Figure 2. 8 Total P vs. soluble Fe(II). (a) NaN_3 treatment; (b) SW treatment; (c) AQDS 0.2 treatment; (d) HA 1.24 treatment; (e) HA 4.96 treatment. All data have been fit with a 2nd order polynomial trendline.

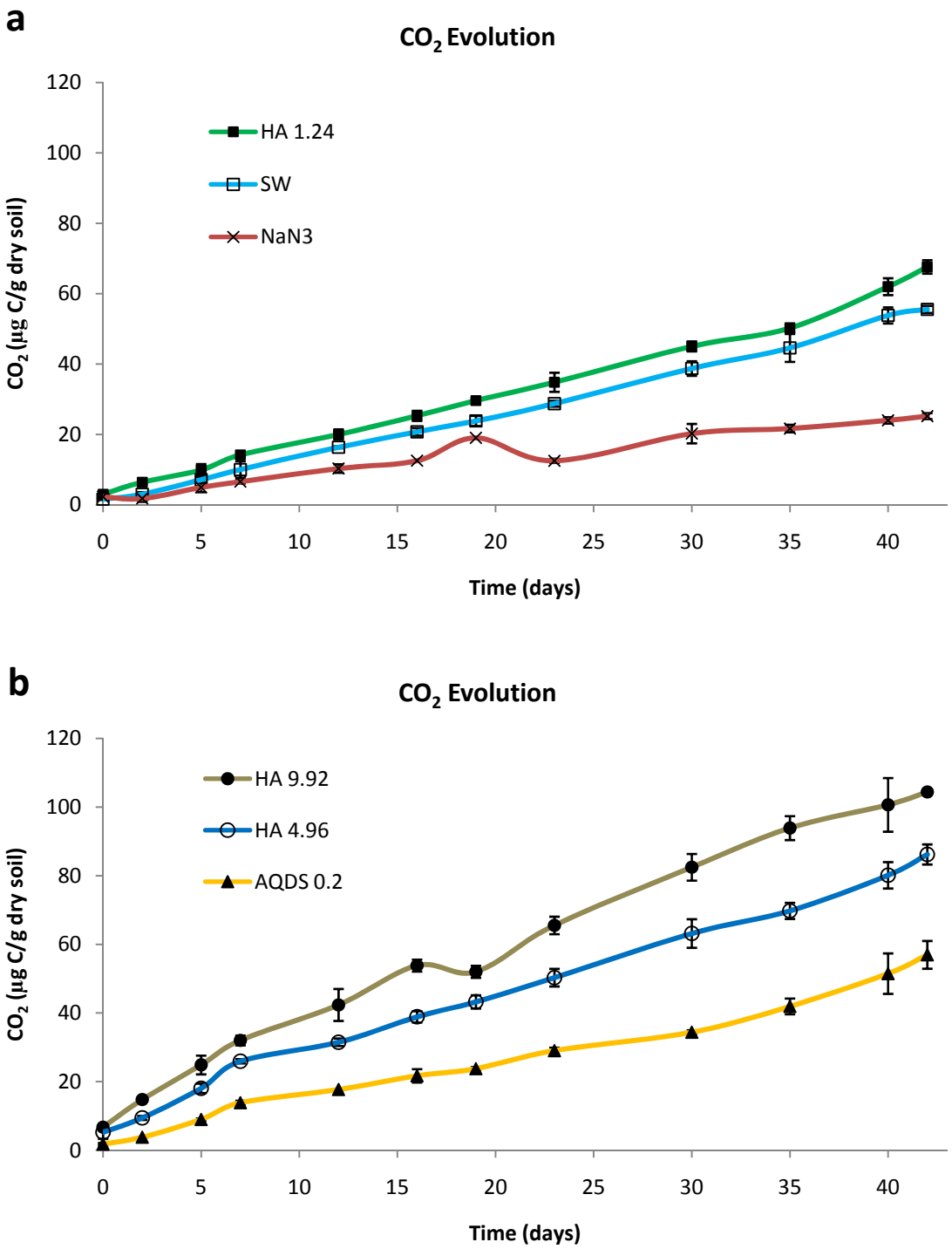

Figure 2. 9 Incubation CO_2 evolution. (a) CO_2 Evolution during the incubation for NaN_3, SW, and HA 1.24 treatments. (b) CO_2 Evolution during the incubation for AQDS 0.2, HA 4.96, and HA 9.92 treatments. Data are means ± one standard deviation.

a

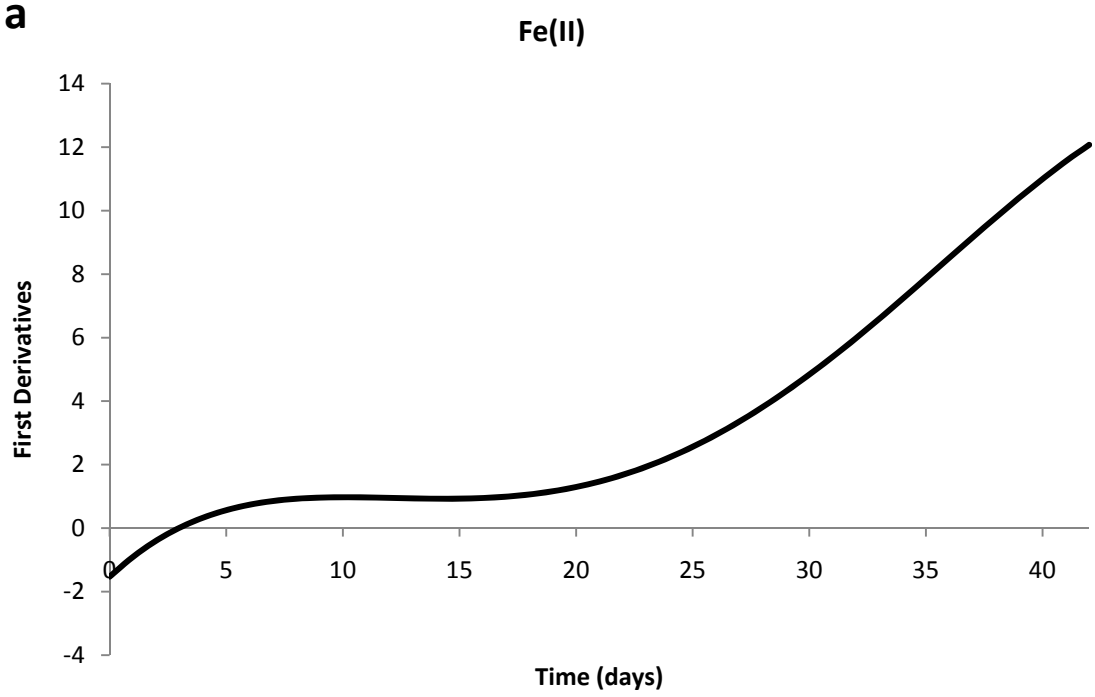
Fe(II)
First Derivatives
14
12
10
8
6
4
2
0
-2
-4
0
5
10
15
20
25
30
35
40
Time (days)

b

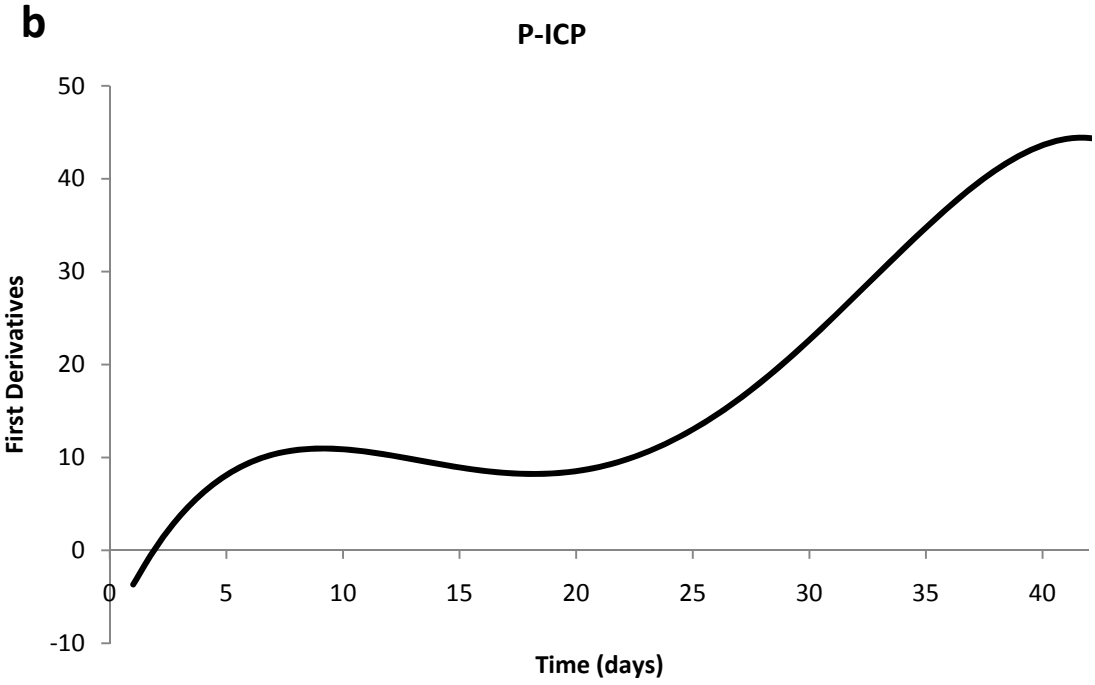
P-ICP
First Derivatives
50
40
30
20
10
0
-10
0
5
10
15
20
25
30
35
40
Time (days)

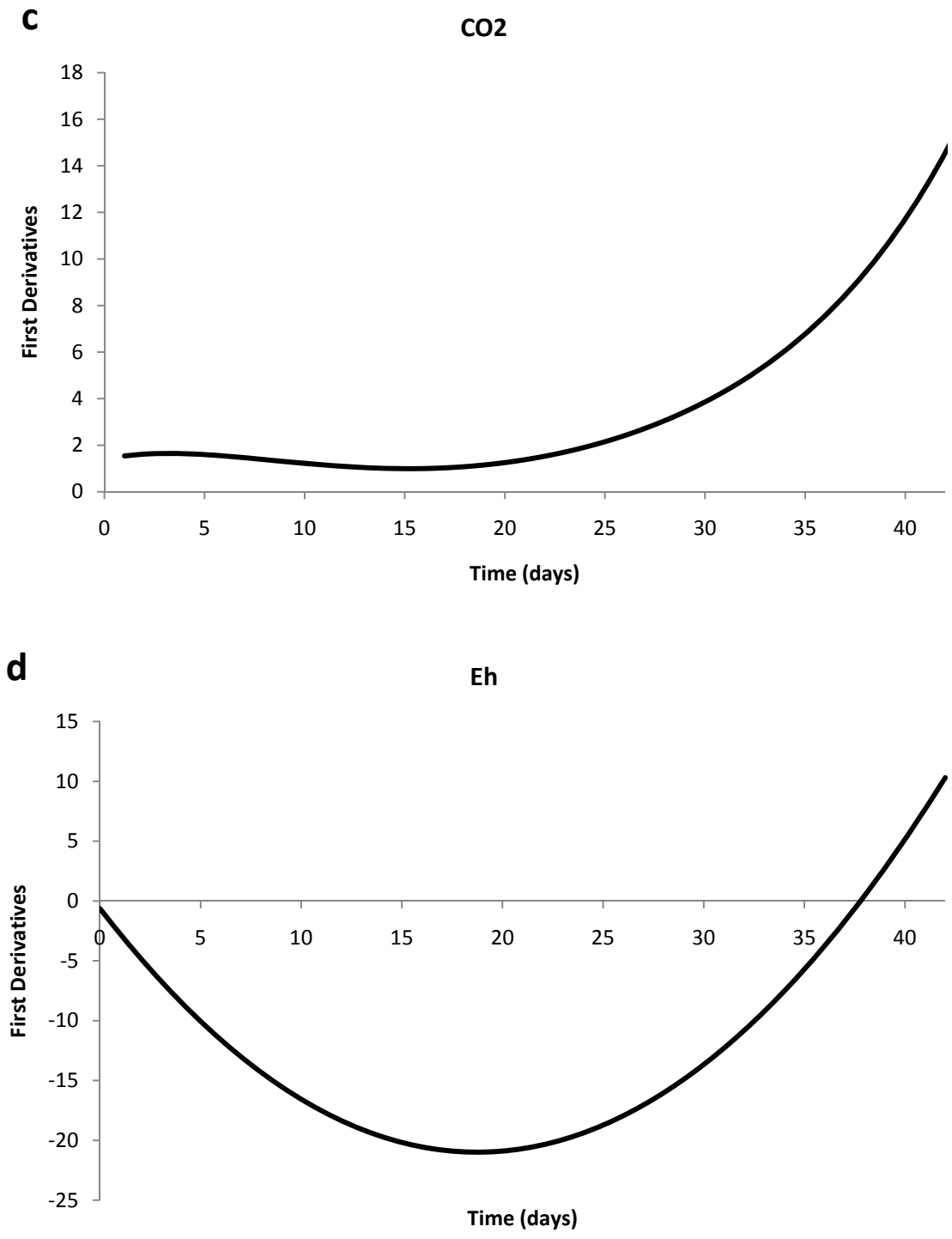

Figure 2. 10 First derivative analysis of AQDS parameters. (a) Soluble Fe(II); (b) total soluble P; (c) CO_2; (d) Eh. Data are 1st derivatives of a best fit polynomial trendline, which represents a corresponding chemical parameter, plotted against incubation time. Day 20 marked a simultaneous shift toward a more positive rate for Fe(II), P-ICP, and CO_2 (related to day 20 Eh) during the incubation.

Table 2. 1

Soil Chemical and Physical Characterizations. Values equal ± one standard deviation. (*)Estimated value; (TOM) total organic matter; (TROM) total residual organic matter; (TLOM) total labile organic matter; (TOC) total organic carbon; (TROC) total residual organic carbon; (TLOC)total labile organic carbon; (HA) extracted humic acid; (Fe_{CBD}) citrate-bicarbonate-dithionite extracted Fe; (Fe_{CA}) citrate-ascorbate extracted Fe; (Fe_{TOT}) total Fe; ($Fe_{NH\text{-}HCl}$) hydroxylamine hydrochloride extracted Fe; (P_{CBD}) citrate-bicarbonate-dithionite extracted P; (P_{CA}) citrate-ascorbate extracted P; (P_{TOT}) total P.

Parameter	Value	Replicate(s)
pH	6.67 ± 0.05	3
Particle Size (%)		
Sand	23.53 ± 0.69	3
Silt	46.11 ± 5.91	3
Clay	30.36 ± 5.5	3
Bulk Density (g/cm^3)	0.66 ± 0.03	6
Porosity (%)	54.66 ± 1.99	6
TOM (%)	5.37 ± 0.11	10
TROM (%)	2.56 ± 0.11	10
TLOM (%)	2.81*	
TOC (%)	1.82 ± 0.05	7
TROC (%)	0.54 ± 0.03	7
TLOC (%)	1.28*	
HA (%)	0.74	1
Fe_{CBD} (g/kg)	2.86 ± 0.01	3
Fe_{CA} (g/kg)	2.22 ± 0.01	3
Fe_{TOT} (g/kg)	28.52	3
$Fe_{NH\text{-}HCl}$ (mg/kg)	437.48 ± 5.47	3
P_{CBD} (mg/kg)	78.39 ± 5.31	3
P_{CA} (mg/kg)	51.25 ± 2.02	3
P_{TOT} (mg/kg)	428.67 ± 13.88	3

Table 2. 2

HA Fe and P Characterizations. Values equal ± one standard deviation. (Fe_{TOT}) Total Fe; ($Fe_{NH\text{-}HCl}$) hydroxylamine hydrochloride extracted Fe; (Fe(II)) 0.5 M HCl extracted Fe(II); (P_{TOT}) total P.

Parameter	Value	Replicate(s)
Fe_{TOT} (mg/g)	10.11 ±0.15	3
$Fe_{NH\text{-}HCl}$ (mg/g)	1.24 ±0.02	5
Fe(II) (mg/g)	1.15 ±0.09	5
P_{TOT} (mg/g)	6.47 ±0.1	3

Table 2. 3

Elemental Analysis of HA Samples. Percentages (%) of C,H,N,S, and O for extracted humic acid (HA Ex) and IHSS Elliott Soil standard humic acid (HA St) samples.

Sample	% C	% H	% N	% S	% O
HA Ex	50.42	5.21	4.73	0.43	39.21
HA St	54.11	4.24	4.04	0.23	37.38

Table 2. 4

SAS regression output for incubation Fe(II), Total Fe, Total P, and CO_2. (*) Pr < 0.05.

Parameter	tmt	Pr>F	Adj R^2	β_1	SE β_1
Fe(II)	NaN_3	<0.0001	0.47	0.006	0.0013
	SW	<0.0001	0.92	0.7	0.0364
	AQDS 0.2	<0.0001	0.834	0.571	0.0456
	HA 1.24	<0.0001	0.955	0.895	0.0343
	HA 4.96	<0.0001	0.981	1.356	0.0336
	HA 9.92	<0.0001	0.979	1.798	0.0462
Fe-ICP	NaN_3	0.023	0.142	-0.012	0.0052
	SW	<0.0001	0.895	0.655	0.0396
	AQDS 0.2	<0.0001	0.91	0.792	0.0447
	HA 1.24	<0.0001	0.939	0.839	0.0379
	HA 4.96	<0.0001	0.975	1.227	0.0347
	HA 9.92	<0.0001	0.973	1.614	0.0471
P-ICP	NaN_3	0.0002	0.382	2.39	0.549
	SW	<0.0001	0.888	7.707	0.484
	AQDS 0.2	<0.0001	0.935	8.713	0.412
	HA 1.24	<0.0001	0.876	8.655	0.5752
	HA 4.96	<0.0001	0.878	7.18	0.4721
	HA 9.92	0.5493	-0.02	0.464*	0.7669
CO_2	NaN_3	<0.0001	0.91	0.55	0.0324
	SW	<0.0001	0.992	1.29	0.021
	AQDS 0.2	<0.0001	0.974	1.23	0.036
	HA 1.24	<0.0001	0.989	1.47	0.0271
	HA 4.96	<0.0001	0.991	1.85	0.0317
	HA 9.92	<0.0001	0.983	2.28	0.0531

CHAPTER 3: REDOX POTENTIAL FLUCTUATION IN A TEMPERATE PASTURE SOIL

Abstract

The present study measured the redox potential (Eh) fluctuation in an Appalachian pasture soil (12-15% slope) during the summer and autumn of 2007 and 2008. This Eh data complements a 42 day anaerobic laboratory incubation of the same field soil in which soluble Fe(II), soluble total Fe, soluble total P, CO_2 evolution, and Eh were determined. The purpose for collecting field Eh was to satisfy a condition set forth by the incubation experiment– that sufficient Eh values exist in the field to facilitate bacterial-reduction of Fe(III)/P surface complexes. Stable redox potentials, as low as -200 mV over a 60 day interval, were measured during the field experiment. Seasonal Eh fluctuation in the soil was shown to be related to soil moisture and frequency of precipitation.

Introduction

Redox potential is a governing parameter of all biological and chemical systems in the environment (Madigan et al., 2003). Enzymatic reactions of soil microorganisms and soil mineral transformations under reducing conditions have been extensively studied (Lovley and Phillips, 1988; Lovley et al., 1996; Benz et al., 1998; Zachara et al., 1998; Zhang et al., 2003; Marsili et al., 2008). In particular, new models have been proposed to explain how tropical soils, classically thought to be continuously oxidized or display minor seasonal redox changes, can greatly influence Fe and P cycling through microbial reduction of Fe(III) oxyhydroxides (Peretyazhco and Sposito, 2005; Chacon et al., 2006).

The reduction of metals in the field by native bacteria is important from both a microbiological and agronomic standpoint. Specifically, the reduction of Fe oxyhydroxides in the soil can release adsorbed P into solution. In soils of low fertility, even small amounts of P solubilized from Fe(III)-reduction could be critical for plant development (Peretyazhco and Sposito, 2005).

Most research with Fe(III) reducing bacteria has been conducted outside of the natural system (Kostka and Nealson, 1998). Consequently, this data cannot be directly applied to the field. However, several parameters have the potential to link laboratory experiments to naturally occurring anaerobic-processes in the environment. Examples include pH, temperature, redox potential, native microbial population, and soil-specific electron mediators such as humic acid (HA) (Lovley et al., 1996; Peretyazhco and Sposito 2005).

In this study, Eh was measured in the field to complement a 42 day anaerobic, laboratory incubation of the same field soil (Ch. 2). Soluble Fe(II), soluble total Fe, soluble total P, CO_2

evolution, and Eh were determined during the laboratory incubation. Soluble Fe(II) and total P were shown to increase with decreasing Eh. The purpose for collecting field Eh was to verify that sufficient Eh values exist in the field to facilitate bacterial-reduction of Fe(III)/P surface complexes.

Materials and Methods

Redox data were collected from a slightly concave position on a NW-facing sideslope (12-15% slope) located at the West Virginia University Agronomy Farm in Morgantown, WV (39° 39' 16.70" N, 79° 54' 7.16" W). Dekalb (loamy-skeletal, mixed, mesic Typic Dystrochrepts) and Gilpin (Fine-loamy, mixed, mesic Typic Hapludults) are the dominant residual soils in the area and are generally more acid than the surrounding soils (Wright et al., 1982). The site does not receive frequent (i.e. annual) applications of lime or fertilizer, and does not presently contain grazing livestock. It is topographically variable, including steep slopes and natural drainages, with grass (harvested for livestock forage) serving as the main source of productivity. The vegetation was examined in the field to identify potential indicator species for wet and/or poorly drained soil. A species of the *Cyperaceae* family was observed (similar to field sedges), but exact identification was not possible due to lack of maturity.

Platinum redox electrodes used to measure field Eh values were constructed using the design philosophies of Patrick et al. (1996) and Wafer et al. (2004) with modifications (Figure 3. 1). Each of nine electrodes was assembled by first heating the end of a 30 cm length x 10 mm diameter glass tube with a propane torch. When the heated end constricted to just greater than 1.0 mm in diameter, 4.0 mm of a 15 mm length x 1.0 mm diameter solid platinum wire (Sigma-Aldrich, St Louis, MO, USA) (that had been cleaned with sandpaper) was inserted into the malleable opening. This end was carefully heated again, with slow rotation along the length of

the glass tube, until 4.0 mm of glass had sealed against the platinum wire. The platinum inside the electrode was 4.0 mm long, and the platinum exposed on the outside was 7 mm long.

Separately, a 1.6 mm diameter x 3 mm deep hole was drilled into the end of a 3.18 mm diameter low-fume-bare bronze brazing rod (LFBB) (Radnor Welding Products, Radnor, PA, USA) cut to a length of 37.5 cm. The rod was vertically clamped to a wooden surface, and the drilled end was carefully heated with a propane torch and filled with 1.5 mm diameter electrical rosin core solder (Lenox, East Longmeadow, MA, USA). After the solder had filled the hole and had cooled, it was indirectly heated again with the torch. The glass tube/platinum assembly was then quickly lowered over the rod, so that the suspended platinum inside the tube seated into the molten solder. Sufficient time was allowed to pass for the solder to cool, and the strength of the junction was checked.

A piece of adhesive-lined polyolefin, 6.35 mm diameter, heat-shrink tubing (McMaster-Carr Supply Co., Atlanta, GA, USA) was then slipped over the bronze rod, so that it covered the length up to the platinum junction, and left 10 mm of bronze exposed at the opposite end. The entire assembly was heated very slowly above the flame of a Bunsen burner until the tubing adhered tightly to the rod. After cooling, shaved red sealing wax (Fisher Scientific, Pittsburgh, PA, USA) was emptied into the glass tube, covering the platinum junction, and was then carefully melted over a Bunsen burner. The open end of the electrode was sealed with a small amount of silicone rubber, which was then covered and sealed with 12.7 mm diameter heat-shrink tubing (McMaster-Carr Supply Co., Atlanta, GA, USA). An overlapping piece of 6.35 mm diameter heat-shrink tubing was then used to cover the seal formed between the 12.7 mm diameter heat-shrink tubing and the insulated bronze rod.

A layer of 5.0 cm wide x 3.18 mm thick rubber insulation tape (Thermwell Products Co., Inc., Mahwah, NJ, USA) was wrapped around ¼ of the glass probe's length, starting near the platinum end, but not completely covering it. The probe was inserted into a 31 cm length x 1.27 cm diameter PVC pipe. Silicone rubber was applied to the bronze-end of the pipe, and a drilled PVC cap was slipped over the bronze rod. The top of the cap was also sealed with silicone rubber. The glass/platinum junction at the opposite end of the probe was left exposed by 7 mm. Loctite Marine epoxy (Henkel, Hagen, Germany) was used to seal the end of the pvc pipe against the exposed glass/platinum junction. The platinum wire did not come in contact with the epoxy.

Reference electrodes (Ag/AgCl) were assembled using a method similar to that of Sawyer et al. (1995). A 4 mm diameter Vycor porous-glass frit (#G0100) (Princeton Applied Research, Oak Ridge, TN, USA) was attached to the end of a 15 cm length x 4 mm diameter Pyrex glass tube (Fisher Scientific) by heat-shrink Teflon tubing (Princeton Applied Research, # G0100). The glass tube was then filled with a saturated KCl solution and an 11 cm length of 0.5 mm diameter silver wire (Aldrich). Teflon tubing was used as a cap, with 4 mm of silver wire left exposed for electrical contact. The silver wire was electroplated with AgCl by using a counter platinum electrode in circuit with a 9V battery and a 1MΩ resistor (RadioShack, Fort Worth, TX, USA).

An auto-range digital multimeter (RadioShack, Fort Worth, TX, USA), connected to a platinum electrode and a AgCl reference electrode, was used to measure Eh (mV). Probe function was checked by two standard solutions made up of a small fraction of quinhydrone mixed in either a pH 4 or pH 7 buffer (Fisher Scientific) (Patrick et al., 1996; Owens et al., 2005). Probes were first installed at the field site on 8/22/07. Channels were made in the soil with PVC pipe of the same diameter as the platinum electrodes. Probes were then seated into the

soil. The nine electrodes were equally spaced within a 5.0 m^2 area, which centered on a 46 m (down slope) x 23 m (across slope) parameter subsequently used for incubation-soil sampling. Three electrodes were installed at a depth of 10, 15, and 20 cm in a staggered-down slope orientation (Figure 3. 2).

Redox values were recorded, on average, every 3 days from 8/22/07 to 11/28/07. Electrodes were left in the ground through the winter months (December 2007 to February 2008). The second cycle of redox measurements began on 6/04/08 and ended on 10/12/08. Electrodes were removed from the field on 6/05/08 for testing and physical evaluation. Potentials were within ±10 mV of standard solutions. The probes were reinstalled on 6/06/08, and data was recorded, on average, every 2 days after measurements resumed on 6/10/08. Moisture and temperature data were collected from 7/02/08 to 10/12/08. Moisture (%) was measured with a Hydrosense detector (Campbell Scientific, Inc., Logan, UT, USA) and temperature with an HI 9063 microcomputer, k-thermocouple thermometer (Hanna Instruments, Inc., Woonsocket, RI, USA). Continuous precipitation data (daily totals) for the entire experiment were obtained from the Morgantown Municipal Airport, located 2 km from the field site.

Results and Discussion

For the 8/22/07 to 11/28/07 period, Eh values showed oxidizing conditions, which approached +400 to +600 mV by Julian day 274 (Figure 3. 3). It is important to note that a total of 62.23 mm of rainfall was observed between Julian days 231and 233, which could explain why some of the probes displayed an average Eh of -100 mV on Julian day 234 (the first day of 2007 data collection). Beginning on Julian day 294, a series of precipitation events marked a slight, average drop in Eh (approximately +600 mV to +400 mV), which continued until Julian day 332.

It is important to note that little precipitation was observed between Julian days 234 and 279, explaining the oxidizing conditions during this period.

Redox values stabilized around -200 mV through the entire month of June 2008 (Figure 3. 4), ending by mid August 2008 (Julian day 244 for field redox 7/02/08 to 10/12/08 data) (Figure 3. 5). During the month of May 2008, steady precipitation was observed for 20 out of 31 days including 27.18 mm of rainfall on Julian day 152, which could explain why some of the deeper probes displayed an average Eh of -200 mV on Julian day 156 (the first day of 2008 data collection). The corresponding precipitation data is reinforced by the soil moisture data. Both of these parameters together explain the Eh fluctuation observed in 2008. The strong correspondence between soil moisture, precipitation, and Eh in 2008 is critical, because it not only supports the precipitation/Eh relationship proposed for 8/22/07 to 11/28/07, but also demonstrates seasonal redox changes that are dependent upon precipitation in the field. Finally, Eh values as low as -200 mV were measured between the upper 10 and 20 cm of soil during the summer of 2008, based upon electrode depth.

Conclusion

The data provide evidence that Eh fluctuation is sufficient to display Fe(III) reduction in the top 10-20 cm of an Appalachian pasture soil on a 12-15% slope. The reduction potential of the Fe(III)/Fe(II) redox couple is approximately +50 mV at pH 7 in soils (Masscheleyn et al., 1990). During this study, stable Eh values as low as -200 mV persisted for approximately 60 days in the summer of 2008. Seasonal Eh fluctuation during the field experiment corresponded strongly to soil moisture and frequency of precipitation.

Reduction of Fe(III) minerals in pasture soils is of agronomic importance. Such mineral transformations have been shown to increase the concentration of plant available P in nutrient

limited environments. Also, any P released by the microbial reduction of Fe minerals, during high frequencies of precipitation, could theoretically add to P concentrations in runoff. Such Eh-dependent processes could be important for both highly fertilized and natural soils. Knowledge of the mechanisms controlling this cycle could allow for more accurate mineral/nutrient modeling and more efficient land-management practices in temperate pasture soils.

References

Benz, M., Schink, B., Brune, A., 1998. Humic acid reduction by *Propionibacterium freudenreichii* and other fermenting bacteria. Applied and Environmental Microbiology 64, 4507-4512.

Chacon, N., Silver, W.L., Dubinsky, E.A., Cusack, D.f., 2006. Iron reduction and soil phosphorus solubilization in humid tropical forests soils: the roles of labile carbon pools and an electron shuttle compound. Biogeochemistry 78, 67-84.

Kostka, J., Nealson, K.H., 1998. Isolation, cultivation and characterization of iron- and manganese- reducing bacteria. In: Burlage, R.S., Atlas, R., Stahl, D., Geesey, G., Sayler, G. (Eds.), Techniques in Microbial Ecology. Oxford University Press, NY, pp. 58-60.

Lovley, D.R., Phillips, E.J.P., 1988. Novel mode of microbial energy metabolism: organic carbon oxidation coupled to dissimilatory reduction of iron or manganese. Applied and Environmental Microbiology 54, 1472-1480.

Lovley, D.R., Coatest, J.D., Blunt-Harris, E.L., Philipps, E.J.P, Woodward, J.C., 1996. Humic substances as electron acceptors for microbial respiration. Nature 382, 445-448.

Madigan, M.T., Martinko, J.M., Parker, J. 2003. Brock Biology of Microorganisms 10th. Prentice Hall, Upper Saddle River, NJ.

Marsili, E., Rollefson, J.B., Baron, D.B., Hozalski, R.M., Bond, D.R., 2008. Microbial biofilm voltammetry: direct electrochemical characterization of catalytic electrode-attached biofilms. Applied and Environmental Microbiology 74, 7329-7337.

Masscheleyn, P.H., DeLaune, R.K., and Patrick, Jr., W.H., 1990. Transformations of selenium as affected by sediment oxidation-reduction potential and pH. Environmental Science and Technology 24, 91-97.

Owens, P.R., Wilding, L.P., Lee, L.M., Herbert, B.E., 2005. Evaluation of platinum electrodes and three electrode potential standards to determine electrode quality. Soil Science Society of America Journal 69, 1541-1550.

Patrick, W.H., Gambrell, R.P., Faulkner, S.P., 1996. Redox Measurements of Soils. In: Sparks, D.L. (Ed.), Methods of Soil Analysis: Part 3, Chemical Methods. Soil Science Society of America, Madison, WI, pp. 1255-1271.

Peretyazhko, T., Sposito, G., 2005. Iron(III) reduction and phosphorous solubilization in humid tropical forest soils. Geochimica et Cosmochimica Acta 69, 3643-3652.

Sawyer, D.T., Sobkowiak, A., Roberts, J.L., 1995. Electrochemistry for Chemists. John Wiley & Sons, Inc., New York, NY.

Wafer, C.C., Richards, J.B., Osmond, D.L., 2004. Construction of platinum-tipped redox probes for determining soil redox potential. Journal of Environmental Quality 33, 2375-2379.

Wright, E.L., Delp,C.H., Sponaugle, K., Cole, C., Ammons, J.T., Gorman, J., Childs, F.D., 1982. Soil Survey of Marion and Monongalia Counties, West Virginia. USDA, Soil Conservation Service.

Zachara, J.M., Fredrickson, J.K., Li, S.M., Kennedy, D.W., Smith, S.C., Gassman, P.L., 1998. Bacterial reduction of crystalline Fe^{3+} oxides in single phase suspensions and subsurfacematerials. American Mineralogist 83, 1426-1443.

Zhang, Y., Lin, X., Werner, W., 2003. The effect of soil flooding on the transformation of Fe oxides and the adsorption/desorption behavior of phosphate. Journal of Plant Nutrition and Soil Science 166, 68-75.

Figures

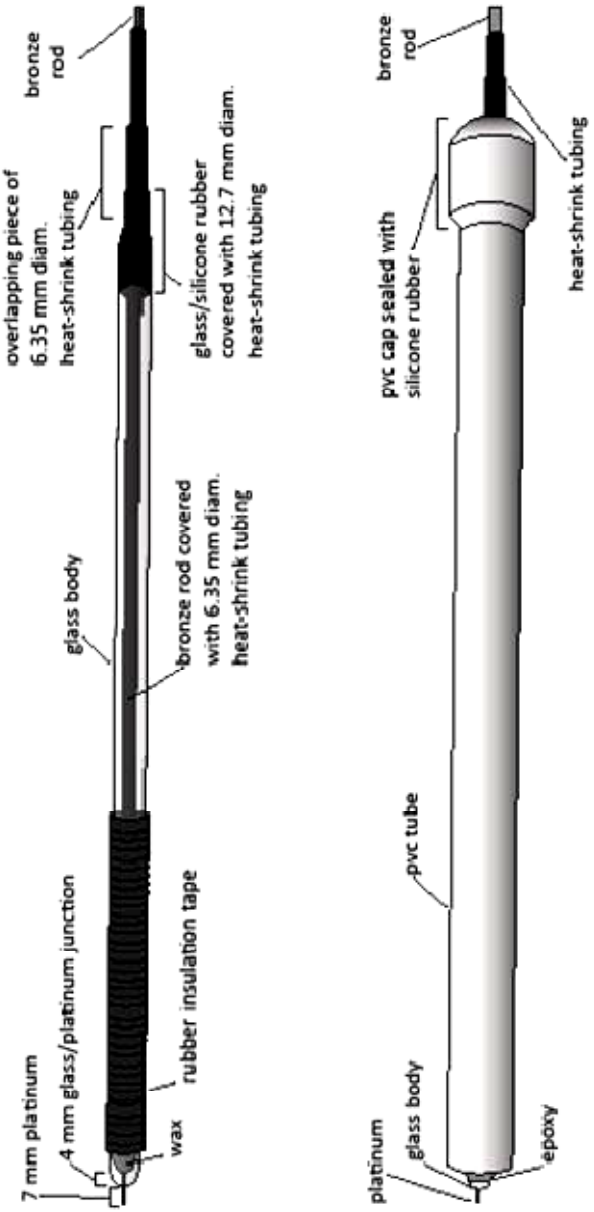

Figure 3. 1 Schematic of platinum electrodes . The figure on the left shows the primary glass/platinum electrode with labeled components. The figure on the right shows the primary electrode encased in a PVC tube with labeled components.

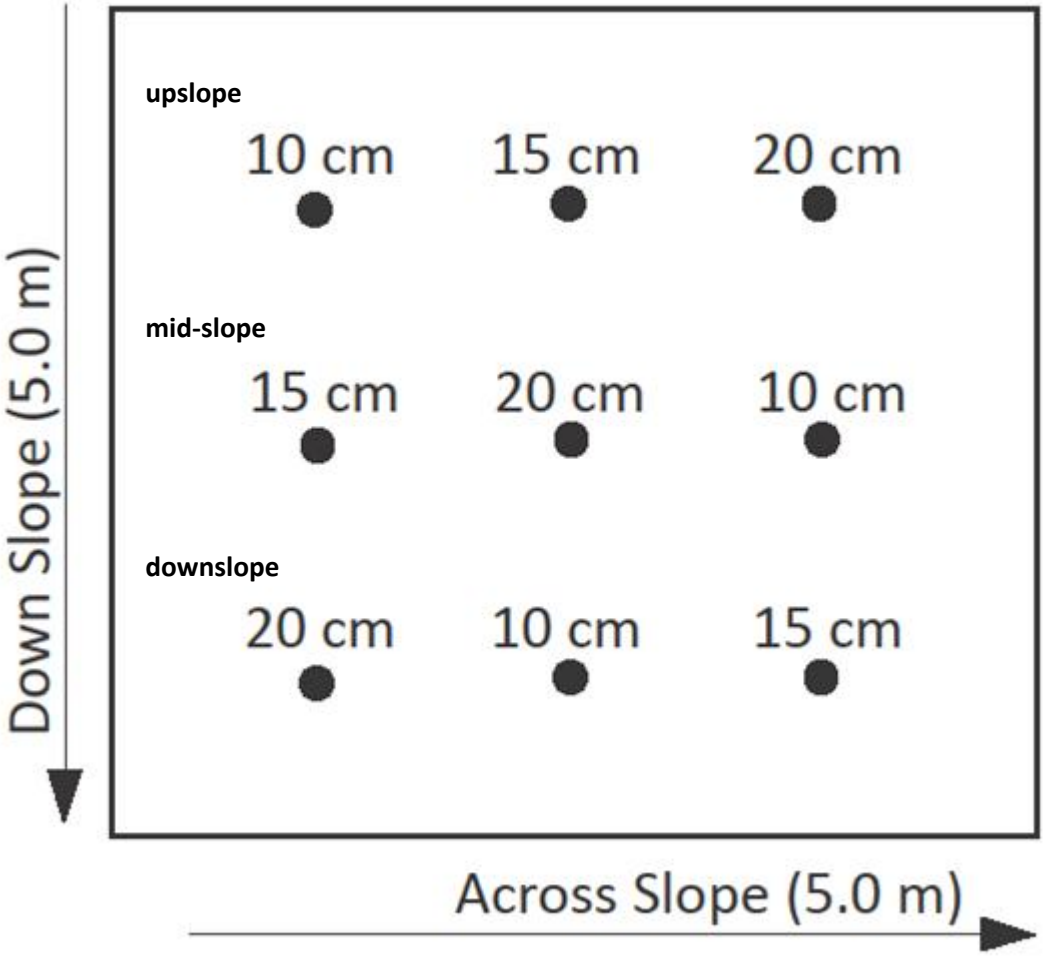

Figure 3. 2 Schematic of platinum electrode orientation in the field. Schematic shows each probe labeled by depth and relative position within a 5.0 m^2 area.

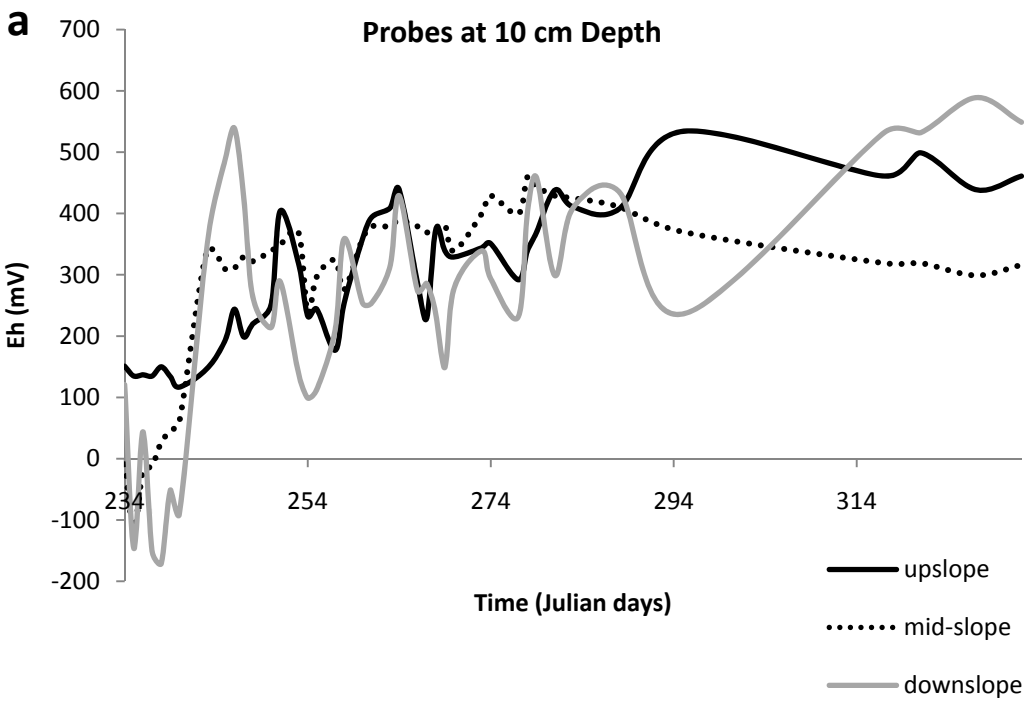
a
Probes at 10 cm Depth
Eh (mV)
700
600
500
400
300
200
100
0
-100
-200
234
254
274
294
314
Time (Julian days)
upslope
mid-slope
downslope

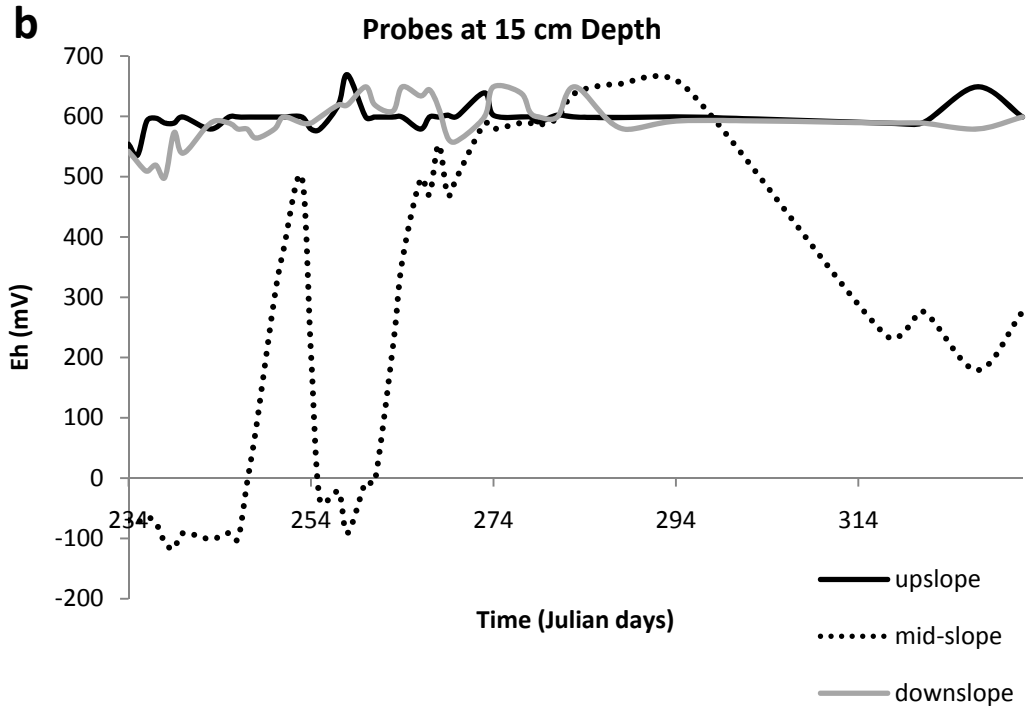
b
Probes at 15 cm Depth
Eh (mV)
700
600
500
400
300
200
100
0
-100
-200
234
254
274
294
314
Time (Julian days)
upslope
mid-slope
downslope

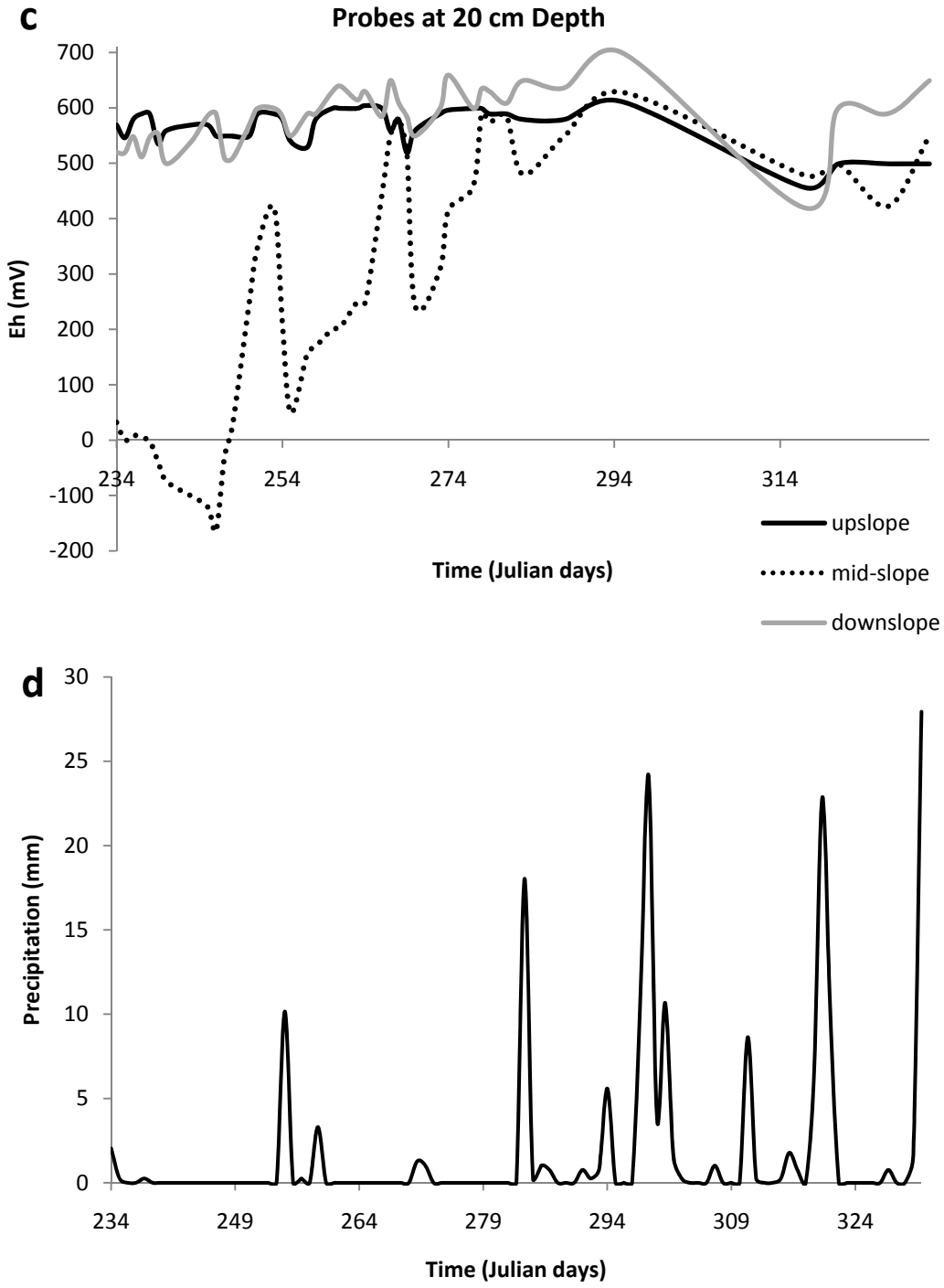

Figure 3. 3 Soil redox potential at (a) 10 cm depth, (b) 15 cm depth, (c) 20 cm depth, and (d) continuous precipitation for the period 22 Aug. 2007 to 28 Nov. 2007.

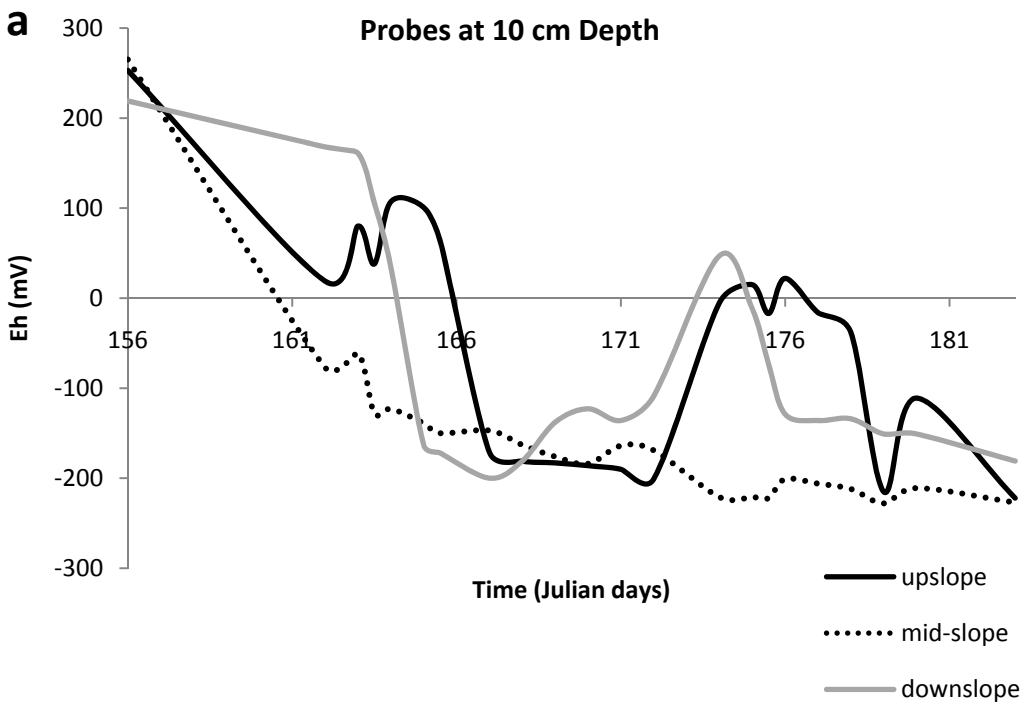
a
Probes at 10 cm Depth
300
200
100
0
-100
-200
-300
Eh (mV)
156
161
166
171
176
181
Time (Julian days)
upslope
mid-slope
downslope

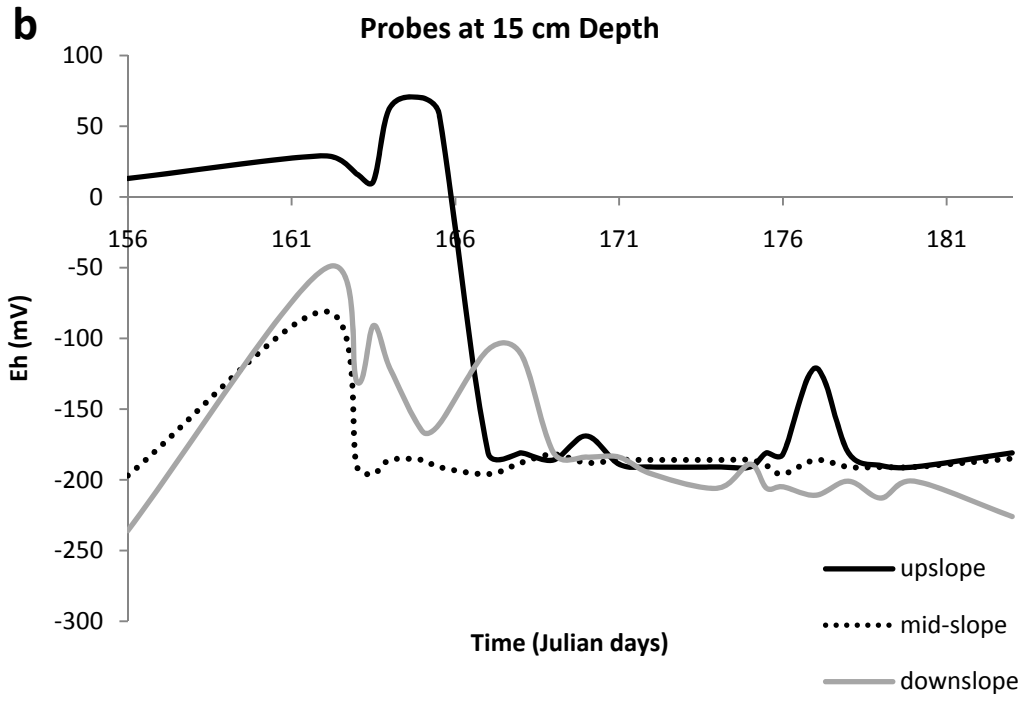
b
Probes at 15 cm Depth
100
50
0
-50
-100
-150
-200
-250
-300
Eh (mV)
156
161
166
171
176
181
Time (Julian days)
upslope
mid-slope
downslope

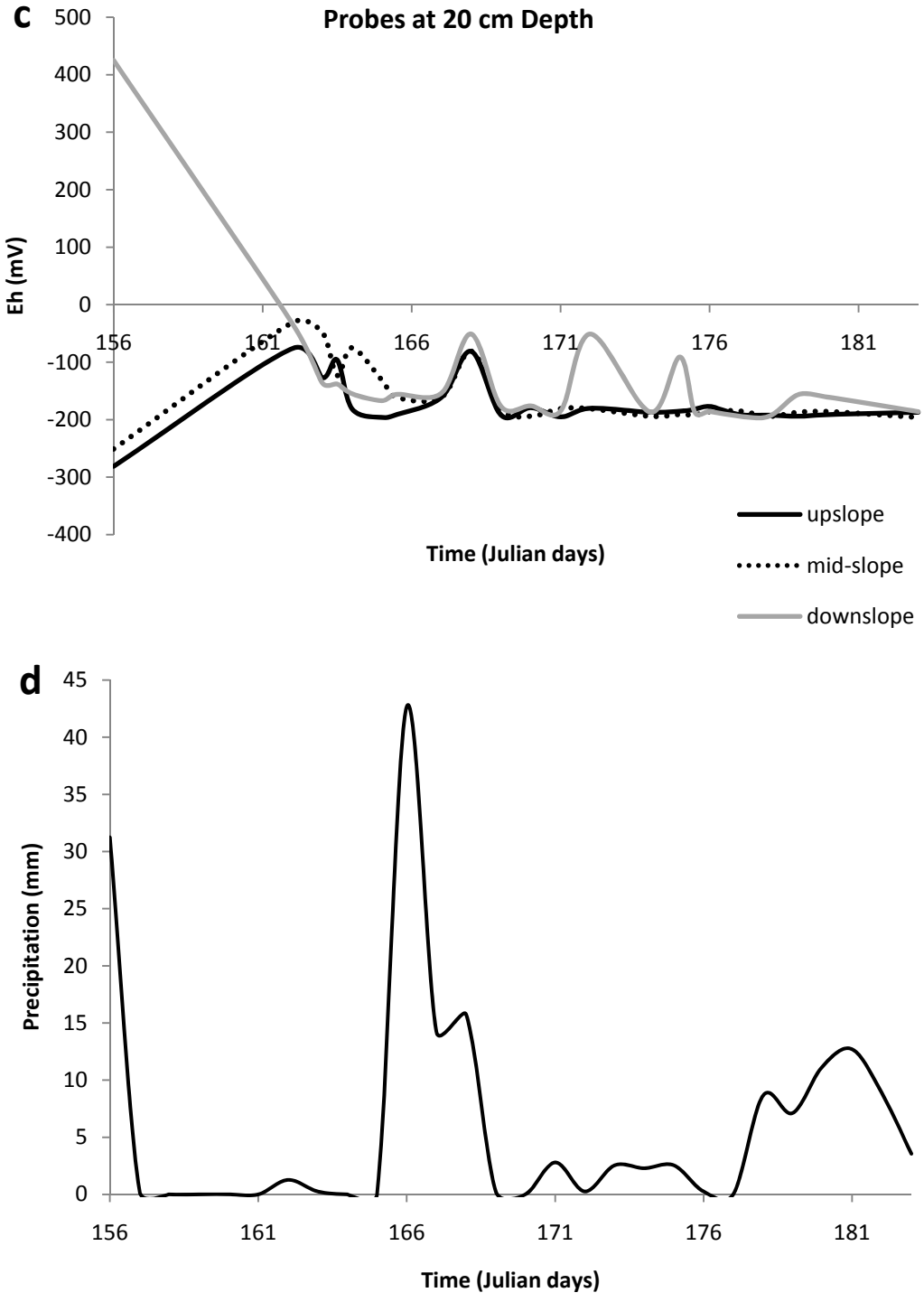

Figure 3. 4 Soil redox potential at (a) 10 cm depth, (b) 15 cm depth, (c) 20 cm depth, and (d) continuous precipitation for the period 4 June 2008 to 1 July 2008.

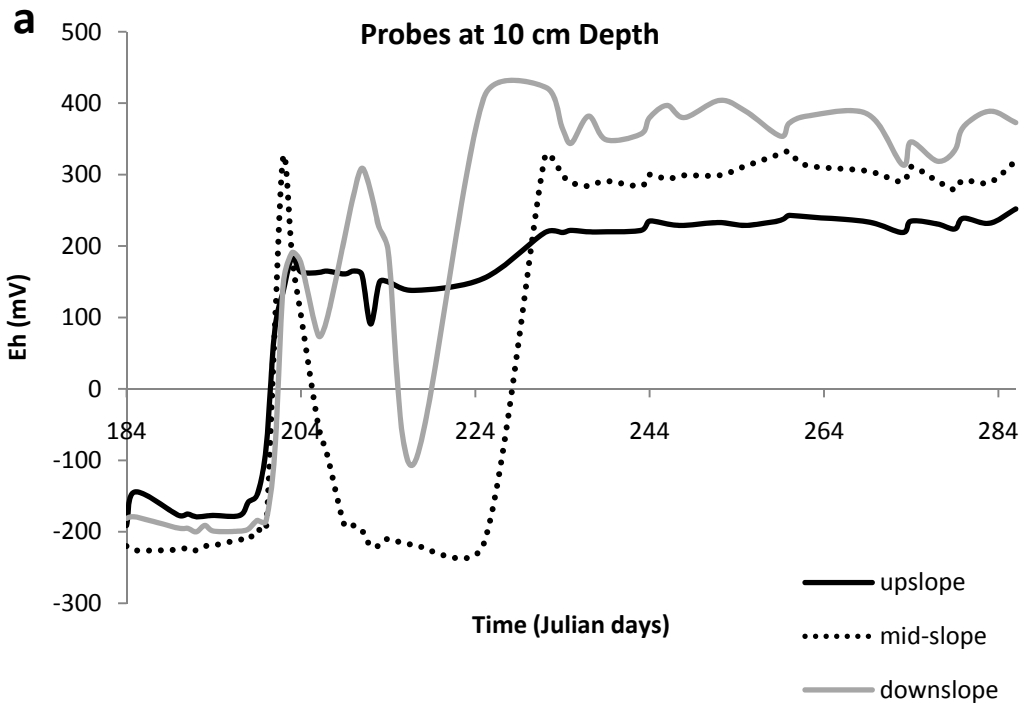
a
Probes at 10 cm Depth
Eh (mV)
500
400
300
200
100
0
-100
-200
-300
184
204
224
244
264
284
Time (Julian days)
upslope
mid-slope
downslope

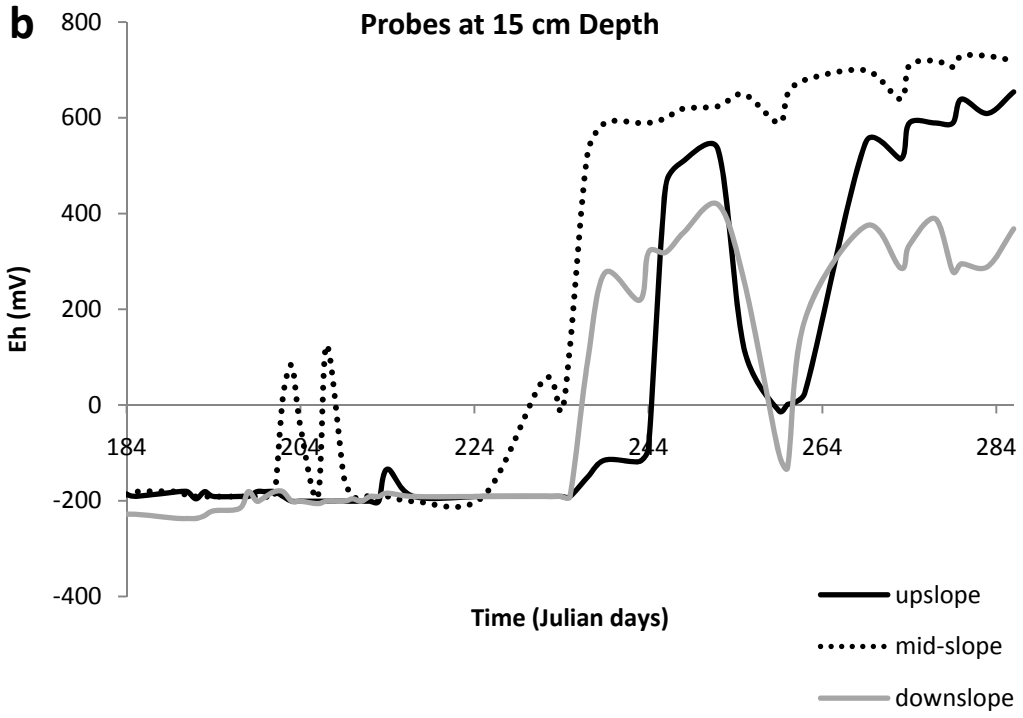
b
Probes at 15 cm Depth
Eh (mV)
800
600
400
200
0
-200
-400
184
204
224
244
264
284
Time (Julian days)
upslope
mid-slope
downslope

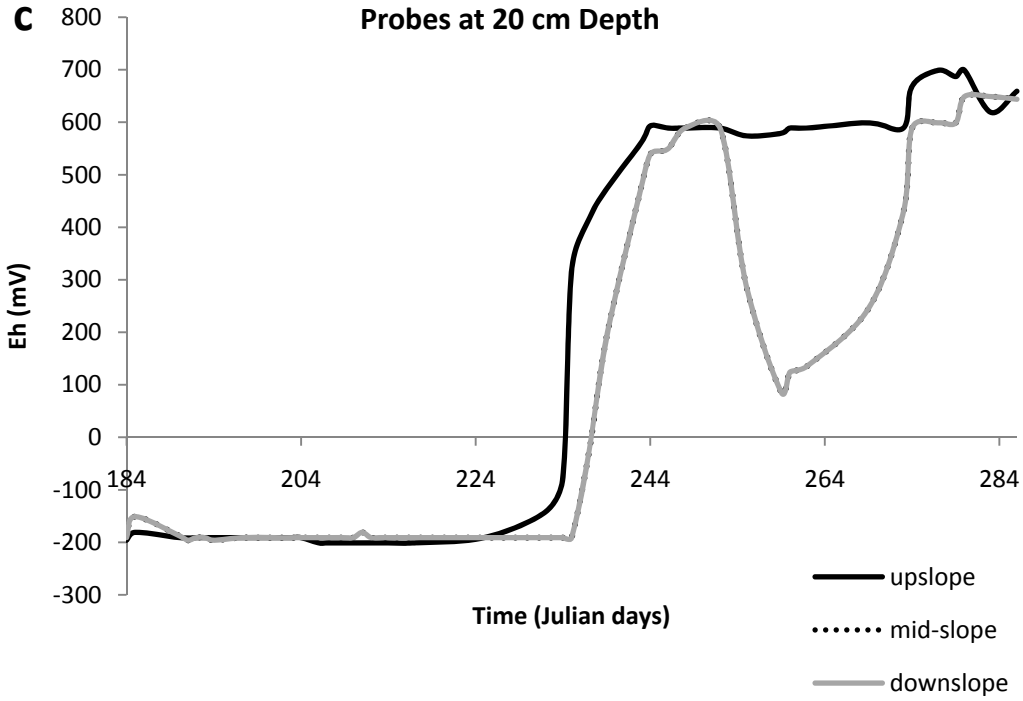
c
Probes at 20 cm Depth
800
700
600
500
400
300
200
100
0
-100
-200
-300
Eh (mV)
184
204
224
244
264
284
Time (Julian days)
upslope
mid-slope
downslope

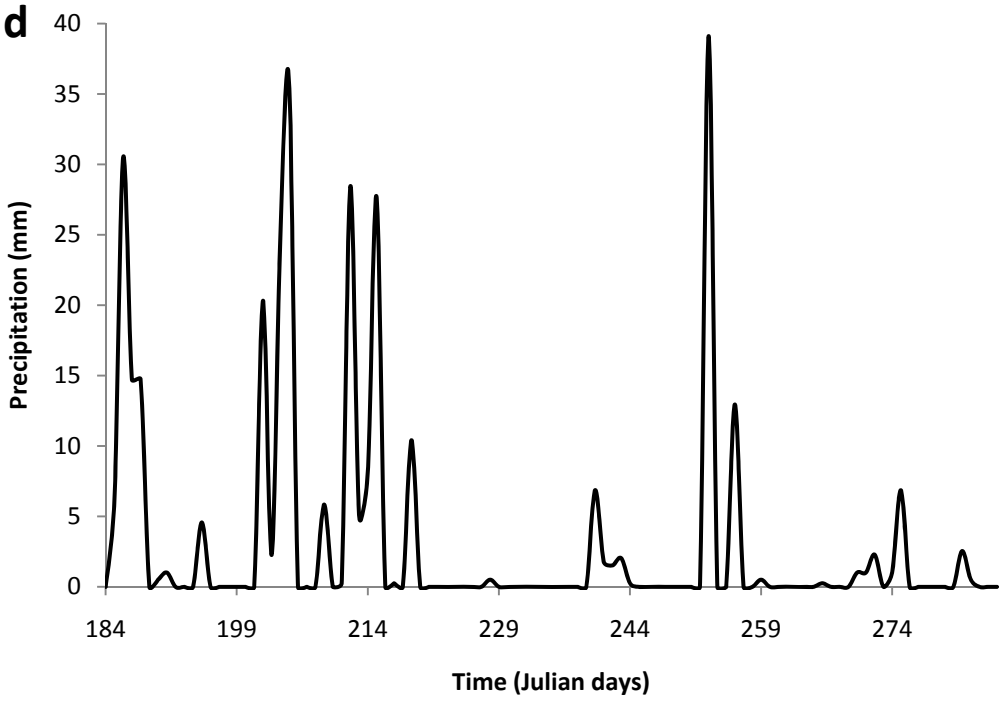
d
40
35
30
25
20
15
10
5
0
Precipitation (mm)
184
199
214
229
244
259
274
Time (Julian days)

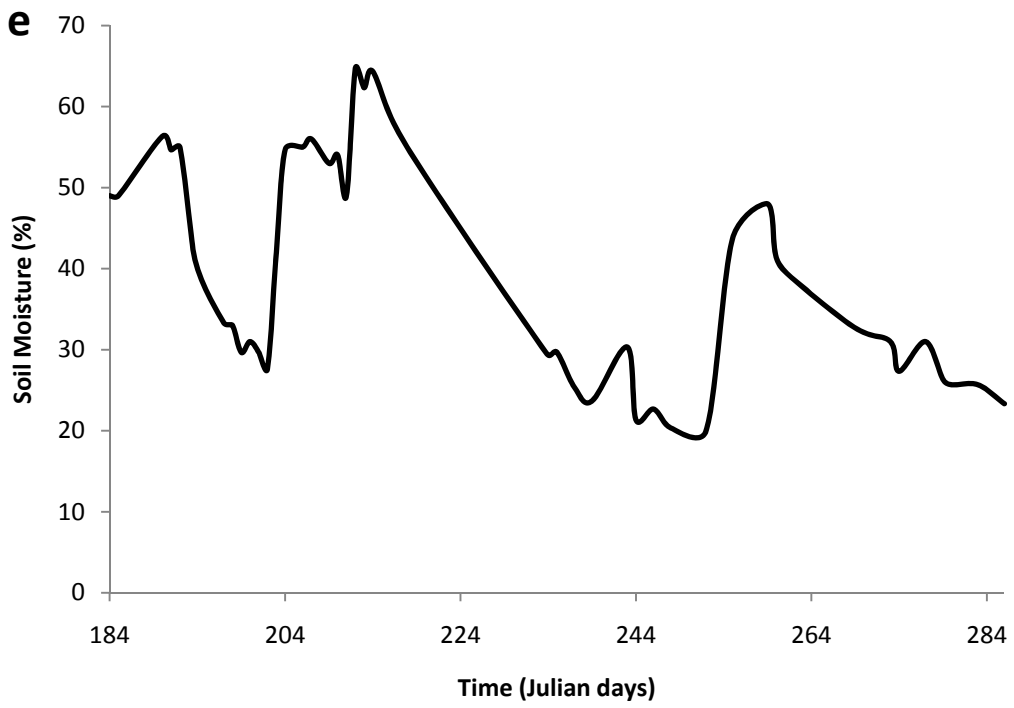

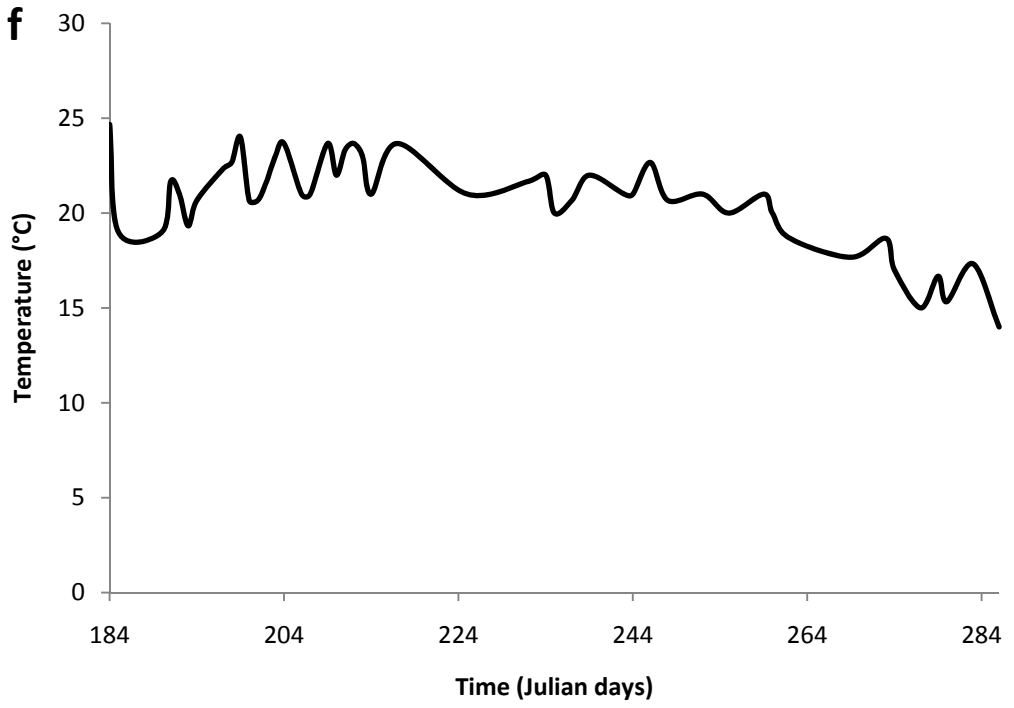

Figure 3. 5 Soil redox potential at (a) 10 cm depth, (b) 15 cm depth, (c) 20 cm depth, (d) continuous precipitation, (e) soil moisture, and (f) soil temperature for the period 2 July 2008 to 12 Oct. 2008. In figure (c), the Eh values of the mid-slope and downslope probes overlap.

CHAPTER 4: CONCLUSIONS

The novelty of the research presented in this thesis most certainly arises from revisiting old ideas and, in some instances, by bypassing tradition. Specifically, the data gives evidence that bacteria can use native humic substances in pasture soils to catalyze Fe reduction and subsequent P solubilization. Based upon the literature, which has historically evaluated similar mechanisms in flooded environments (predominantly anoxic), it had been assumed that topographically variable, agricultural landscapes (those that have not been flooded or otherwise disturbed) do not demonstrate significant Fe reduction and associated P solubilization.

New research has proposed that Fe reduction coupled to P desorption is an important process in predominantly oxidized tropical soils. Little research, if any, has examined this process with the same scrutiny in temperate pasture systems. The data collected in this thesis gives evidence that the microbial reduction of Fe in pastures is linked to P cycling, and that the cycle includes native humic electron mediators. Additionally, by using robust platinum electrodes in the field to measure redox potential over a 2 year period, it was possible to further support the theory that such a mechanism exists in the environment. Laboratory incubation data and field redox data are usually disjoint in the literature. The data presented here offers multiple connections between lab results and the natural system: Eh, pH, temperature, native HA, and native microbial population.

Future research that seeks to define the mechanisms of Fe reduction and P solubilization in temperate pasture soils should consider the many possible angles from which to work. For example, a project might be conducted in which HA is tested for competitive adsorption with P

on Fe(III) oxyhydroxide surfaces. Such research might expand the catalytic role of HA, concerning electron shuttling, to include a purely chemical role by which HA exchanges with P at the Fe-mineral surface in pasture soils.

The same experimental procedure carried out in this thesis (i.e. the lab incubation and the field-data collection) could be carried out in fertilized soils, especially soils that are sources of P-pollution for aquatic environments. Both organic and inorganic materials would increase the concentration of soil phosphorus. Based on the data reported here, it is reasonable to hypothesize that much greater concentrations of P could be lost under anaerobic conditions, related to seasonal changes (frequency of precipitation), from larger, more active agriculture landscapes that apply fertilizers.

From a microbiological standpoint, the successful isolation of novel Fe-reducing bacteria from temperate pasture soils would be extremely relevant to modern microbiology. Potentially, new methods of isolation might have to be developed in order to culture such organisms in the lab. And if a researcher was fortunate enough to obtain a viable isolate, any analytical technique ranging from genetic fingerprinting to electrochemical studies could be used to classify it. Establishment of biogeochemical parameters of the organism could be strengthened by the networking of soil microbiologists and soil chemists– a prospect worth considering in the long run.

From a chemical standpoint, the type of data reported here would be advanced even further by using modern electrochemical techniques. Specifically, potentiostats and electrochemical cells could be used to examine the mechanisms of Fe-surface chemistry in temperate pasture soils. Electrochemical analysis is also used for biological experiments in

much the same way as for chemical experiments. Again, the research could greatly benefit from the networking between the fields of soil microbiology and soil chemistry.

Finally, there is no universal agreement on the chemical structure or biogeochemical relevance of humic substances in soils. Studies could be conducted on the molecular structure of novel HA extracted from different locations. For example, laboratory procedures, such as functional group and elemental analysis could supplement FTIR and NMR techniques to develop new methods for HA characterization. Quinonoid, phenolic, and Fe(III) containing functional groups could collectively serve as a starting point for characterization, since these groups are associated with the electron-mediating capacity of humic substances. Ultimately, a project could attempt to correlate quinone concentration (for example) with a certain region of the ^{13}C-NMR spectrum common to humic substances, thereby removing some of the ambiguity that inhibits proper peak assignment. Different methods for size separation and fractionation could also be explored in the future. One such idea might involve using ultrasound at different frequencies and time intervals on a HA sample, which could then be characterized with ^{13}C-NMR. Theoretically, ultrasound treatments could break the bonds between certain chemical groups in HA, possibly rendering segments of the ^{13}C-NMR spectrum with higher resolution.

APPENDICES

Appendix 1 preliminary ferrozine and ammonium-molybdate experiments

Ferrozine Detection Limits for Fe(II)

Detection Limit Definition	mg/L
Instrument Detection Limit	0.16
Lowest Limit of Detection	0.27
Method Limit of Detection	0.74
Limit of Quantification	1.60
Practical Quantification Limit	3.70

Ammonium-Molybdate Detection Limits for P

Detection Limit Definition	µg/50 mL
Instrument Detection Limit	0.57
Lowest Limit of Detection	1.14
Method Limit of Detection	1.41
Limit of Quantification	5.70
Practical Quantification Limit	7.05

Ferrozine and ammonium molybdate change with time graphs

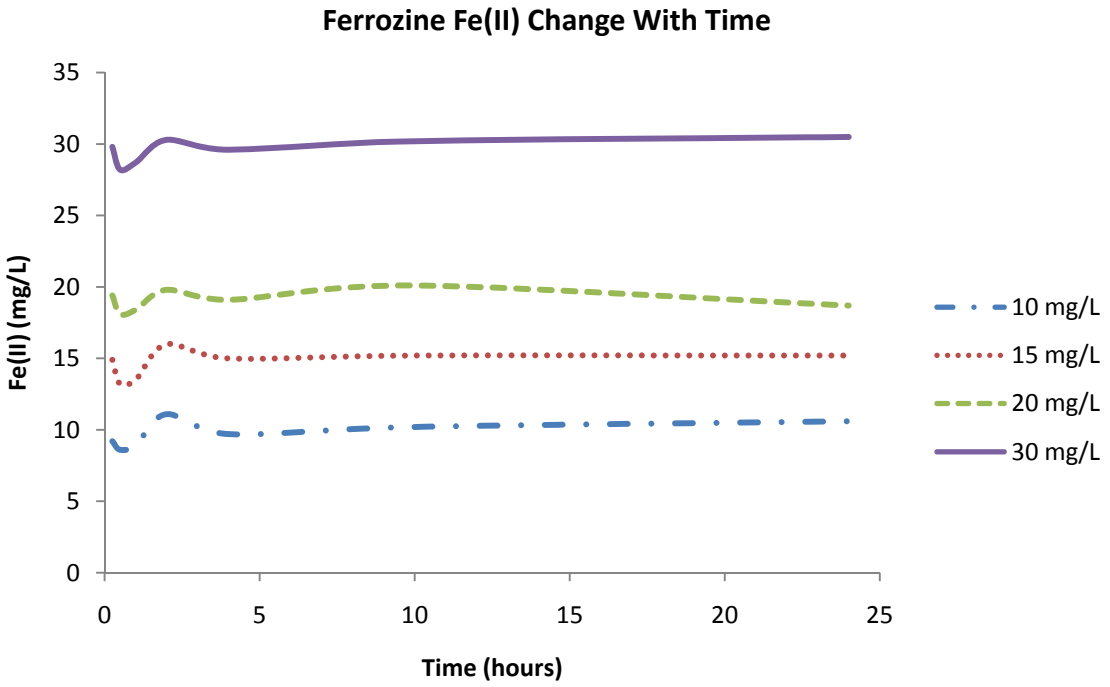

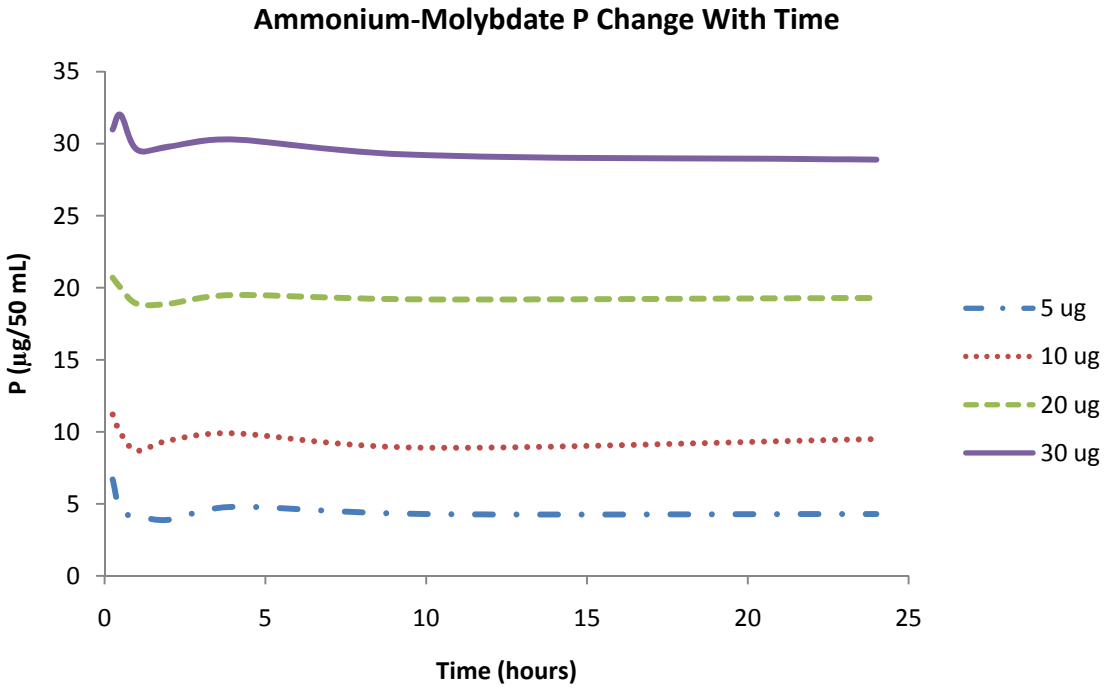

Appendix 2 Propylene Oxide (PO) Treatment Results and Discussion

Propylene Oxide Treatment: pH, Eh, Fe, P, and CO_2

The PO treatment displayed the second lowest rates for chemical parameters measured during the incubation, excluding P-ICP and pH. The slopes for Fe(II) and Fe-ICP were 0.16 and 0.17 mg kg^{-1} day respectively. Concentrations of PO P-ICP (PO P-ICP slope = 5.26 µg kg^{-1} day) showed the largest degree of variation compared to other treatments. This is important to address, since the PO treatment seemed to act as a microbial inhibitor, but simultaneously showed higher levels of solubilized P-ICP than any other treatment. When the P-ICP graphs and Fe graphs were compared to those for CO_2 (PO CO_2 slope = 0.87 µg g^{-1} day), it was observed that the PO treatment, unlike all other treatments, deviated strongly only for P-ICP. In other words, CO_2 evolution did not support the observed levels of P solubilization observed for the PO treatment, which would have supported a metabolic mechanism for P release over time. This observation implies an abiotic-chemical reaction between propylene oxide and soil that influences P solubilization. The reaction might be partially explained by propylene oxide interactions with carboxyl groups in organic-phosphate complexes or through surface reactions at the mineral surface (Wolf et al., 1989). Also, the error around data averages was larger for the PO treatment than any other treatment. For these reasons, the PO treatment could not be considered analogous to the NaN_3 treatment as an effective inhibitor, and was graphically separated from all other treatments. The above information concerning the PO treatment was derived from the following figures.

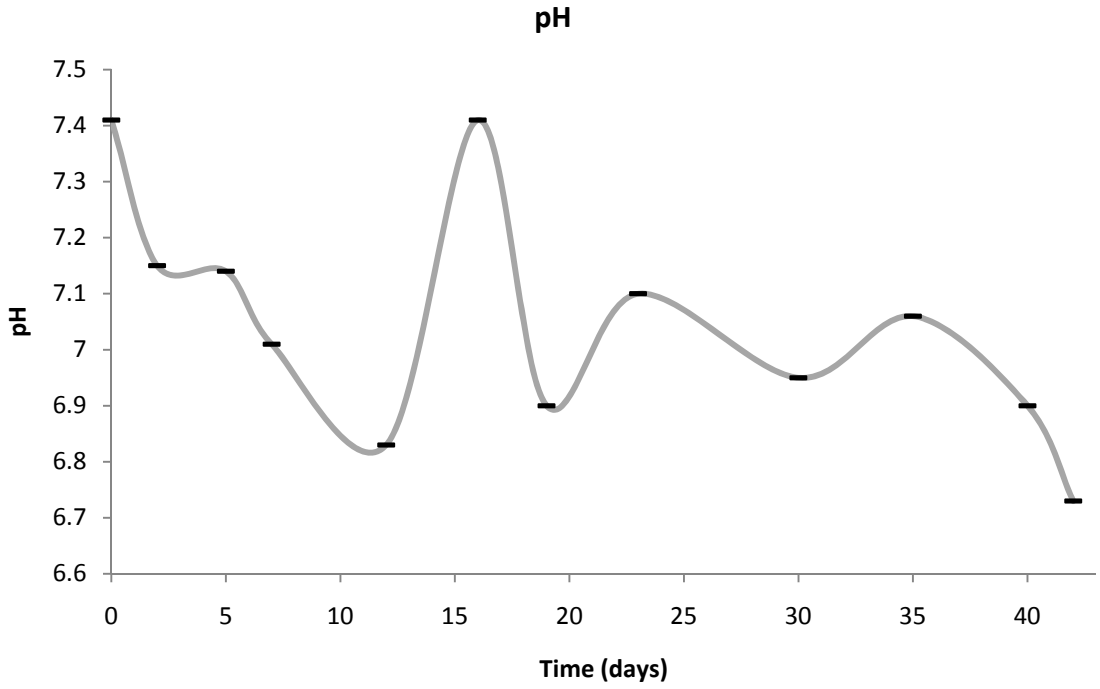
pH
7.5
7.4
7.3
7.2
7.1
7
6.9
6.8
6.7
6.6
pH
0
5
10
15
20
25
30
35
40
Time (days)

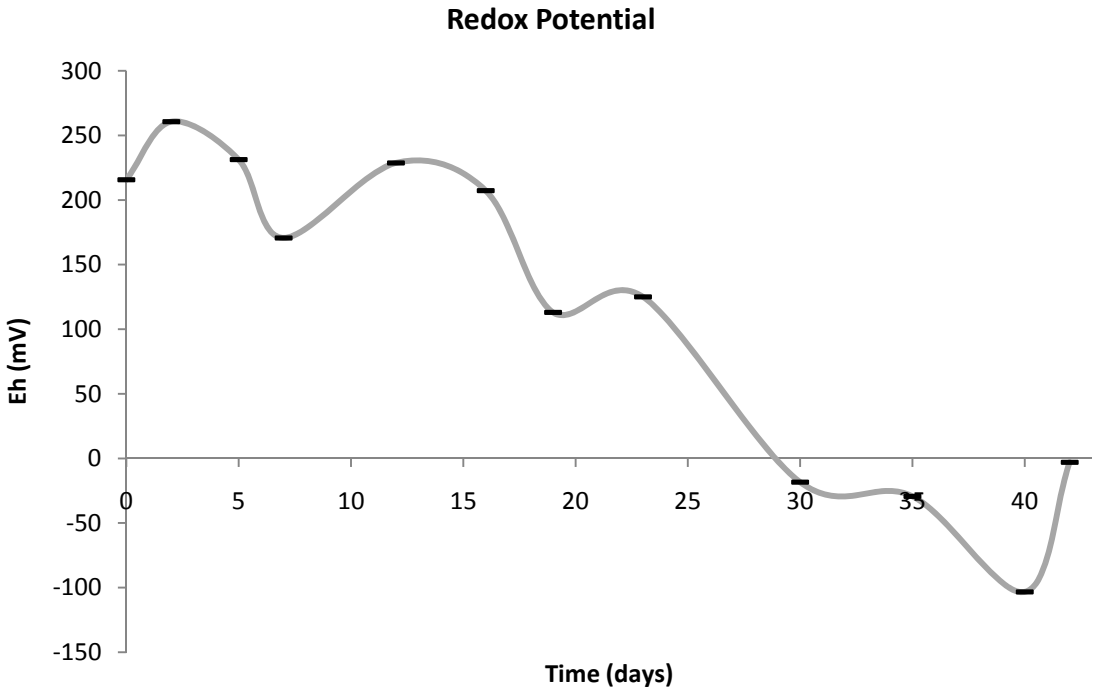
Redox Potential
300
250
200
150
100
50
0
-50
-100
-150
Eh (mV)
0
5
10
15
20
25
30
35
40
Time (days)

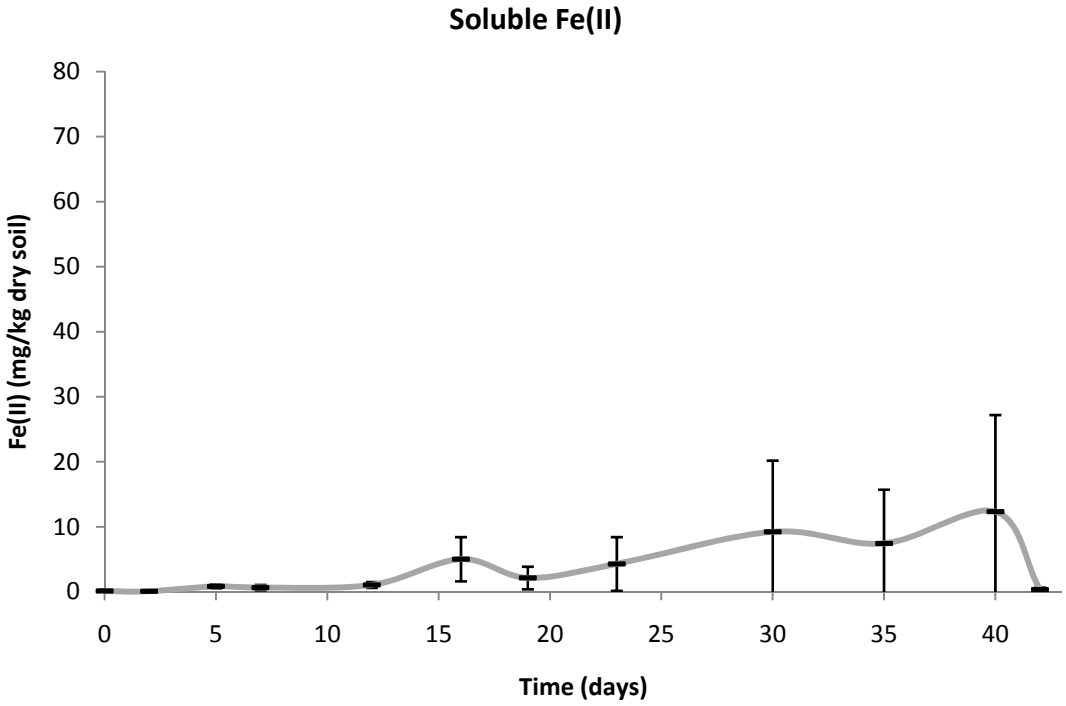
Soluble Fe(II)
Fe(II) (mg/kg dry soil)
80
70
60
50
40
30
20
10
0
0
5
10
15
20
25
30
35
40
Time (days)

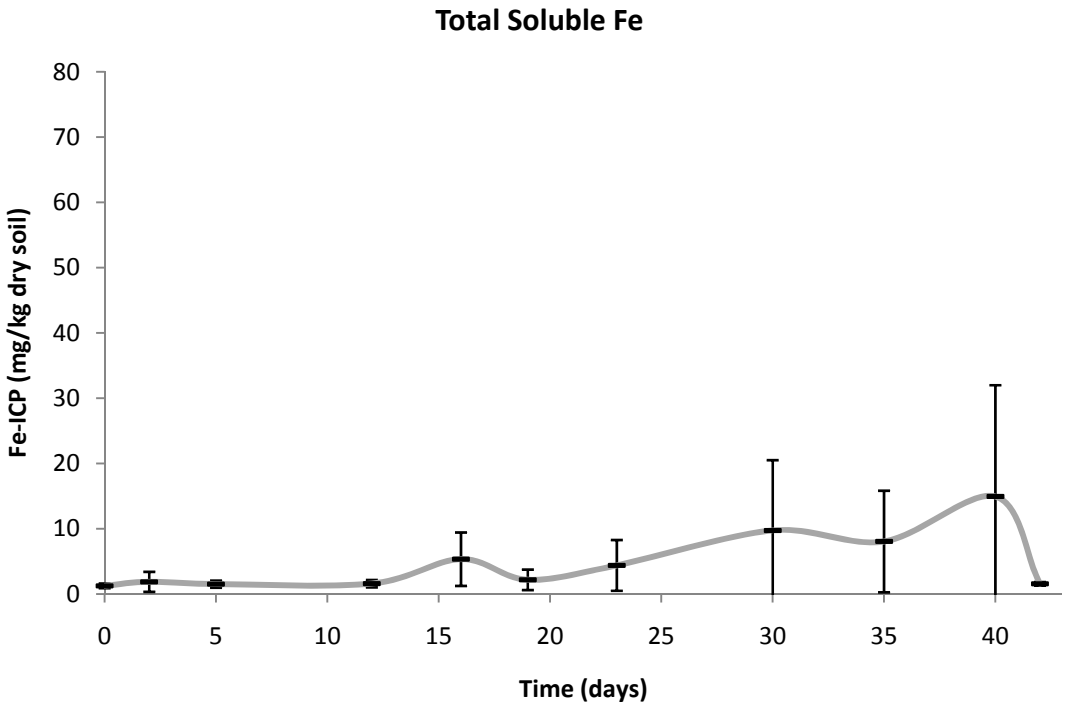
Total Soluble Fe
Fe-ICP (mg/kg dry soil)
80
70
60
50
40
30
20
10
0
0
5
10
15
20
25
30
35
40
Time (days)

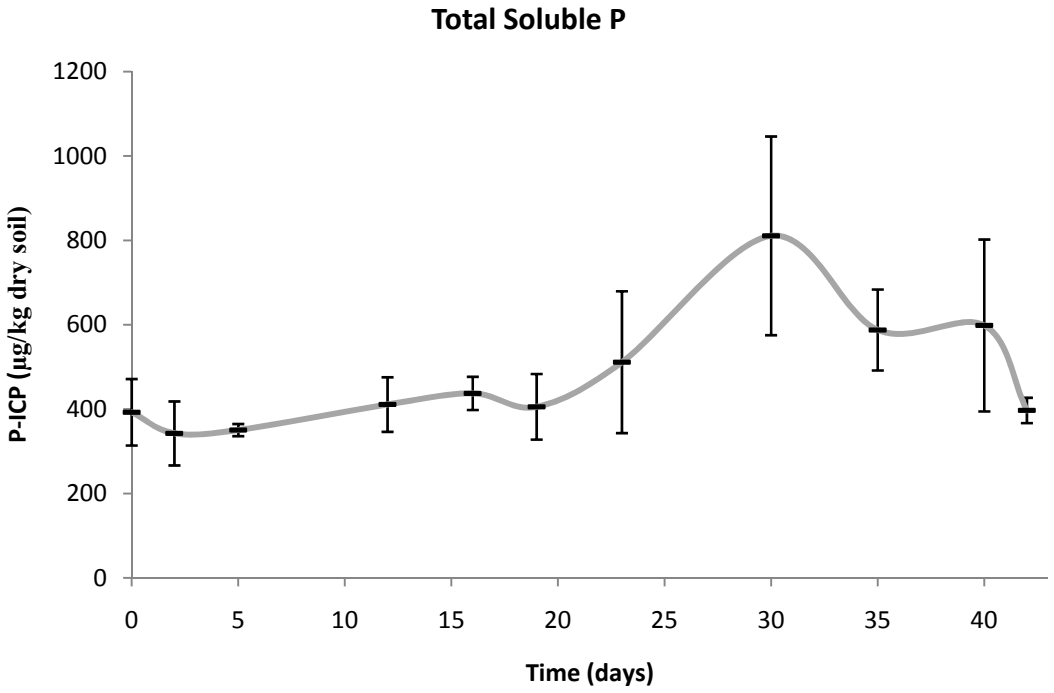
Total Soluble P
P-ICP (µg/kg dry soil)
1200
1000
800
600
400
200
0
0
5
10
15
20
25
30
35
40
Time (days)

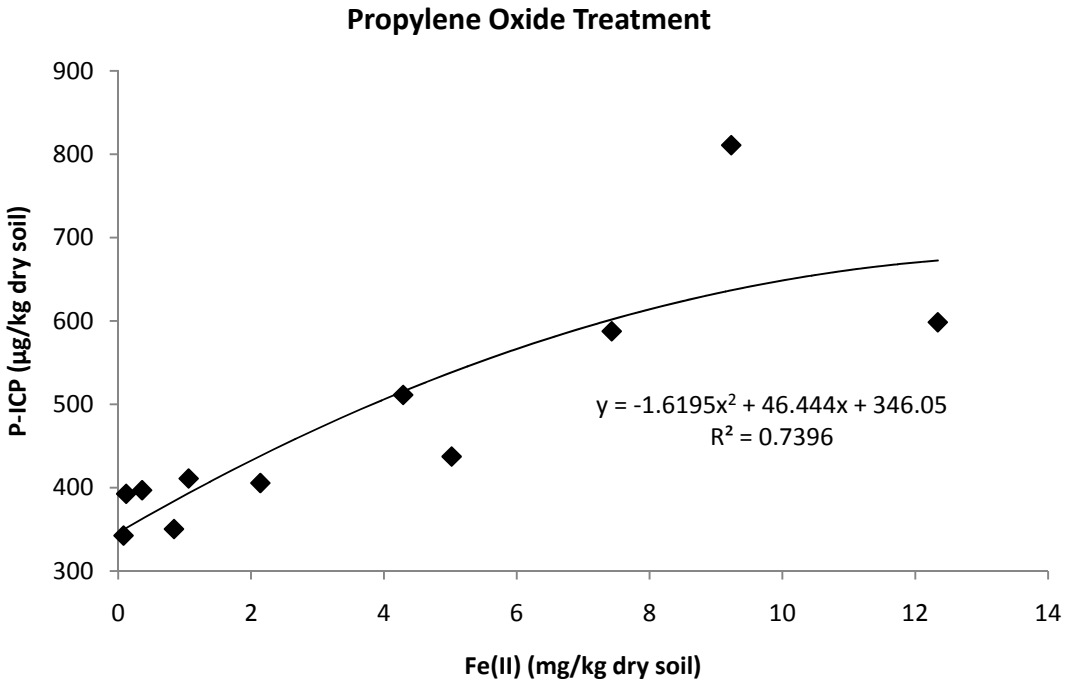
Propylene Oxide Treatment
P-ICP (µg/kg dry soil)
900
800
700
600
500
400
300
0
2
4
6
8
10
12
14
Fe(II) (mg/kg dry soil)
y = -1.6195x² + 46.444x + 346.05
R² = 0.7396

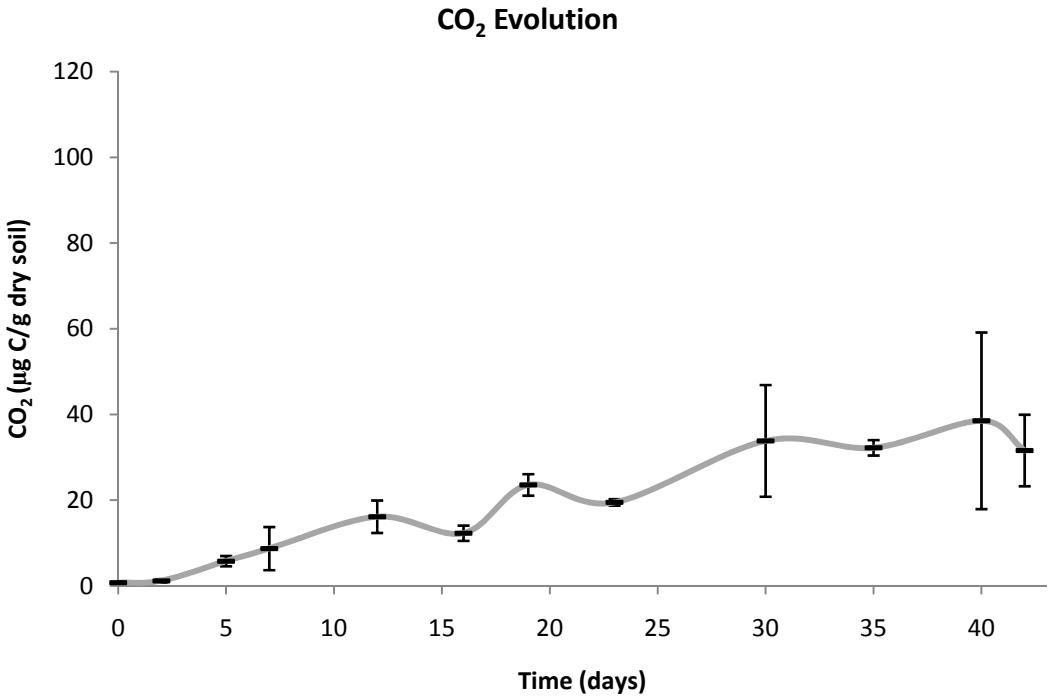

The above figures show all PO oxide data that were omitted from the main text.

Appendix 3 SAS regression analysis

Soluble Fe(II)

tmt	df	MSE	Pr>F	Adj R^2	β_0	SE β_0	β_1	SE β_1
NaN_3	29	0.01	<0.0001	0.47	0.026	0.0307	0.006	0.0013
PO	31	35.728	0.0414	0.103	0.351	1.813	0.158	0.074
SW	32	8.914	<0.0001	0.92	-3.744	0.9048	0.7	0.0364
AQDS 0.2	31	13.521	<0.0001	0.834	-2.135	1.1519	0.571	0.0456
HA 1.24	32	7.935	<0.0001	0.955	-3.501	0.8536	0.895	0.0343
HA 4.96	32	7.61	<0.0001	0.981	-2.05	0.836	1.356	0.0336
HA 9.92	32	14.361	<0.0001	0.979	-1.197	1.148	1.798	0.0462

(*) Pr < 0.05

Soluble Total Fe

tmt	df	MSE	Pr>F	Adj R^2	β_0	SE β_0	β_1	SE β_1
NaN_3	29	0.166	0.023	0.142	1.314	0.128	-0.012	0.0052
PO	31	42.154	0.0447	0.099	1.031	1.97	0.169	0.0804
SW	32	10.575	<0.0001	0.895	-1.99	0.9854	0.655	0.0396
AQDS 0.2	31	12.996	<0.0001	0.91	-1.426	1.129	0.792	0.0447
HA 1.24	32	9.679	<0.0001	0.939	-1.701	0.9428	0.839	0.0379
HA 4.96	32	8.096	<0.0001	0.975	0.831	0.8623	1.227	0.0347
HA 9.92	32	14.979	<0.0001	0.973	3.43	1.173	1.614	0.0471

(*) Pr < 0.05

Soluble Total P

tmt	df	MSE	Pr>F	Adj R^2	β_0	SE β_0	β_1	SE β_1
NaN_3	29	1862.23	0.0002	0.382	40.727	13.543	2.39	0.549
PO	31	22796	0.0085	0.183	365.14	45.805	5.263	1.87
SW	32	1576.84	<0.0001	0.888	0.592	12.033	7.707	0.484
AQDS 0.2	31	1100.1	<0.0001	0.935	32.77	10.39	8.713	0.412
HA 1.24	32	2229.88	<0.0001	0.876	30.254	14.31	8.655	0.5752
HA 4.96	32	1502.04	<0.0001	0.878	184.776	11.7446	7.18	0.4721
HA 9.92	32	3963.7	0.5493	-0.02	451.282	19.0786	0.464*	0.7669

(*) Pr < 0.05

CO_2 Evolution

tmt	df	MSE	Pr>F	Adj R^2	β_0	SE β_0	β_1	SE β_1
NaN_3	29	6.47E-12	<0.0001	0.91	2.74	0.798	0.554	0.0324
PO	31	6.12E-11	<0.0001	0.717	1.97	2.37	0.865	0.0969
SW	32	2.98E-12	<0.0001	0.992	0.439	0.523	1.29	0.021
AQDS 0.2	31	8.41E-12	<0.0001	0.974	1.5	0.909	1.23	0.036
HA 1.24	32	4.95E-12	<0.0001	0.989	2.34	0.674	1.47	0.0271
HA 4.96	32	6.75E-12	<0.0001	0.991	7.46	0.787	1.85	0.0317
HA 9.92	32	1.9E-11	<0.0001	0.983	11.9	1.32	2.28	0.0531

(*) Pr < 0.05

Appendix 4 Additional NMR experiments

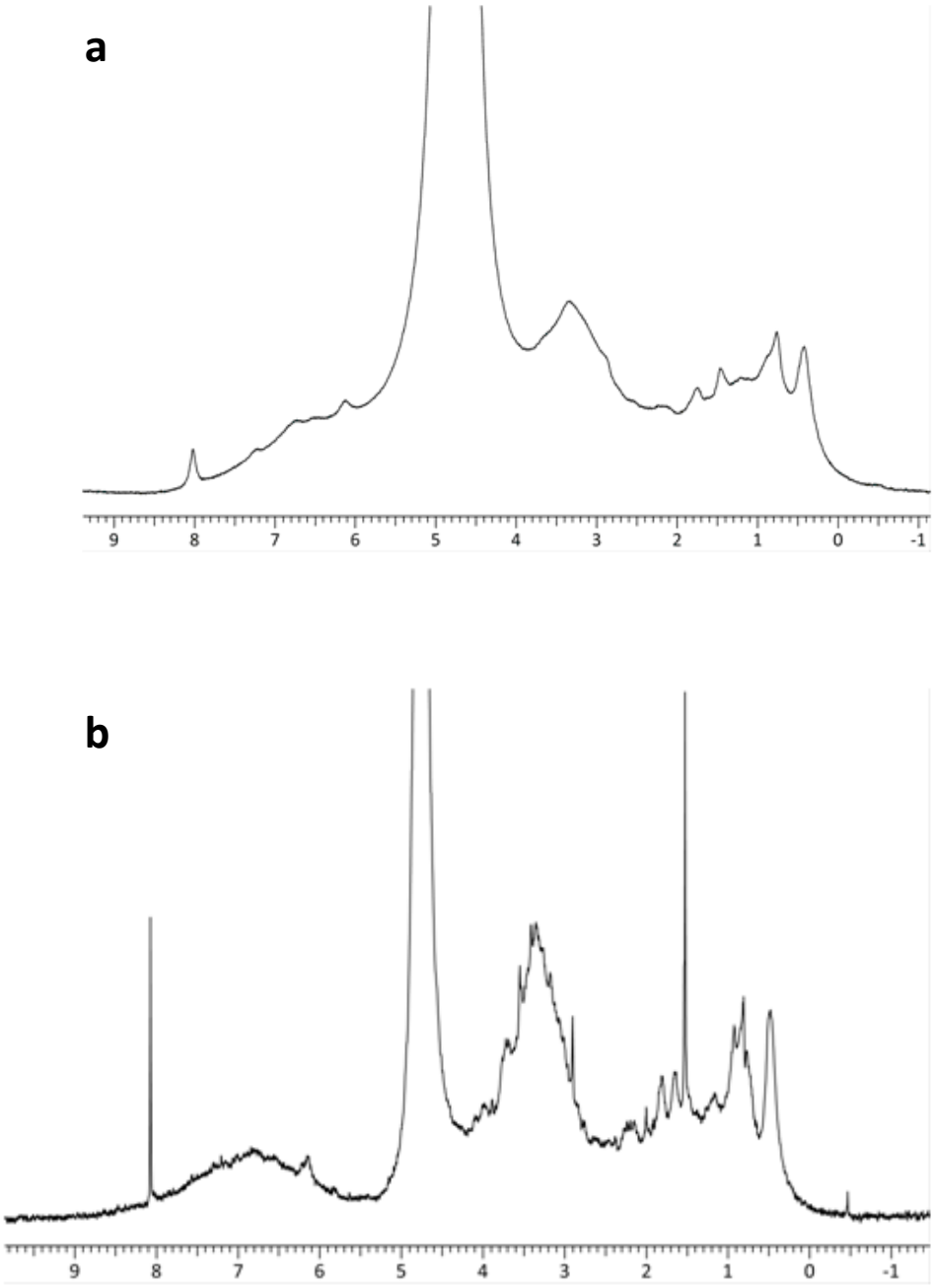

^{1}H-NMR spectra of HA samples. (a) Humic acid extracted from soil. (b) IHSS Elliott Soil standard. Samples prepared in 3 M NaOD in D_2O.

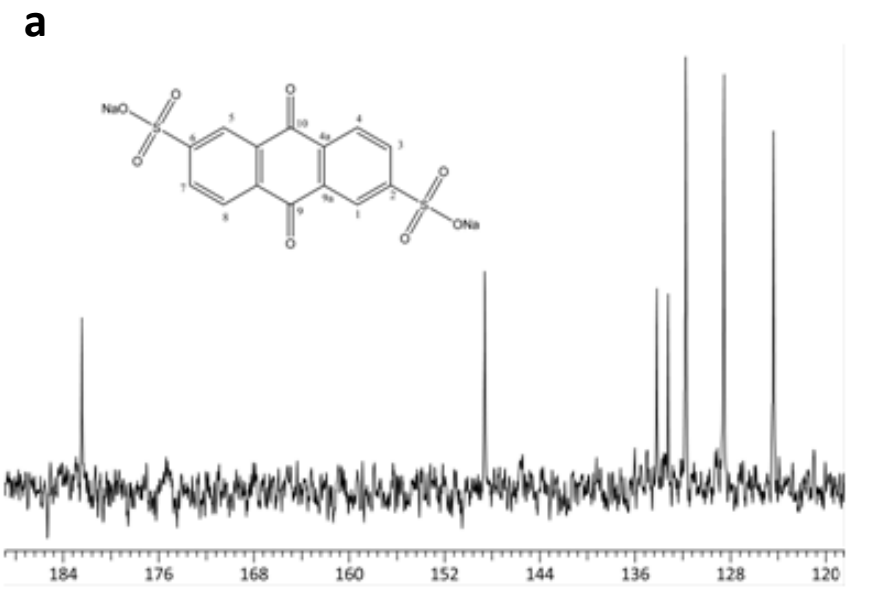

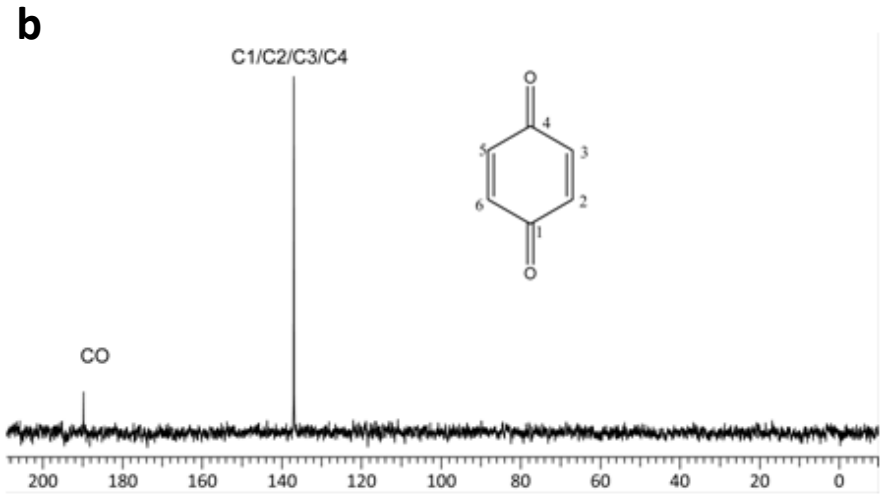

^{13}C-NMR of AQDS and benzoquinone. (a) 40 mg AQDS (used in the incubation experiment) and (b) 40 mg p-benzoquinone prepared in 1 ml D_2O.

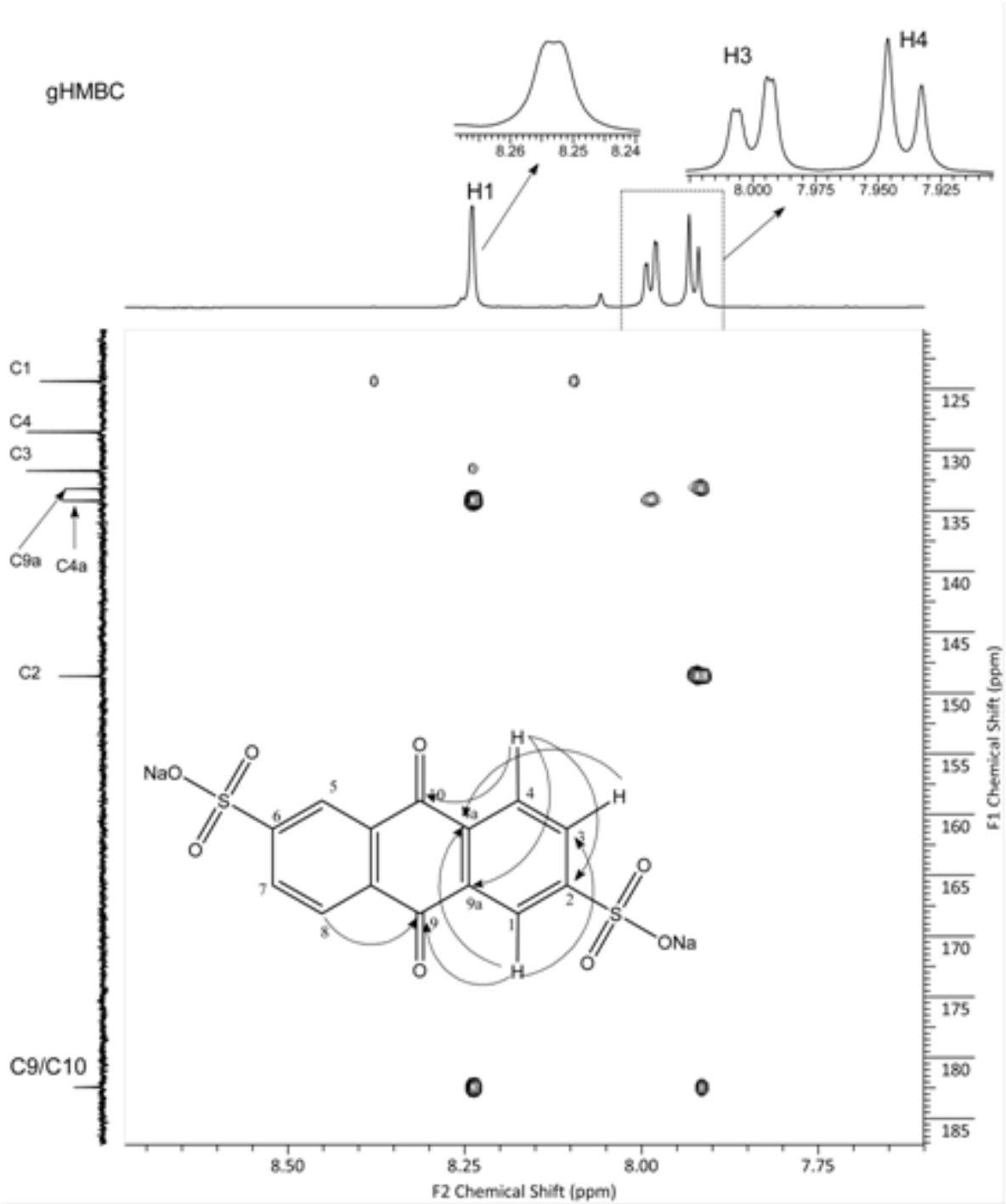

Heteronuclear Multiple Bond Correlation (HMBC) NMR of AQDS used during the incubation. F2 chemical shift is for ^{1}H and F1 chemical shift is for ^{13}C. Arrows around AQDS molecule show H-C J-couplings. The figure shows, and confirms, which H atoms are nearest to which C atoms. The correct molecular structure of AQDS was confirmed by the HMBC NMR experiment. AQDS (40 mg) was prepared in 1 ml D_2O.